Information and Communication Theoretical Modeling and Analysis of the Gut-Brain Axis

by

Beyza Ezgi Örtlek

Doctor of Philosophy

in

Electrical and Electronics Engineering

KOÇ ÜNİVERSİTESİ

September, 2025

Information and Communication Theoretical Modeling and Analysis of the Gut-Brain Axis

Koç University

Graduate School of Sciences and Engineering

This is to certify that I have examined this copy of a doctoral dissertation by

Beyza Ezgi Örtlek

and have found that it is complete and satisfactory in all respects,
and that any and all revisions required by the final
examining committee have been made.

Committee Members:

_____

Prof. Özgür Barış Akan (Advisor)

_____

Prof. Alper T. Erdoğan

_____

Prof. Fatih Alagöz

_____

Prof. Özgür Gürbüz

_____

Asst. Prof. Murat Kuşcu

Date: _____

To my dearest family, Semiran, Hüsamettin, and Cevdet Bilgehan Örtlek,

To my dearest aunt Yılşen and my dearest Ömer,

And to my beloved uncle, Fatih Kemâl Gargun, whose kindness, generosity, and pure-heartedness taught us to do good, help others, keep learning, and always look ahead.

ABSTRACT

Information and Communication Theoretical Modeling and Analysis of the Gut-Brain Axis
Beyza Ezgi Örtlek
Doctor of Philosophy in Electrical and Electronics Engineering
September, 2025

The gut-brain axis (GBA) represents one of the most sophisticated and crucial communication networks in the human body. However, a quantitative understanding of its signaling mechanisms has remained elusive, as conventional approaches fail to capture the inherently stochastic, nonlinear, and multi-scale nature of intra-body communication. The most promising paradigm to address these challenges is Molecular Communication (MC). Understanding biological signaling from an information and communication theoretical perspective provides insight into the fundamental dynamics of these systems. Therefore, this thesis applies MC principles to the GBA to establish a comprehensive and quantitative communication framework.

Building on this objective, the thesis constructs a multi-scale understanding of the GBA through a deliberate progression from a foundational single channel to a complete, bidirectional communication network. The research first develops a channel model for the propagation of a single microbial metabolite (p-cresol), deriving its impulse response and linking gut dysbiosis to a neurological outcome. It then advances the analysis to a complete end-to-end model of molecular-to-neural communication, modeling the short-chain fatty acid (SCFA)-driven vagal nerve pathway and quantifying its information-theoretic performance. Finally, the work culminates in a novel system-level model of the bidirectional communication within GBA that incorporates closed-loop feedback between the hypothalamic-pituitary-adrenal (HPA) axis, immune system, and gut barrier. This framework is used to analyze the system's transition into a pathological state and quantify its corresponding loss of channel capacity.

Collectively, the developed communication framework provides the tools to unravel the fundamental signaling mechanisms within the GBA, allowing for a de-

tailed analysis of how signaling disruptions contribute to disease progression. This in-depth, quantitative understanding creates a foundation for a new generation of medical technologies, providing a roadmap for ICT-inspired diagnostic tools and therapeutic strategies to detect and repair communication failures. Furthermore, it lays the essential theoretical groundwork for future Internet of Bio-Nano Things (IoBNT) applications to restore healthy information flow within the body.

ÖZETÇE

Bağırsak-Beyin Ekseni'nin Bilgi ve İletişim Kuramsal Modellemesi ve Analizi

Beyza Ezgi Örtlek

Elektrik ve Elektronik Mühendisliği, Doktora

Eylül, 2025

Bağırsak-beyin ekseni (BBE), insan vücudunda bulunan en karmaşık ve hayati haberleşme ağlarından birisidir. Ancak, geleneksel yaklaşımların vücut içi haberleşmenin stokastik, doğrusal olmayan ve çok ölçekli doğasını yakalamada yetersiz kalması nedeniyle, bu eksendeki sinyal mekanizmalarının nicel olarak anlaşılması henüz tam olarak sağlanamamıştır. Bu zorlukların üstesinden gelmek için en umut verici yaklaşım Moleküler Haberleşme'dir (MH). Biyolojik sinyalleşmenin bilgi ve iletişim kuramı perspektifinden ele alınması, bu sistemlerin temel dinamikleri hakkında içgörü sağlar. Bu nedenle bu tez, BBE için kapsamlı ve niceliksel bir haberleşme çerçevesi oluşturmak amacıyla MH ilkelerini uygulamaktadır.

Bu amaç doğrultusunda tez, temel bir tekil kanaldan başlayıp bütünleşik ve çift yönlü bir haberleşme ağına uzanan kademeli bir ilerleyişle, BBE'ne ilişkin çok ölçekli bir kavrayış inşa etmektedir. Araştırma ilk olarak, tek bir mikrobiyal metabolitin (p-cresol) yayılımı için bir kanal modeli geliştirerek bu kanalın dürtü yanıtını türetmekte ve bağırsak disbiyozu ile nörolojik bir sonuç arasındaki nedensel ilişkiyi ortaya koymaktadır. Ardından çalışma, moleküler düzeyden nöral iletime uzanan bütünleşik bir uçtan uca model geliştirerek kısa zincirli yağ asitleri ile uyarılan vagus sinir yolunu modellemekte ve bu haberleşme kanalının bilgi-kuramsal performansını nicel olarak ölçmektedir. Son olarak çalışma, hipotalamus-hipofiz-adrenal ekseni, bağışıklık sistemi ve bağırsak bariyeri arasında kapalı döngü geri bildirimini içeren, BBE'deki çift yönlü haberleşmeye yönelik özgün bir sistem-düzeyi model ile çalışma tamamlanmaktadır. Geliştirilen bu model sistemin patolojik bir duruma geçişini analiz etmek ve buna eşlik eden kanal kapasitesi kaybını ölçmek için kullanmaktadır.

Sonuç olarak, bu tezde geliştirilen haberleşme çerçevesi, BBE'ni oluşturan temel

sinyal mekanizmalarını çözümlemek için gerekli araçları sağlamaktadır. Bu sayede, sinyal akışındaki bozulmaların hastalıkların oluşum ve ilerleyişine olan etkisinin detaylı bir şekilde analiz edilmesine olanak tanımaktadır. Elde edilen bu derinlemesine ve niceliksel anlayış, haberleşme hatalarını tespit edip onarmak üzere tasarlanmış, bilgi ve iletişim teknolojilerinden (BİT) ilham alan yeni nesil tanı ve tedavi stratejileri için bir yol haritası sunarak geleceğin tıp teknolojilerine zemin hazırlamaktadır. Dahası bu çalışma, vücuttaki sağlıklı bilgi akışını yeniden sağlamayı amaçlayan gelecekteki Biyo-Nano Nesnelerin İnterneti (BNNİ) uygulamaları için gerekli olan temel teorik altyapıyı oluşturmaktadır.

ACKNOWLEDGMENTS

I would like to express my deepest gratitude and sincere thanks to my supervisor, Prof. Özgür Barış Akan, for his exceptional mentorship, guidance, and unwavering encouragement throughout every stage of this research. Without his endless support and belief in my capabilities, completing this thesis would have been impossible. More than an academic supervisor, Prof. Akan has been a true mentor whose wisdom extends beyond the academic realm and will continue to guide me throughout my professional and personal life. I consider myself truly privileged and honored to have been his student.

I also sincerely thank Prof. Alper T. Erdoğan and Prof. Fatih Alagöz for agreeing to supervise this thesis and for guiding it with their valuable comments and suggestions throughout this process. I am especially grateful to Prof. Erdoğan, who has always supported and advised me since my undergraduate years. His continued belief in me, first as my undergraduate advisor and now as a member of my thesis committee, has been a great source of encouragement. His guidance has profoundly shaped my academic journey. My gratitude also extends to Prof. Özgür Gürbüz and Asst. Prof. Murat Kuşcu for taking part in my thesis committee and for their valuable comments.

I also want to sincerely thank Dr. Meltem Civaş for her invaluable guidance and support throughout this journey. My special thanks are to Dilara Aktaş for her collaboration and companionship.

I extend my deepest gratitude to my family, whose unwavering support has been my foundation. To my father, Hüsamettin, and my mother, Semiran, for their endless love and belief in every decision I have made. To my brother, Cevdet Bilgehan, my playmate since the day he was born and my favorite person in the

world, thank you for your constant support and companionship. I could not have accomplished anything without them. This achievement belongs as much to them as it does to me. A very special thanks to my grandmother, Hamiyet Dündar, who has always believed in me and wished for my success. I am also grateful to my aunts, Yılşen, Samiye, and Semiha, for their love and encouragement. I wish to honor the memory of my uncle, Fatih Kemâl Gargun, father of Doğa and İdil. His lesson to "always look ahead" encourages us to move forward together, and we will accomplish incredible things in his memory to make him proud.

My deepest gratitude is for Ömer. His patient support, endless encouragement, and strong belief in me were my sanctuary through every challenge. His presence filled the most difficult days with warmth and joy, and his support was the constant strength that carried me to the finish line. I will always be thankful for his love and for standing by my side.

Finally, I would like to express my warmest thanks to my dear friends who have been with me every step of this journey. To Habibe Cansu Demirel, for the countless nights we worked side by side, your support made those long hours meaningful. To Esra Başaran, for all our talks and debates that always ended with laughter and brought us closer. And my warmest, most special thanks to Tuba Görmez, my best friend since our undergraduate years. Thank you for standing by me during the hardest times and for always supporting me when I needed it most. Without your friendship and encouragement, this journey would not have been the same. I feel truly fortunate to have you in my life.

TABLE OF CONTENTS

List of Tables **xii**

List of Figures **xiii**

Introduction **1**

Chapter 1: Modeling of Microbial Molecule Transmission in the Gut-Brain Axis **11**

1.1 Introduction 11

1.2 Molecular Communication System Model 14

1.3 Numerical Evaluation 19

1.4 Conclusion 24

Chapter 2: End-to-End Molecular-to-Neural Signaling in the Gut-Brain Axis **26**

2.1 Introduction 26

2.2 Literature Review 29

2.3 System Model 33

2.3.1 Vagus Nerve Activation Model 35

2.3.2 Receiver Model 38

2.4 Theoretical Analysis and Simulations 45

2.4.1 Mutual Information 48

2.4.2 Delay Analysis 51

2.5 Discussion 54

2.6 Conclusion 56

Chapter 3: Closed-Loop Bidirectional Communication in the Gut-Brain Axis **58**

3.1 Introduction 58

3.2 System Model 63

3.2.1 Model Architecture and Signal Propagation 63

3.2.2 Molecular Communication Framework 65

3.3 Theoretical Analysis and Simulations 70

3.3.1 Time-Domain Response to Stress Scenarios 71

3.3.2 Bifurcation Analysis and Tipping Points 73

3.3.3 Frequency Domain Analysis 75

3.3.4 Quantitative Performance Metrics: DC Gain and Bandwidth . 80

3.3.5 Information-Theoretic Channel Capacity 81

3.4 Discussion 85

3.5 Conclusion 87

Chapter 4: Conclusion **89**

Bibliography **95**

LIST OF TABLES

1.1 List of Parameters used in Analysis 19

2.1 Hodgkin-Huxley Model Parameters 42

3.1 Model Parameters 69

LIST OF FIGURES

1.1 Biological Representation of MC System 13
1.2 Scheme of the MC channel model for p-cresol signaling in ASD. . . . 15
1.3 **(a)** Impulse Response for MC System. **(b)** Concentration of Signaling Molecule at Rx. **(c)** Enzyme Kinetics at Rx. 20
1.4 Numerical analysis for MC system with respect to changing blood vessel diameter. 22
1.5 Numerical analysis for MC system with respect to changing distance between Tx & Rx. 23
1.6 Numerical analysis for MC system with respect to changing Rx dimension. 24

2.1 Biological Representation of MC System (Created in https://BioRender.com). 30
2.2 Illustration of ligand-receptor binding.(Created in https://BioRender.com). 31
2.3 Scheme of the MC channel model for SCFA-driven vagus nerve signaling withing GBA. 34
2.4 SCFA-driven cytosolic calcium oscillation and membrane potential for changing k_1 values. (a) Cytosolic calcium oscillations, and (b) Membrane potential (V_m) for $k_1 = 1.50\mu M/s$. (c) Cytosolic calcium oscillations, and (d) Membrane potential (V_m) for $k_1 = 3.82\mu M/s$, . . 39
2.5 Zoomed-in view of SCFA-driven neural responses with varying GPCR activation rates. (a) Action potential generation, and (b) corresponding neurotransmitter concentration for lower activation rate ($k_1 = 1.52\,\mu$M/s); (c) Action potential generation, and (d) corresponding neurotransmitter concentration for higher activation rate ($k_1 = 3.82\,\mu$M/s). 44

2.6 Zoomed-in view of SCFA-driven responses for varying SCFA concentrations. (a) Cytosolic calcium dynamics in response to different SCFA levels, and (b) corresponding membrane potential changes. . . 46
2.7 Mutual information and mean signaling delay as a function of SCFA concentration. As SCFA concentration increases, mutual information improves while signaling delay decreases, indicating enhanced communication efficiency. 47
2.8 Mutual information vs GPCR activation rate. 49
2.9 Action potential and mutual information vs GPCR activation rate. . 50
2.10 Delay vs GPCR activation rate. 53

3.1 Illustration of bidirectional communication along the gut–brain axis via the HPA axis. (Created in https://BioRender.com). 59
3.2 Closed-loop communication within the gut–brain axis via the HPA axis. (Created in https://BioRender.com). 64
3.3 Comparative dynamics of the GBA network under three simulated stress scenarios. The columns depict the system's response to (a) a Healthy Baseline, (b) an Acute Stress event (a 12-hour pulse starting at hour 48), and (c) a Chronic Stress profile (initiated at hour 48). The rows display the time-course for the key signaling molecules: Endotoxin, TNF-α, ACTH, and Cortisol. 70
3.4 Dynamics of the acute inflammatory cascade following a transient endotoxin leakage. 72
3.5 Results of the numerical bifurcation sweep identifying critical thresholds for system stability. 74
3.6 Magnitude and phase response of the linearized GBA channel. 79
3.7 Information-theoretic channel capacity as a function of stress-induced leakage rate (k_{leak}). 83

3.8 Detailed analysis of channel capacity for healthy and chronic stress states. 84

INTRODUCTION

The survival of living organisms depends on fast, reliable, and energy-efficient communication across all scales, from molecular interactions to macro-scale physiological processes. These processes involve generating and encoding signals, transmitting them through inherently noisy media, and decoding them via specific receptors to inform higher-order regulatory mechanisms that maintain homeostasis. Although we have deep biological insights at individual scales, a critical gap remains in our quantitative, system-level understanding of how information is represented and processed across whole physiological systems. This gap has direct clinical implications, as dysregulated communication is a fundamental reason for a broad spectrum of disorders. A principled framework that conceptualizes biological systems as information-processing communication networks can therefore clarify underlying signaling mechanisms, identify novel biomarkers, and ultimately guide interventions that can be designed to restore healthy communication.

Traditional engineering approaches are not suitable for capturing the complexity of biological signaling. The conventional methods typically assume continuous waveforms, linear time-invariant media, and additive Gaussian noise. By contrast, intra-body signaling is discrete and stochastic at low molecular copy numbers. Signal transmission is governed by nonlinear diffusion, advection, and chemical reactions, while receivers such as cellular receptors exhibit saturation and adaptation. Furthermore, the heterogeneous environments within the body introduce memory effects, and significant delays arise from multi-step reaction cascades and axonal conduction. The extensive existence of feedback loops and molecular cross-talk constructs a deeply interconnected system where the same molecule can play multiple contextual roles. Addressing these complexities thus requires an inherently molecular,

probabilistic, dynamical, and multi-scale theoretical framework [1, 2].

Molecular Communication (MC) theory provides this foundation by establishing a rigorous framework to analyze biological signaling as a communication system [3, 4]. This paradigm maps biological components onto functional blocks, where entities such as neurons or endocrine cells serve as transmitters. These transmitters encode information by modulating the type, concentration, or timing of the molecules they release. These molecular signals propagate through a channel, like the bloodstream, where they are impaired by diffusion-based dispersion, noise from interfering molecules, and significant delays from biochemical processes. Finally, target cells serve as receivers, employing specialized protein receptors to capture the molecules. The binding event initiates an intracellular cascade that decodes the message and translates molecular patterns into specific functional responses. This formal mapping enables the application of information-theoretic metrics such as channel capacity, mutual information, and delay analysis to quantitatively assess the efficiency, robustness, and failure modes of these biological communication pathways [5].

Guided by MC principles, this thesis conceptualizes the human body as a sophisticated communication network. Among the body's many interconnected systems, the gut-brain axis (GBA) represents an ideal testbed for this approach due to its immense importance and inherent complexity. The GBA integrates dense microbial metabolism with epithelial sensing, vagal afferent signaling, immune activation, endocrine pathways, and central neural circuits that govern mood, stress, appetite, and metabolism. [6].

The human gastrointestinal (GI) tract is a highly specialized and continuous organ system responsible for the intricate processes of digestion, nutrient absorption, endocrine signaling, and immune surveillance [7]. It is structurally defined as a series of hollow organs joined in a long, muscular tube that extends from the mouth to the anus. This anatomical pathway includes the mouth, esophagus, stomach, the small intestine (which comprises the duodenum, jejunum, and ileum), the cecum, the colon (which constitutes the large intestine), the rectum, and the anal canal. [7, 8].

The primary role of the GI tract is the mechanical and chemical breakdown of consumed macronutrients into absorbable components that include monosaccharides, amino acids, and fatty acids. Following digestion, the GI tract facilitates the absorption of these nutrients along with water, electrolytes, and vitamins into the circulatory system. This absorptive function is vastly enhanced by the immense surface area of the GI tract, which is amplified by structural specializations such as folds, finger-like projections called villi, and microscopic cellular extensions known as microvilli [7, 9].

In addition to its digestive functions, the GI tract functions as a major endocrine organ. It contains specialized enteroendocrine cells within its lining. The scattered enteroendocrine cells along the epithelium sense luminal nutrients and microbial products, and release peptide hormones, including gastrin, secretin, cholecystokinin, peptide YY, and glucagon-like peptide-1. These hormones tune motility, secretion, gastric emptying, and metabolic homeostasis, and they also act on vagal afferents and central circuits that regulate appetite and energy balance [10].

Moreover, the GI tract serves a crucial role in immune defense as a major barrier between the internal milieu and the external environment. This protective function is managed by gut-associated lymphoid tissue (GALT). This immune tissue continuously monitors the contents within the GI tract, maintaining a delicate balance between tolerating beneficial gut microbiota and mounting defenses against pathogenic organisms. Therefore, the GI tract is an integrated and complex system essential for processing nutrients, regulating physiological processes, and protecting the host [11].

The human gut is not a sterile tube but a dynamic ecosystem inhabited by densely populated microorganisms, collectively known as the gut microbiota. This complex and dynamic community consists of trillions of bacteria, archaea, viruses, and fungi, which function together as a vital metabolic organ. The gut microbiome significantly extends the biochemical and physiological capabilities of the human host. It carries out vital functions that the human genome cannot perform and plays a critical role in maintaining overall health and regulating disease states [12].

A principal metabolic activity of commensal gut bacteria is the anaerobic fermentation of complex dietary carbohydrates and fibers that resist digestion in the upper GI tract. This process yields short-chain fatty acids (SCFAs) as major end products, most prominently acetate, propionate, and butyrate. These molecules are not merely metabolic waste but serve as crucial signaling compounds. They act as ligands for specific free fatty acid receptors, including GPR41 and GPR43, which are expressed on the surface of vagal afferents, epithelial cells, immune cells, and enteroendocrine cells. Through the signaling pathways, SCFAs enhance barrier function (e.g., by stimulating mucus), modulate local and systemic immunity, and influence the secretion of gut peptides. Moreover, these fatty acids can directly stimulate sensory fibers of the vagus nerve, establishing a direct neural communication channel to the brain [13, 14, 15].

The microbial metabolites, including SCFAs, secondary bile acids, and tryptophan derivatives, critically influence central nervous system (CNS) function and behavior through multiple integrated pathways. They can act through endocrine routes by entering systemic circulation and interacting with the blood-brain barrier, through immune mechanisms by modulating the production and release of cytokines, and through direct neural pathways by activating afferent vagal nerve fibers. In this manner, the gut microbiota is an essential component of the GBA, linking microbial metabolic output to host neurobiology and physiological status [16, 17, 14, 18, 19].

The intricate functions of the GI tract are regulated through a sophisticated neural network comprising the CNS, autonomic nervous system (ANS), and enteric nervous system (ENS). The CNS, consisting of the brain and spinal cord, serves as the supreme command center that integrates sensory information from the gut and coordinates complex physiological responses. The ANS provides the neural pathways connecting the CNS with peripheral organs through sympathetic and parasympathetic divisions that generally exert opposing effects on gastrointestinal function. The sympathetic division typically inhibits digestive processes during stress responses, while the parasympathetic division, particularly through the vagus nerve, promotes digestive secretions and motility at rest. Most remarkably, the

ENS represents an intrinsic nervous system embedded within the gastrointestinal wall, containing approximately 100 million neurons that can operate autonomously to control local gut functions including peristalsis, secretion, and blood flow, while maintaining constant bidirectional communication with the CNS [20].

These neural systems constitute the structural foundation of the GBA. The GBA is a bidirectional communication network that integrates neural, endocrine, immune, and microbial signaling pathways between the GI tract and the nervous system [6, 21, 22]. This sophisticated biological system operates through several parallel communication routes:

- **Neural Pathways:** The vagus nerve (Cranial Nerve X) serves as the primary neural route for gut-brain communication, containing approximately 80% afferent and 20% efferent fibers. [23]. Vagal afferent neurons, with cell bodies in the nodose ganglia, transmit a vast array of sensory information from the gut lumen to the nucleus tractus solitarius (NTS) in the brainstem. These signals convey crucial information about mechanical distension, nutrient composition, osmolarity, and local hormonal environment [24]. In turn, vagal efferent neurons, originating primarily in the dorsal motor nucleus of the vagus (DMV), carry regulatory signals from the brain to the gut, to finely tune gut motility, secretion, and inflammatory responses [25]. Spinal afferents provide complementary neural pathways, conveying nociceptive and inflammatory signals critical for visceral pain perception and protective reflexes [26, 27].

- **Endocrine Pathways:** Gut hormones released from specialized enteroendocrine cells (EECs) function as crucial signaling molecules in the GBA. The EECs express receptors that detect specific ligands such as nutrients and microbial metabolites, and then trigger the release of peptides like ghrelin, cholecystokinin (CCK), peptide YY (PYY), and glucagon-like peptide 1 (GLP-1) [28]. These hormones act both locally on vagal afferents and enteric neurons and systemically by entering the bloodstream to influence the CNS, ultimately regulating appetite, mood, and cognition [29, 30]. A central endocrine com-

ponent of the GBA is the hypothalamic-pituitary-adrenal (HPA) axis, which is the primary stress response system of the body. Gut-derived signals and microbial metabolites can directly modulate HPA axis activity. [31, 32].

- **Immune Pathways:** The GI immune system acts as a critical communication interface within the GBA. Immune activation begins when dendritic cells and macrophages detect microbial signals, triggering the release of cytokines including interleukin 1-β (IL 1-β), interleukin-6 (IL-6), and tumor necrosis factor-α (TNF-α) [33, 34]. These molecular alarm signals reach the brain through three primary routes. The first is the humoral pathway, where cytokines enter the blood circulation to access specialized brain regions lacking a complete blood-brain barrier. The second, the neural pathway, involves the direct activation of afferent vagal and spinal nerves by these cytokines. Finally, the cellular pathway involves immune cell trafficking from the periphery to brain regions [35]. These signals significantly affect neuroinflammation, neurogenesis, and synaptic plasticity [36, 37].

- **Microbial Pathways:** Gut microbes influence brain function through multiple mechanisms, including production of neurotransmitters (GABA, serotonin, dopamine), modulation of tryptophan metabolism, and generation of microbial metabolites (SCFAs, secondary bile acids) that enter circulation and affect brain function. The vagus nerve appears particularly important for mediating microbial effects on brain and behavior [17, 38].

Disruptions in GBA signaling have been implicated in numerous pathological conditions. Functional GI disorders such as irritable bowel syndrome (IBS) and functional dyspepsia involve altered gut-brain communication manifested as visceral hypersensitivity and motility disturbances [39]. Neurological and psychiatric disorders, including depression, anxiety, autism spectrum disorder (ASD), and Parkinson's disease, have been associated with gut microbial alterations and impaired gut-brain signaling [40]. Metabolic disorders such as obesity and type 2 diabetes involve

disrupted energy homeostasis signaling through the GBA. Inflammatory conditions, including inflammatory bowel disease (IBD), demonstrate complex interactions between gut inflammation, microbial dysbiosis, and neural signaling pathways [41, 42].

Despite significant advances in understanding individual components of the GBA, conventional approaches encounter significant limitations in deciphering the dynamic, multi-scale interactions within this complex communication system. The fundamental challenges include:

- **Temporal Dynamics** A primary challenge lies in the vast spectrum of temporal scales at which GBA communication occurs. Signaling events range from millisecond neurotransmission and minute-by-minute hormone release to daily circadian fluctuations and long-term developmental changes in the gut microbiota. Conventional methods often provide static snapshots that cannot capture these dynamic interactions.

- **Spatial Complexity** The GBA is hierarchically organized across multiple spatial dimensions, from nanoscale molecular interactions (e.g., metabolite-receptor binding) and microscale cellular synapses to macroscale organ system physiology and organism-level behavior. This multi-scale organization generates emergent properties that cannot be understood through the isolated study of individual components, requiring integrated analytical approaches.

- **System Nonlinearity:** The GBA exhibits complex nonlinear behaviors including feedback loops, threshold responses, and adaptivity. These characteristics make system behavior difficult to understand and predict.

- **Individual Variability:** Each individual has a unique microbiota composition, neural wiring, and physiological responses. This profound individuality creates a significant challenge for conventional research methods. By relying on population averages, these studies generate a generalized physiological model that does not account for the specific signaling characteristics of any single person.

These limitations underscore the necessity for novel theoretical and computational frameworks to integrate multi-omics data, multi-scale system dynamics, and predict emergent network behaviors. Traditional communication paradigms, which are developed for electromagnetic wave propagation through engineered channels, fundamentally fail to capture the essential characteristics of biological signaling. Communication within the GBA operates through stochastic molecular diffusion, nonlinear reaction kinetics, and complex biochemical interactions within heterogeneous environments. To address these challenges, we adopt MC as the analytical backbone for modeling information generation, propagation, distortion, and integration across neural, endocrine, immune, and microbial routes of the GBA network.

This thesis is dedicated to the development of a comprehensive and quantitative framework for the GBA. It addresses the fundamental challenge of understanding the GBA by reframing it not merely as a biological system, but as a complex, multi-scale molecular communication network. To this end, MC and information theory are established as the primary analytical frameworks for modeling and evaluating the information flow within this communication system. We develop theoretical models that explicitly capture the stochastic, nonlinear, and feedback-driven nature of intra-body signaling.

The overarching objective of this research is to establish a formal methodology that translates the biological mechanisms of the GBA into quantifiable, communication-theoretic principles. This approach involves identifying the core components of the system, including transmitters, channels, receivers, and noise sources, and then applying performance metrics from information theory. Metrics like mutual information and channel capacity are used to rigorously evaluate the efficiency and robustness of signaling within the GBA. The ultimate goal is to provide a rigorous, analytical foundation for studying the GBA, to enable a more precise and predictive understanding of its complex signaling dynamics.

This objective is driven by several core motivations:

- *Develop a multi-scale modeling framework* that bridges the gap between molecular-binding events (nanoscale), cellular activation (microscale), and organ-level

physiological responses (macroscale).

- *Investigate and incorporate feedback mechanisms* to move beyond one-way communication models and toward a realistic, closed-loop representation of the GBA, which is crucial for understanding homeostasis.

- *Leverage information-theoretic metrics* such as mutual information, delay, and capacity to quantitatively assess the efficiency, robustness, and failure modes of gut-brain signaling in health and disease conditions.

- And to pave the way for IoBNT applications by creating validated models that can eventually inform the design of bio-compatible nano-devices for monitoring and modulating the GBA.

This vision is realized through a structured progression of theoretical and computational models, each chapter addressing a different layer of the communication problem:

- **Chapter 1** introduces an MC-based channel model for the propagation of microbial molecules (e.g., p-cresol) from the gut to the brain, establishing a baseline for analyzing this specific communication channel [43].

- **Chapter 2** presents an end-to-end model for SCFA-driven vagus nerve signaling. The proposed model integrates molecular receptor kinetics, intracellular calcium dynamics, and Hodgkin-Huxley neuronal models to map a gut-derived molecular signal to a neural output, and quantifies the channel performance with mutual information and delay [44].

- **Chapter 3** culminates this effort by developing a novel, end-to-end model for the bidirectional GBA. It integrates the hypothalamic-pituitary-adrenal (HPA) axis, immune signaling, and gut barrier integrity into a closed-loop feedback system. This model is used to simulate the transition from health to chronic stress pathology, identify dynamical tipping points, and perform

a frequency-domain analysis to quantify the information-theoretic capacity of the GBA as a communication channel [45].

Collectively, this work provides a communication-theoretic framework to advance understanding of the GBA. By establishing a rigorous theoretical foundation based on MC principles, we offer a principled methodology to analyze how information is generated, propagated, distorted, and decoded across coupled neural, endocrine, and immune routes. By turning biological mechanisms into explicit channel models with noise, memory, and feedback, the thesis enables systematic evaluation of signaling efficiency, latency, and robustness and informs targeted diagnostic protocols and therapeutic strategies. These insights lay the groundwork for interventions that restore healthy communication patterns within the GBA and for future Internet of Bio-Nano Things (IoBNT) devices that safely monitor and modulate these pathways.

Chapter 1

MODELING OF MICROBIAL MOLECULE TRANSMISSION IN THE GUT-BRAIN AXIS

1.1 Introduction

Molecular communication (MC) is a bio-inspired communication technique that aims to mimic biological and chemical communication mechanisms and provide a theoretical framework for molecular-level processes from an information and communication theoretical (ICT) perspective [1]. Understanding molecular signaling processes existing in nature via MC enables envisioning the Internet of Bio-Nano Things (IoBNT) technology, which also is a concept central to the long-term vision of this work. This IoBNT technology employs seamless communication between the natural and artificial nano-biological functional devices integrated into the Internet infrastructure [46, 47]. Revealing the fundamentals of molecular nanonetworks from an ICT perspective also enables many of the foreseen IoBNT applications that further provide novel and effective ICT-based diagnosis and treatment techniques for human diseases.

In multicellular organisms like humans, cells have evolved various signaling mechanisms to accomplish the transmission of important biological information. From single cells to complex biological systems, each biological nanonetwork inside the human body is connected and communicates using molecular interactions and action potentials [4]. For instance, distinct signaling channels connect nerve cells in the human central nervous system (CNS) to bacteria in the gastrointestinal (GI) tract, and any failure in these communication networks will deteriorate human health and lead to diseases [48]. This intricate, bidirectional communication network is called the gut-brain axis (GBA). The GBA integrates signaling from the gut and its vast

microbial community with the brain, influencing a wide range of physiological and psychological processes through neural, endocrine, and immune pathways [49].

Disruptions in the signaling mechanism of this vital axis have been implicated in numerous conditions, including Autism Spectrum Disorder (ASD) [50]. Autism is a spectrum disorder that refers to heterogeneous neurodevelopmental disorders caused by differences in the brain and failures in various communication channels, such as the dopamine pathway and intracellular signaling mechanisms in neurons [51]. Social communication deficits and repetitive and unusual sensory-motor behaviors are associated with an ASD, and children with ASD have difficulties communicating with other people. These symptoms of autism can be seen in the range from mild to severe, so that autism is defined as a spectrum disorder [52].

Apart from the main symptoms, most people with ASD suffer from a number of co-occurring physical and mental health conditions. Anxiety and GI symptoms are common comorbidities associated with ASD that can lead to depression, chronic constipation, food intolerance, abdominal pain, and diarrhea are gastrointestinal problems [53]. The gut microbiome affects the development of the brain and behaviors via the gut-brain axis, so abnormalities of gut microbiota are also associated with ASD or common mood disorders [54].

Alterations in gut microbiota composition result in gastrointestinal and neurobehavioural problems in people, especially children with ASD [55]. Mainly, alternations in *Clostridia*, *Bacterioides*, and *Lachnospiraceae* compositions induce the production of several toxic side products, such as indolpyruvate, serotonin (5-HT), 4-ethylphenylsulfate (4-EPS), and p-cresol [56, 57] while reducing expression of gastrointestinal tight junction proteins. Decreased level of gastrointestinal tight junction proteins causes increasing gut permeability. Increased gut permeability further leads to leakage of toxic molecules, such as 4-EPS and/or p-cresol, into blood circulation [58], [59]. Hence, the accumulation of p-cresol molecules has been suggested as a biomarker for ASD in humans [60].

The gut bacteria can synthesize p-cresol via two distinct pathways, producing synthetic enzymes humans cannot express. It has been shown that several bacterial

strains, such as *Clostridium* and *Ruminococcus*, which are known to produce p-cresol, overgrow in the gut flora of patients with ASD [61]. *Clostridium difficile* expresses p-hydroxyphenylacetate (p-HPA) decarboxylase and produces p-cresol through fermentation of tyrosine [62]. *Pseudomonas stutzeri* and *Pseudomonas mendocina* express toluene monooxygenase, and thus, produce p-cresol from toluene [63, 64].

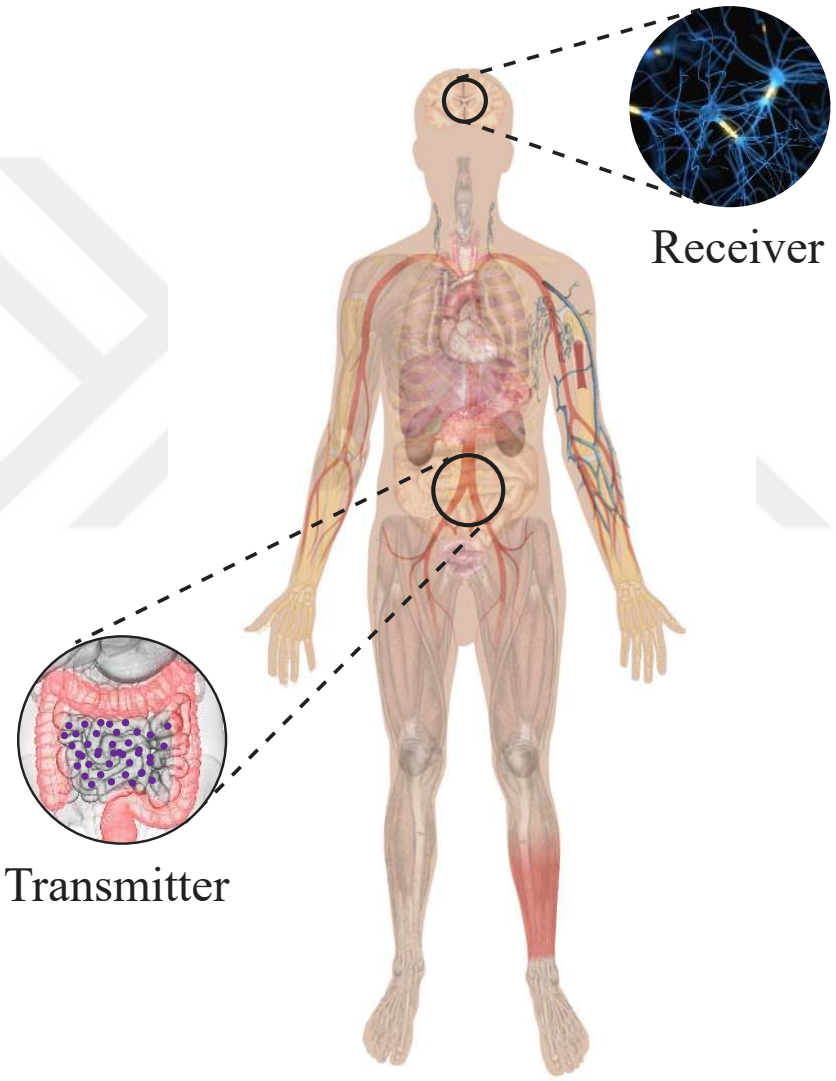

Figure 1.1: Biological Representation of MC System

Although two distinct pathways are involved in p-cresol production, the main pathway occurs through the fermentation of tyrosine and phenylalanine, which are the amino acids generated from dietary proteins. These amino acids are first metabo-

lized to 4-hydroxyphenylacetic acid and then converted to the p-cresol by decarboxylation of the 4-hydroxyphenylacetic acid molecule. Produced p-cresol molecules pass through the epithelial gut barrier via diffusion and enter the bloodstream [65, 66].

P-cresol molecules propagate through the circulatory system and cross the blood-brain barrier (BBB) and irreversibly inactivate the Dopamine β-Hydroxylase (DBH) [67]. Inactivation of DBH causes excess dopamine and a reduced level of norepinephrine in the CNS. An excessive amount of dopamine damages the neurons [68] which further leads to autistic-like behaviors such as social deficits and stereotyped behaviors [69, 70].

Uncovering the fundamental principles and precise mechanisms for signaling across the microbiota-gut-brain axis in ASD from an ICT perspective will pave the way for outstanding applications in the IoE domain, e.g., early diagnosis of ASD, continuous health monitoring with intrabody nanosensor networks, and ICT-based diagnosis and treatment techniques. To achieve this ambitious goal, this chapter takes a foundational first step by establishing an MC-based channel model for a single, clinically relevant signaling pathway within the GBA. The main focus of this chapter is to develop a communication-theoretic model for p-cresol propagation from the gut to the brain, characterize its impulse response, and analyze the impact of key physiological parameters on signal transmission.

The remainder of this chapter is organized as follows. Section II introduces the MC-based channel model for this designated signaling network and derives its impulse response. Section III presents numerical results to validate the model and explore its parametric sensitivity. Finally, Section IV concludes the chapter and outlines how these findings serve as a basis for the more complex models developed subsequently in this thesis.

1.2 Molecular Communication System Model

The gut-brain axis is characterized by an intercommunication of the aforementioned natural communication routes detailed in Sections I. Here, we investigate the molecular communication-based modeling of the p-cresol signaling in ASD through the

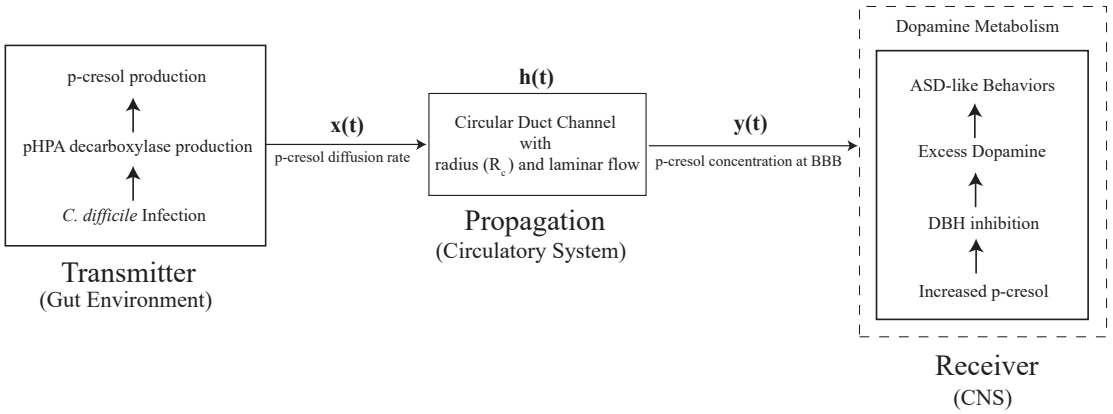

Figure 1.2: Scheme of the MC channel model for p-cresol signaling in ASD.

gut-brain axis. After the increase in *Clostridium difficile* species in the gut environment, p-cresol concentration increases, and these molecules are released into the bloodstream. In this section, we introduce an MC-based model for this communication scheme. First, we identify four major communication elements, which are the transmitter, signal channel, and receiver as follows:

- *Transmitter:* The transmitter represents the gut environment and assumed as volume transmitters.
- *Signal:* The concentration of p-cresol molecules is represented as the signal.
- *Channel:* The gut-brain axis, indicating the gut environment to CNS through the bloodstream, is denoted as the channel.
- *Receiver:* The receiver represents the dopaminergic neuron cell.

Transmission, propagation, and reception are three main processes that underline the communication mechanism of p-cresol molecules throughout the gut-brain axis. In the proposed work, p-cresol molecules, i.e., signaling molecules, are produced in the human gut environment and transmitted to the bloodstream by freely diffusing across the leaky gut epithelium. To achieve a realistic model, the gut environment is represented as a volume transmitter that the p-cresol molecules are generated

instantaneously, and the surface of the transmitter is transparent and does not impede the diffusion of signal molecules [71]. Volume transmitter models for the gut environment enables neglecting the effect of particle generation and the impact of the release mechanism into the bloodstream.

The transmitted p-cresol molecules propagate through the bloodstream under the influence of advection and diffusion. The propagation of emitted signal is guided partly by the blood velocity and pressure inside the channel. The propagated signal through the brain capillaries [72], is received by BBB for further signaling process.

In this work, we propose an approximate communication model built upon the advection-diffusion equation. Here, c(d,t) denotes normalized concentration of p-cresol molecules that $dVc(d,t)$ gives average fraction of molecules within the differential volume dV at coordinate d and time t, i.e.,

$$\frac{\partial c(d,t)}{\partial t} = D\nabla^2 c(d,t) - \nabla.(\upsilon(d,t)c(d,t)) \tag{1.1}$$

where D is the diffusion coefficient, and ∇ is the Nabla operator. We assume that the p-cresol molecules freely diffuse from the intestinal barrier and are released into the blood vessel uniformly at $z = 0$. After propagation through the circulatory system, assumed as a circular duct channel with radius R_c and laminar flow, p-cresol molecules enter the brain via diffusing directly through the BBB. Inside the brain, p-cresol molecules bind the enzyme and inhibit enzyme activity.

The propagation channel, e.g., blood vessel, is considered as a straight impermeable cylindrical duct with radius R_c that can be described by cylindrical coordinates $[r, \psi, z]$, where $0 \leq r \leq R_c$, $0 \leq \psi \leq 2\pi$ and $-\infty \leq z \leq \infty$. The duct is assumed to be filled with a fluid of viscosity η, and steady flow occurs through the z-direction with flow velocity, $\upsilon(r)$, which is defined as $\upsilon(r) = \left[0, 0, \upsilon_0\left(1 - \frac{r^2}{R_c^2}\right)\right]$.

This velocity vector is used to model flow in blood vessels and is known as the Poiseuille flow profile [73]. Since the propagation process occurs in an MC environment, the advection-diffusion equation in (1) can be simplified as,

$$\frac{\partial c(d,t)}{\partial t} = D\nabla^2 c(d,t) - \upsilon(d)\frac{\partial c(d,t)}{\partial z} \tag{1.2}$$

Due to its Newtonian fluid nature, the blood flow-mediated propagation process can be modeled as a flow-dominated regime inside a circular duct. In the flow-dominant regime, flow-based transport is considered, and it is assumed that particles are not diffused inside the duct [73]. For flow dominant regime, spatial distribution of concentration, $c(r,t)$ and flow velocity $\upsilon(r)$ is defined as

$$\begin{aligned} c(r,t) &= \frac{1}{\pi R_c^2}\delta(z - \upsilon(r)t) \\ \upsilon(r) &= 2\upsilon^{eff}(1 - \frac{r^2}{R_c^2}) \end{aligned} \tag{1.3}$$

Under the assumption of one-dimensional diffusion with constant drift for the blood flow model in which no interaction occurs between particles, the impulse response of the modeled MC channel is stated as,

$$h(t) = \int_{V_{Rx}} c(r,t)dV_{Rx} \tag{1.4}$$

where V_{Rx} is the volume of Rx, which is assumed as a passive receiver, and υ^{eff} denotes the mean velocity in the propagation channel, which is a function of applied pressure. υ^{eff} is defined to model laminar flow in a bounded environment since the flow velocity increases toward the center of a tube for viscous fluid, and υ^{eff} gives a good approximation for flow velocity.

The dimension of the passive receiver is defined as l_r, l_ψ, l_z coordinated at $[R_c - l_r \leq r_{Rx}\ R_c, |\psi_{Rx}| \leq l_\psi/2, |z_{Rx} - d_z| \leq l_z/2]$. The impulse response of the flow dominant regime is derived by integrating (4) over V_{Rx}, and the result is obtained as [73],

$$h(t) = \begin{cases} 0, & t \leq t_1 \\ \left[\dfrac{l_\psi(2R_c l_r - l_r^2)}{2\pi R_c^2} - \dfrac{2l_\psi d_z - l_\psi l_z}{8\pi \upsilon^{eff} t}\right], & t_1 < t < t_2 \\ \dfrac{l_\psi l_z}{4\pi \upsilon^{eff} t}, & t \geq t_2 \end{cases} \tag{1.5}$$

where t_1 and t_2 are defined as

$$\begin{aligned} t_1 &= \frac{d_z - l_z/2}{2\upsilon^{eff}(1-(1-l_r/R_c)^2)} \\ t_2 &= \frac{d_z + l_z/2}{2\upsilon^{eff}(1-(1-l_r/R_c)^2)} \end{aligned} \tag{1.6}$$

In our system model for p-cresol signaling, the concentration of p-cresol molecules released from Tx is defined as $N_{p,Tx}$, the expected concentration of signaling molecules at the Rx, $N_{p,Rx}$, calculated in (7) and (8) by using the observation probability of p-cresol molecules in the brain.

$$N_{p,Rx} = N_{p,Tx} h(t) \tag{1.7}$$

$$N_{p,Rx} = \begin{cases} 0, & t \leq t_1 \\ N_{p,Tx}\left[\frac{l_\psi(2R_c l_r - l_r^2)}{2\pi R_c^2} - \frac{2l_\psi d_z - l_\psi l_z}{8\pi \upsilon^{eff} t}\right], & t_1 < t < t_2 \\ N_{p,Tx}\frac{l_\psi l_z}{4\pi \upsilon^{eff} t}, & t \geq t_2 \end{cases} \tag{1.8}$$

The properties of the introduced MC system model are investigated in Section III by performing numerical analysis.

Table 1.1: List of Parameters used in Analysis

Parameter	**Value**	**Units**	**Reference**
R_c	4	μm	[74]
l_r	0.2	μm	[75]
l_ψ	$\pi/2$		
l_z	7.2	μm	[75]
λ	$6.0900x10^3$	$M^{-1}s^{-1}$	[76]
v_{eff}	1	$\mathrm{mm}s^{-1}$	
d_z	200	μm	

1.3 Numerical Evaluation

The derived analytical results are used to perform numerical simulations for both system impulse response and enzyme kinematics. The impulse response of the proposed system is demonstrated in Fig. 1.3(**a**) with respect to the determined observation probability (5) with system parameters provided in Table 1.1.

Fig. 1.3(**b**) shows that transmitted p-cresol molecules reach the BBB in a very short time since it propagates to Rx with blood flow assistance. Blood flow-directed

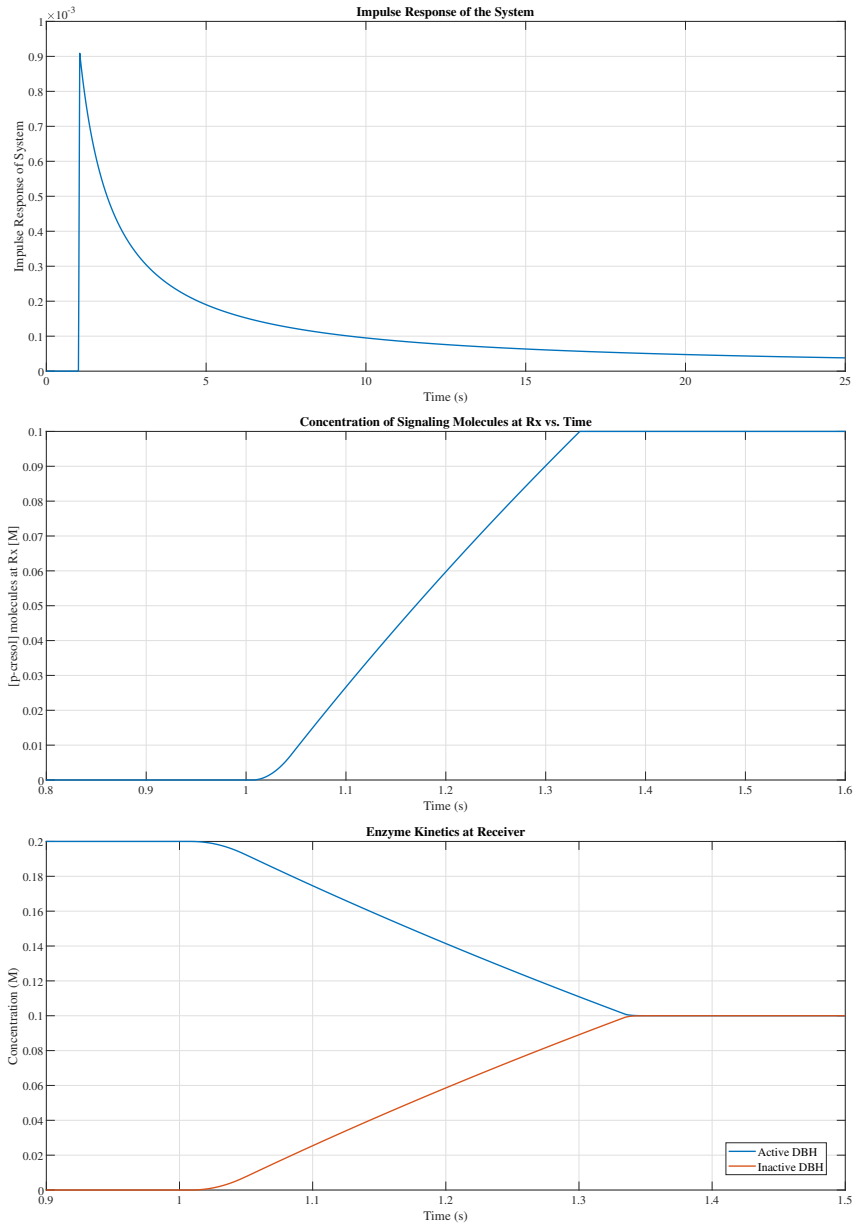

Figure 1.3: **(a)** Impulse Response for MC System. **(b)** Concentration of Signaling Molecule at Rx. **(c)** Enzyme Kinetics at Rx.

propagation decreases response time, and p-cresol concentration inside the brain increases within a short period.

After the propagation process, received signal molecules bind the active DBH enzymes with association rate $\lambda = 6.09x10^3$ M^{-1} sec^{-1} and inactivate DBH enzymes

within a very short period ($\sim$ 1 sec) since DBH has high affinity towards p-cresol molecules compared with dopamine molecules. For simulation enzymatic reaction inside Rx, the concentration of transmitted p-cresol is specified as $N_{p,Tx} = 0.1$ M and the initial number of DBH enzymes (unbound, active) is defined as $N_{\text{DBH}} = 0.2$ M. Further numerical simulations are performed to show that received p-cresol molecules directly inhibit the DBH enzyme by binding the enzyme with high affinity. As shown in Fig. 1.3**(c)**, all received molecules bind the free DBH enzymes in a short time ($\sim$ 0.3 sec) and act as DBH inhibitors. Inhibiting DBH activity further leads to excess dopamine levels inside the brain since they cannot be converted to norepinephrine by DBH. Excess dopamine levels in the brain induce ASD-like behaviors, e.g., repetitive behaviors and social deficits.

According to results of numerical analysis in Fig. 1.3, it can be concluded that increased p-cresol concentration inside the gut environment results in enhanced system response. It means that changing bacteria composition that produces p-cresol directly affects the brain chemistry of people with ASD. This further indicates that controlling the gut microbiota can improve people's health and life standards.

To emphasize the effect of each parameter on the system impulse response and further reception process, numerical analysis is performed for changing conditions as shown in Fig. 1.4-1.6. For each case, only one parameter is changed, and the effect of that specific parameter is investigated. In the first case, (Fig. 1.4), the radius of the blood vessel is alternated and specified as $[3\mu m, 4\mu m, 5\mu m]$. Increasing the diameter of the blood vessel results in decreased observation probability of signal molecules at Rx. For higher vessel diameters, signal molecules propagate slower through the channel, and the system's response time decreases. This results delay in the enzymatic reaction process inside the Rx, as shown in Fig. 1.4 (bottom).

In the second case, (Fig. 1.5), the distance between Tx-Rx is alternated and specified as $[20\mu m, 200\mu m, 2mm]$. Increasing the distance between Tx-Rx (d_z) dramatically affects the system's impulse response and prolongs the response time. Since signaling molecules arrive at Rx within an extended time period for increasing d_z value, enzymatic reactions are delayed inside Rx. For instance, for $d_z = 20\mu m$, all

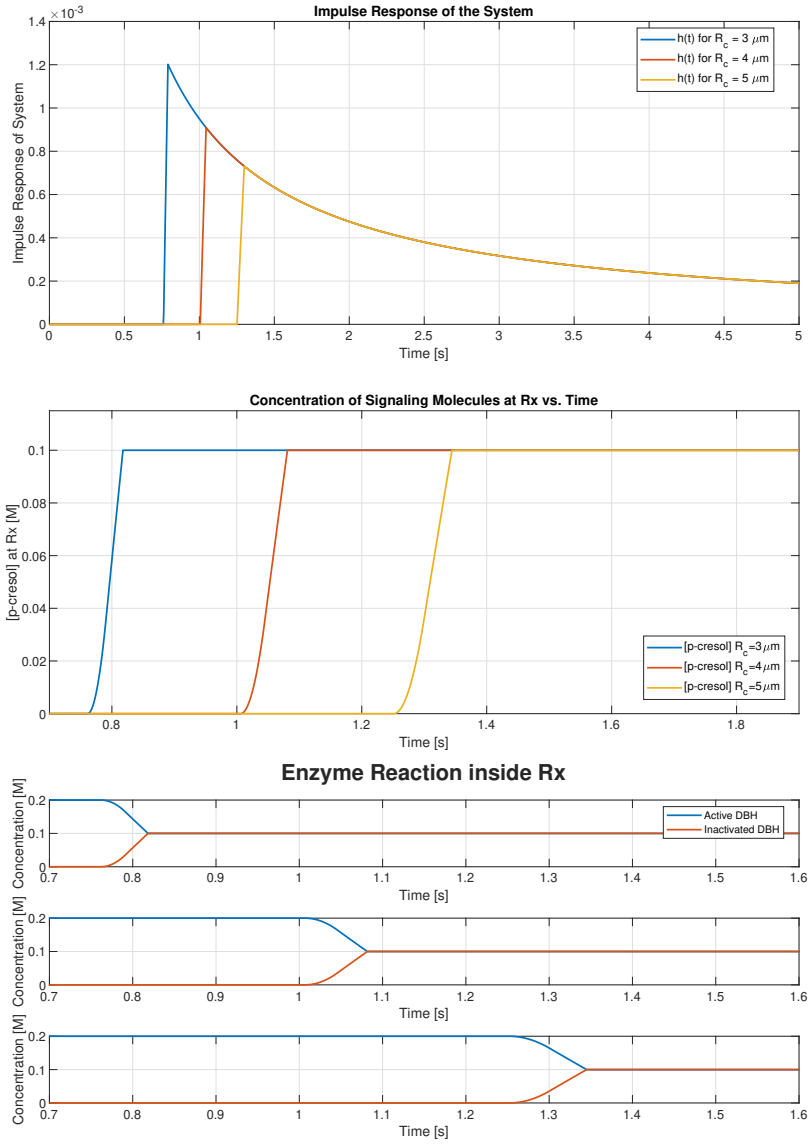

Figure 1.4: Numerical analysis for MC system with respect to changing blood vessel diameter.

released p-cresol molecules received to Rx within 0.1 sec, and enzymatic reactions occur very fast compared to case, $d_z = 2mm$.

For investigating the effects of Rx's physical properties on the system, l_r is varied as $[0.15\mu m, 0.2\mu m, 0.25\mu m]$ since the size of the receiver dendrite can change. As shown in Fig. 1.6, the observation probability of signal molecules at Rx increases while the Rx dimension increases. This further decreases the response time of the

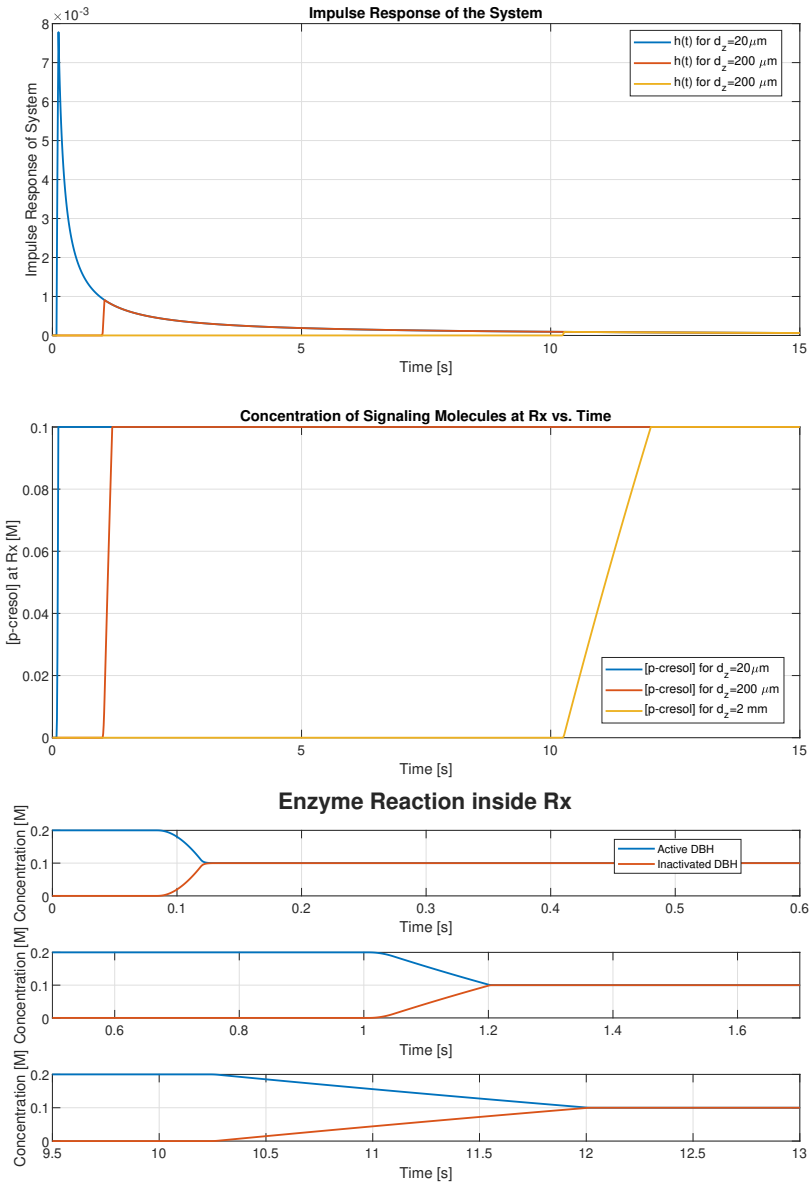

Figure 1.5: Numerical analysis for MC system with respect to changing distance between Tx & Rx.

system and accelerates the further signaling processes inside Rx. Small changes in Rx dimensions directly alter the system impulse response shown in Fig. 1.6.

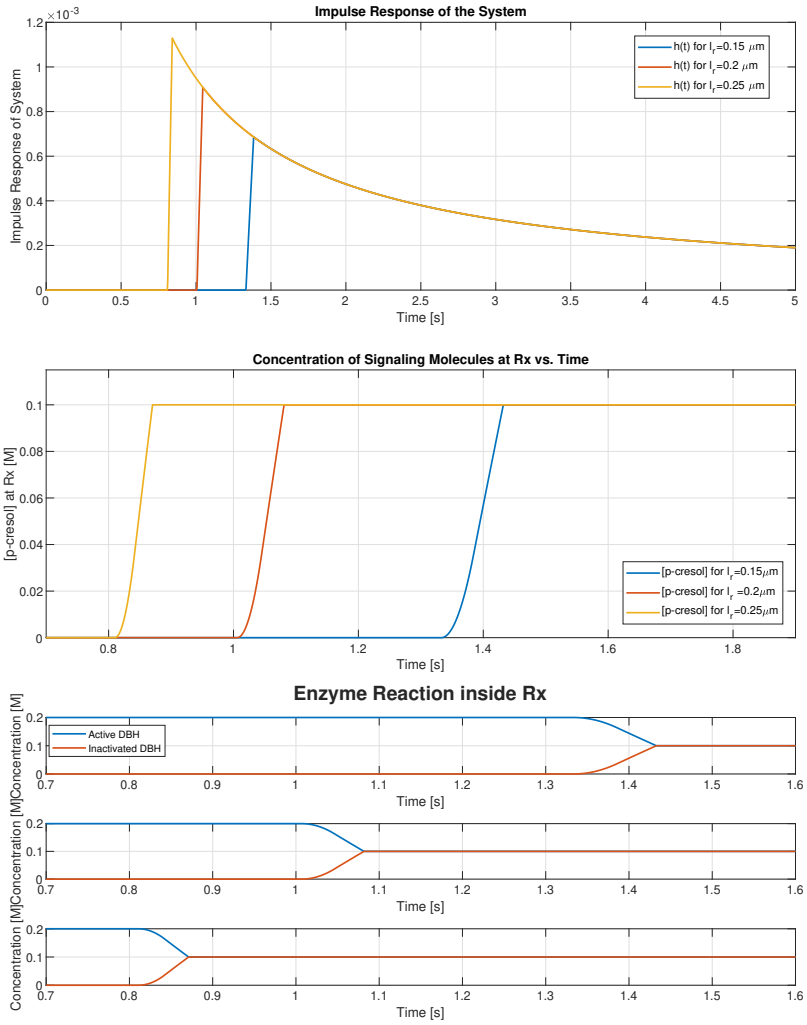

Figure 1.6: Numerical analysis for MC system with respect to changing Rx dimension.

1.4 Conclusion

This chapter demonstrated that specific gut metabolites can play a direct role in the pathogenesis of neurological conditions like Autism Spectrum Disorder (ASD). Specifically, the work focused on p-cresol, a toxic metabolite produced by gut microbiota that is reported at elevated levels in children with autism. We showed that gut dysbiosis leads to an overproduction of this compound, which then propagates through the bloodstream to the brain. Upon reaching the central nervous system, the p-cresol molecules inhibit the Dopamine β-Hydroxylase (DBH) enzymes, and

ultimately disrupt dopamine metabolism in a way that contributes to abnormal behaviors associated with ASD.

To quantify this communication process, we proposed an MC-based channel model for p-cresol signaling using a flow-dominant transmission protocol. The input-output relationship between elevated p-cresol level and its neurological impact was characterized using communication engineering tools. Numerical analysis was performed to validate the derived mathematical models and reveal how the channel's physical properties, such as blood vessel dimensions and transmission distance, affect the system response.

Ultimately, this chapter has developed a MC-based channel model for p-cresol signaling in the gut–brain axis, quantitatively linking gut-microbial production to neural outcomes. By characterizing the impulse response and parametric dependencies of this channel, we have laid the necessary groundwork for the subsequent chapters. The principles and methods utilized here will be expanded upon to analyze more complex end-to-end signaling cascades and the bidirectional, feedback-controlled network that constitutes the gut-brain axis.

Chapter 2

END-TO-END MOLECULAR-TO-NEURAL SIGNALING IN THE GUT-BRAIN AXIS

2.1 Introduction

Molecular communication (MC) is a bio-inspired communication paradigm in which molecules serve as information carriers, facilitating communication among biological and artificial nanomachines [1, 77]. Unlike conventional electromagnetic communication systems, MC relies on biochemical interactions and diffusion processes to transfer information, mimicking natural biological communication mechanisms such as neurotransmission, immune responses, and hormonal signaling. This paradigm naturally supports emerging biomedical applications, including the Internet of Bio-Nano Things (IoBNT), enabling innovative solutions in healthcare, diagnostics, and personalized medicine [78, 47].

One of the most promising applications of MC is understanding complex signaling mechanisms in biological systems. A particularly compelling example is the gut-brain axis (GBA), a highly intricate network that connects the gastrointestinal (GI) tract with the central nervous system (CNS) via dynamic molecular signaling processes. In this context, electrical and molecular signals are interconverted and propagated through natural communication pathways, including neural (vagal), endocrine (hormonal), immune, and metabolic routes. Conventional communication paradigms do not adequately represent the spatial, temporal, and stochastic characteristics of these biochemical interactions. Traditional communication methods employ electromagnetic waves as information carriers, assuming continuous wave or packet transmission through linear channels with additive noise and deterministic error rates. These frameworks cannot represent diffusion-based transport, the dis-

crete nature of molecular particles, or the reaction kinetics that are fundamental to molecular signaling [1]. By applying MC principles, this work aims to model and analyze a crucial gut-to-brain signaling pathway within the GBA, offering insights into the underlying molecular communication dynamics.

Existing studies have explored different aspects of GBA; however, exploring the GBA through the perspective of MC is a relatively new and developing field, with only a few pioneering studies addressing the complex communication mechanisms involved. For instance, [79] introduced the Microbiome-Gut-Brain Axis (MGBA) as a biomolecular communication network, providing a foundation for integrating wearable and implantable IoBNT devices while presenting infrastructural challenges in minimally invasive MC and electrical signal transmission through a comprehensive network perspective. Nevertheless, prior studies, including electrophysiological recordings and systems-level frameworks, cannot often fully capture essential features of biological signaling, such as molecular noise, spatial diffusion, and temporal delays. In contrast, MC provides a holistic and mechanistic modeling framework that inherently incorporates these dynamics via advection-diffusion and ligand-receptor interactions, making it a suitable methodology for quantitatively analyzing Short-Chain Fatty Acid (SCFA)-driven vagus nerve signaling within the GBA.

In our previous study [43], we delved into the foundational aspects of MC within the GBA, establishing a basis for understanding how molecular signals regulate complex physiological interactions. There, we developed an MC-based model specifically for p-cresol, providing a comprehensive analysis of its propagation mechanisms within the GBA. By characterizing the impulse response of the MC channel and performing extensive numerical simulations, valuable insights were obtained into how variations in system parameters, such as transmitter-receiver distances and receiver dimensions, influence p-cresol signaling in autism spectrum disorder (ASD). These findings enhance understanding of the molecular mechanisms underlying ASD and demonstrate the potential of applying communication theoretical frameworks to unravel biological processes through the GBA.

Expanding the theoretical foundations of MC in the GBA, [80] introduces the

concept of a Molecular Quantum (MolQ) communication channel at the synapse, modeling neurotransmitter diffusion processes. Although their approach provided significant insights into synaptic communication dynamics, it did not address upstream molecular signaling events such as gut microbial metabolite interactions or intracellular signaling cascades triggered by gut-derived signals.

These pioneering studies collectively establish the foundation for understanding the GBA through MC frameworks, demonstrating the feasibility and potential benefits of applying advanced communication theories to biological systems. Despite these advancements, the field remains in its infancy, with many biological signaling mechanisms within the GBA yet to be fully elucidated. Motivated by this, this chapter introduces a comprehensive MC-based model explicitly examining SCFA-mediated gut-to-brain signaling via the vagus nerve, representing the first investigation of this pathway from an MC perspective. The developed model integrates receptor binding kinetics, intracellular signaling cascades, and neuronal activity, providing a systematic analysis of signaling efficiency and reliability through mutual information and delay metrics. Thus, in contrast to previous work focusing on general network frameworks [79], specific metabolites such as p-cresol [43], or synaptic neurotransmitter dynamics [80], our approach explicitly integrates upstream molecular events with downstream neural signaling processes, providing a more comprehensive representation of SCFA-driven vagus nerve signaling within the GBA. By conceptualizing this pathway as a communication channel, the study aims to:

- Model SCFA-dependent receptor binding kinetics, capturing how ligand concentration influences receptor activation and neuronal response.

- Describe the action potential generation and propagation process along the vagus nerve, including noise factors that may influence signal fidelity.

- Analyze neurotransmitter release dynamics in the nucleus tractus solitarius (NTS), linking the firing rate from vagal afferents to downstream signaling in the brain.

- Conduct an information-theoretic analysis of the pathway, evaluating metrics such as mutual information and delay resilience.

The rest of the chapter is organized as follows. Section 2.2 presents a comprehensive literature review providing the physiological background for GBA and SCFA-mediated signaling. Section 3.2 introduces the system model, detailing the SCFA-driven vagus nerve signaling mechanisms within the GBA. Section 3.3 presents the theoretical analysis and simulations, where the proposed MC framework is evaluated using information-theoretic metrics such as mutual information and delay. Section 3.4 discusses the simulation results, highlighting the impact of SCFA-induced G-protein activation rates on communication efficiency and signaling delays. Finally, Section 3.5 concludes the chapter and suggests directions for future research.

2.2 Literature Review

The GBA facilitates information transfer through multiple physiological routes, including neural, endocrine, immune, and metabolic pathways [6]. Among these pathways, neural signaling, particularly mediated by the vagus nerve, provides rapid and direct communication between gut microbiota-derived signals and the CNS. This relationship is depicted in Figure 2.1. Focusing specifically on neural pathways allows for a detailed exploration of how precise molecular interactions can trigger immediate physiological responses, which is essential for understanding the modulation of CNS activity by gut-derived signals. The vagus nerve provides a well-established biological system for MC-based modeling. Its characterized molecular signaling mechanisms, continuous anatomy, and defined physiological outputs make it appropriate for end-to-end communication analysis.

As a major parasympathetic nerve, the vagus nerve (*cranial nerve X*), plays a central role in the GBA by transmitting sensory signals between the gut and the brain. Originating in the medulla oblongata, the vagus nerve extends extensively through the neck, thorax, and abdomen, earning the nickname "wanderer nerve" due to its widespread innervation [81, 82]. Its sensory fibers, known as vagal afferents,

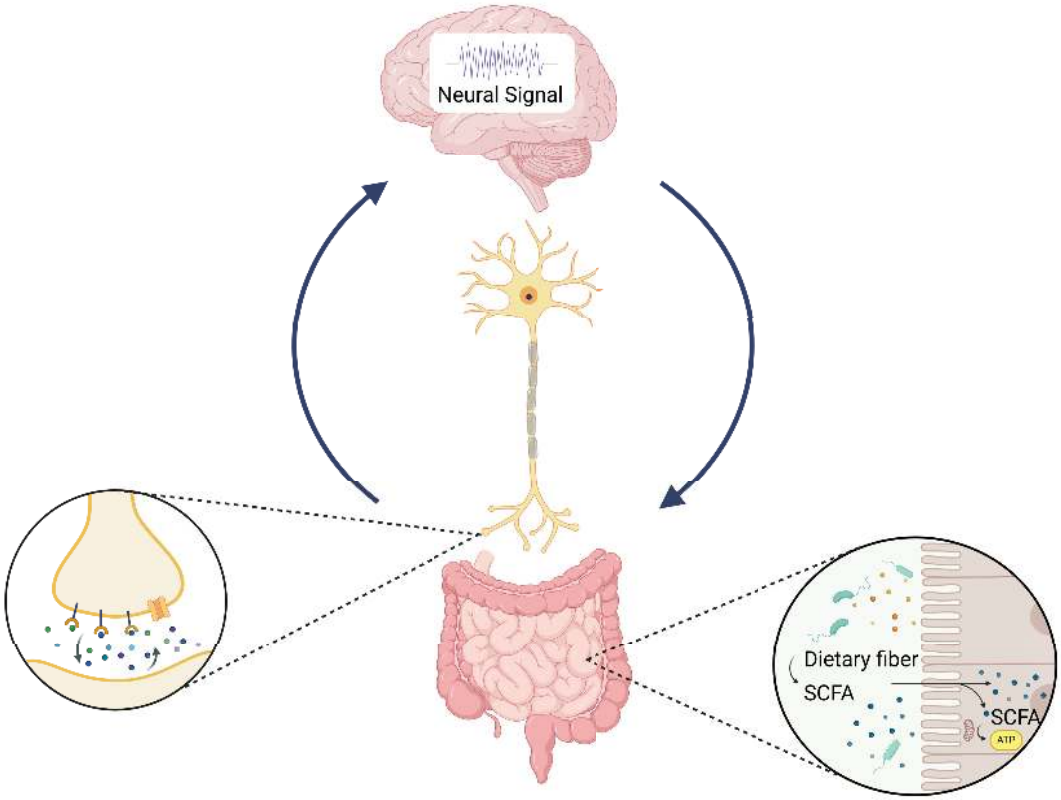

Figure 2.1: Biological Representation of MC System (Created in https://BioRender.com).

arise from the nodose ganglion and innervate the gastrointestinal mucosa, functioning as key chemosensors of the luminal environment [83]. Vagal afferents contain specialized receptors sensitive to a wide range of gut-derived signals, including hormones, nutrients, and microbial metabolites such as SCFAs [23, 84], enabling the detection and transmission of gut-derived molecular information to the NTS in the brainstem, where it integrates with higher-order brain functions [24, 85].

SCFAs, primarily acetate, propionate, and butyrate, are metabolic byproducts produced by gut microbiota through the fermentation of dietary fibers. Beyond their role in energy metabolism and gut homeostasis, SCFAs also act as signaling molecules mediating communication from the gut to the brain via immune, endocrine, and neural pathways [86, 87].

In the neural pathway, SCFAs bind to G-protein-coupled receptors (GPR41/FFAR3)

on vagal afferent neurons, provoking neuronal signals that propagate along the vagus nerve to the brain. This binding triggers intracellular signaling cascades that lead to calcium-mediated membrane depolarization, action potential generation, and ultimately neurotransmitter release at the NTS [13, 88, 23]. Modeling these molecular interactions enables a systematic representation of gut-derived neuronal signaling within the MC framework.

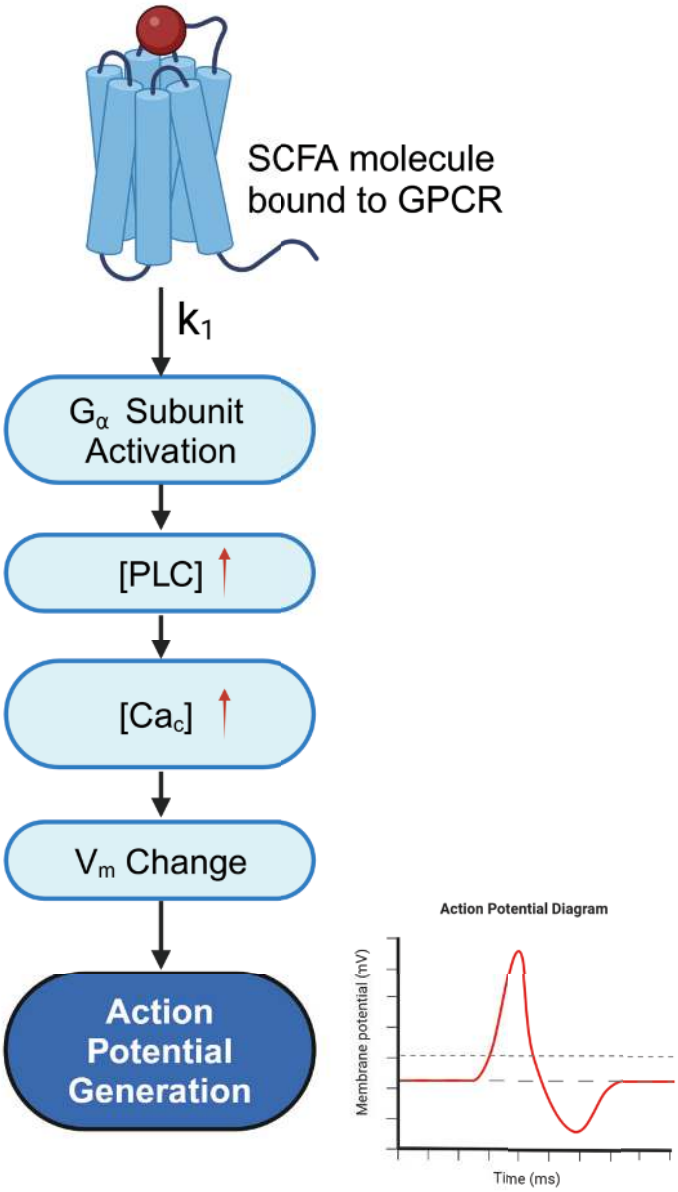

Figure 2.2: Illustration of ligand-receptor binding.(Created in https://BioRender.com).

This study specifically focuses on the gut-to-brain signaling pathway, wherein SCFAs produced by the gut microbiota bind to G-protein-coupled receptors (GPCRs) on vagal afferent neurons. Figure 2.2 illustrates the sequential intracellular signaling events, including receptor binding, G-protein alpha subunit activation, PLC-mediated calcium signaling, membrane depolarization, and neurotransmitter release at the NTS [14, 43]. This detailed biological representation shown in Figure 2.2 provides the foundation for the proposed MC-based modeling framework that enables systematic quantitative analysis. Integrating MC principles into this communication pathway allows the evaluation of information transfer and signaling efficiency, supporting the development of IoBNT-based diagnostic and therapeutic tools targeting SCFA-related communication deficiencies.

Dysregulation of SCFA signaling has been linked to various pathological conditions, including inflammatory bowel disease, colorectal cancer, obesity, type 2 diabetes, and neurological disorders such as depression, anxiety, and autism spectrum disorders [89, 90, 86, 14]. These associations underscore the importance of quantitatively characterizing how SCFA fluctuations influence neural signaling within the GBA, particularly via the vagus nerve [89, 90, 86, 14].

Existing research efforts, including pioneering MC-based studies, have established foundational insights into the gut-brain axis, highlighting its complexity and the significant role of SCFAs as critical signaling mediators [91, 13]. However, a substantial gap remains in fully capturing the detailed mechanisms of SCFA-driven neural communication, particularly via vagal afferent pathways. Prior works have predominantly addressed specific components of the signaling cascade [43], or focused on broader network-level representations [79] without an integrated analysis of molecular receptor interactions and subsequent neuronal activity.

To address this gap, this chapter proposes a comprehensive molecular communication framework that explicitly incorporates SCFA receptor-binding kinetics, downstream intracellular signaling, and neuronal transmission along the vagus nerve. By modeling these sequential processes, the study aims to offer a unified analysis of communication efficiency and reliability within the GBA. The developed model allows

quantitative evaluation of key parameters such as signal fidelity, mutual information, and transmission delays. Consequently, this work provides a systematic basis for understanding SCFA-mediated neural communication and establishes the background for future studies aimed at therapeutic and diagnostic applications based on the IoBNT paradigm.

To complement the gut-to-brain direction focused in this study, it is worth noting that the GBA operates bidirectionally. Brain-derived signals influence gut physiology through pathways such as the hypothalamic-pituitary-adrenal (HPA) axis and the autonomic nervous system (ANS). These descending pathways affect gastrointestinal motility, secretion, barrier integrity, and immune modulation, ultimately shaping the gut microbiota composition and SCFA production [21]. Understanding these mechanisms is also important to capture the dynamic nature of the GBA. Future modeling efforts may consider incorporating such brain-to-gut signaling to develop a more holistic MC-based representation of bidirectional GBA communication.

2.3 System Model

The GBA is a complex, bidirectional communication network linking the GI tract to the CNS through neural, endocrine, and immune pathways. This study focuses on communication between gut microbiota and the brain via SCFA-driven vagus nerve signaling, where SCFAs produced by gut microbiota bind to GPCRs on vagal afferent neurons. This binding elevates phospholipase C (PLC) concentrations and cytosolic calcium levels, ultimately generating action potentials that travel along the vagus nerve to the brainstem. Upon reaching the NTS, these neuronal signals modulate physiological and behavioral processes, underscoring the significance of SCFAs in gut-to-brain communication.

Figure 2.3 provides a schematic overview of the proposed molecular communication model, representing the gut environment as the transmitter, the vagus nerve as the channel, and the CNS as the receiver. Although the GBA operates bidirectionally, this study focuses on the gut-to-brain signaling direction, in which gut-derived

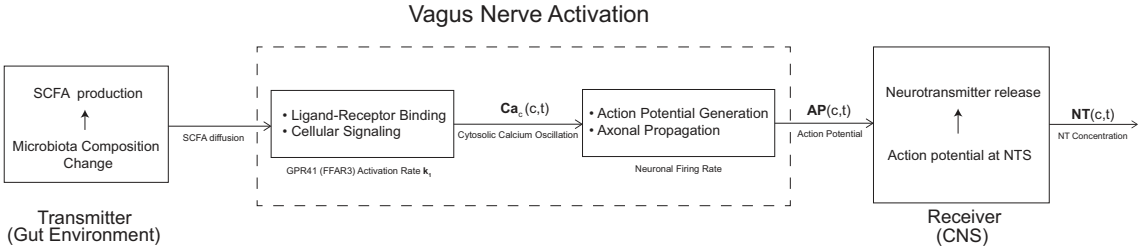

Figure 2.3: Scheme of the MC channel model for SCFA-driven vagus nerve signaling withing GBA.

molecular signals influence CNS activity. As illustrated in Figure 2.3, the proposed model comprises five stages: (i) SCFA binding to GPCRs on vagal afferent neurons, (ii) activation of G-protein alpha subunits ($[G_\alpha]$) and subsequent intracellular signaling cascades involving PLC and calcium dynamics, (iii) membrane depolarization and action potential generation, (iv) signal propagation along the vagus nerve, and (v) neurotransmitter release at the CNS synapse. Conceptualizing this pathway as a molecular communication channel enables quantitative assessment of signaling efficiency and reliability using information-theoretic metrics such as mutual information and delay.

Within the MC framework, the vagal pathway is effectively modeled by considering the concentration of SCFA molecules as the primary input signal. This signal is transmitted through receptor-ligand binding and ultimately converted into electrical signals. The vagal pathway can be conceptualized as a sequence of processes within the MC framework, encompassing the following components:

- **Input Signal**: Gut microbiota-derived SCFA molecules serve as the initial input signal, representing the molecular information transmitted within the GBA channel.

- **Channel and Transmission Mechanism**: The SCFAs diffuse across the gut environment and bind to G protein-coupled receptors (FFAR3/GPR41) on vagal afferent neurons. This binding activates the GPCR complex and

initiates intracellular signaling cascades that lead to the generation of action potentials.

- **Output Signal**: The action potentials propagate along the vagus nerve to the NTS in the brainstem, resulting in the release of neurotransmitters. These neurotransmitters modulate higher brain functions and complete the communication pathway.

The detailed modeling and analysis of these steps are described comprehensively in the following subsections.

2.3.1 Vagus Nerve Activation Model

The MC-based model explains how microbial metabolites in the gut, specifically SCFAs, influence CNS functions through the vagal pathway. The proposed model simulates and analyzes the key signaling events in the SCFA-driven vagus nerve signaling pathway, providing insights into the interactions between gut-derived metabolic signals and CNS activity. While the model offers a framework for understanding the underlying mechanisms of the GBA, it also provides a foundation for future research exploring potential therapeutic applications.

Vagus nerve activation is initiated by the binding of SCFAs, produced by gut microbiota, to G-protein-coupled receptors (FFAR3/GPR41) located on vagal afferent neurons. This binding event triggers the intracellular biochemical signaling cascades, starting from G-protein activation as illustrated in Figure 2.2.

Upon SCFA binding, the G protein alpha subunits ($[G_\alpha]$) are activated. Mathematically, the activation of $[G_\alpha]$ and the following interactions are described by the set of nonlinear ordinary differential equations [92]:

$$\frac{d[G_\alpha]}{dt} = k_1 + k_2[G_\alpha] - k_3[G_\alpha]\frac{[PLC]}{[G_\alpha] + k_4} - k_5[G_\alpha]\frac{[Ca_c]}{[G_\alpha] + k_6}. \tag{2.1}$$

In the governing equation for $[G_\alpha]$, the parameter k_1 represents the production rate of activated G protein alpha subunits induced by SCFA binding to the GPCR complex. This parameter sets the sensitivity of neuronal activation to variations in SCFA levels, essentially governing how quickly and strongly neurons respond to changes in gut-derived SCFA concentrations. The parameter k_2 introduces an autoregulatory component that maintains the concentration of $[G_\alpha]$ at a stable baseline. This self-regulation ensures consistent neuronal signaling and prevents erratic responses as external conditions change.

The parameters k_3, k_4, k_5, and k_6 control the interactions between $[G_\alpha]$, $[PLC]$, and cytosolic calcium $[Ca_c]$, emphasizing the role of ER-related processes in the signaling cascade. Specifically, the parameters k_3 and k_4 regulate the inhibitory influence of the $[PLC]$ on activated $[G_\alpha]$, controlling the strength and saturation threshold of this interaction. The parameters k_5, and k_6 determine how effectively $[Ca_c]$ suppresses $[G_\alpha]$ levels. Together, these parameters ensure precise regulation and stability of the neuronal signaling cascade under varying physiological conditions.

To understand how these factors influence the calcium signaling cascade, it is necessary to consider the dynamics of other key molecules. The concentration of $[PLC]$ is governed by [92]:

$$\frac{d[PLC]}{dt} = k_7[G_\alpha] - k_8\frac{[PLC]}{[PLC] + k_9}. \tag{2.2}$$

Here, k_7 governs the synthesis rate of $[PLC]$, linking $[G_\alpha]$ activation directly to the production of $[PLC]$. Thus, increased $[G_\alpha]$ levels induce $[PLC]$ generation, stimulating downstream signaling cascades. The parameter k_8 manages the degradation rate of $[PLC]$ by effectively controlling how rapidly $[PLC]$ is removed from the system and so influences the duration and intensity of the signal. Additionally, k_9 describes the Michaelis-Menten constant for $[PLC]$ degradation reaction and influences the sensitivity and responsiveness of the system by modulating how effectively

$[PLC]$ is removed as its concentration varies [92].

Cytosolic calcium concentration $[Ca_c]$ is one of the critical variables driving neuronal excitability since it directly influences the membrane polarization. The dynamics of cytosolic calcium concentration are described by following differential equations [92]:

$$\begin{aligned}\frac{d[Ca_c]}{dt} &= k_{10}[Ca_c][PLC]\frac{[Ca_{ER}]}{[Ca_{ER}]+k_{11}} + k_{12}[PLC] + k_{13}[G_\alpha] \\ &\quad - k_{14}\frac{[Ca_c]}{[Ca_c]+k_{15}} - k_{16}\frac{[Ca_c]}{[Ca_c]+k_{17}}.\end{aligned} \tag{2.3}$$

$$\frac{d[Ca_{ER}]}{dt} = -k_{10}[Ca_c][PLC]\frac{[Ca_{ER}]}{[Ca_{ER}]+k_{11}} + k_{16}\frac{[Ca_c]}{[Ca_c]+k_{17}}, \tag{2.4}$$

where Eq. 2.3 describes the dynamics governing cytosolic calcium concentration $[Ca_c]$, while Eq. 2.4 represents the concentration dynamics of calcium within the endoplasmic reticulum ($[Ca_{ER}]$). $[Ca_c]$ acts as a dynamically regulated signaling mediator that is influenced by multiple factors. Specifically, $[Ca_c]$ increase via calcium release from the endoplasmic reticulum, and also a calcium influx process initiated by the activation of $[PLC]$ and $[G_\alpha]$. Conversely, calcium efflux mechanisms from the cytosol and also calcium reuptake into the endoplasmic reticulum maintain calcium homeostasis by counterbalancing the elevation in $[Ca_c]$ [92].

The parameters k_{10} and k_{11} regulate calcium release from the endoplasmic reticulum into the cytosol, modulated by the $[PLC]$. On the other hand, the parameter k_{12} represents an additional pathway by which $[PLC]$ directly elevates cytosolic calcium levels, independent of ER stores. Parameter k_{13} captures the influence of $[G_\alpha]$ on calcium influx into the cytosol, providing a direct link between GPCR activation and calcium signaling.

Parameters k_{14}, k_{15}, k_{16}, and k_{17} describe the mechanisms responsible for cytosolic calcium reduction, ensuring the maintenance of calcium homeostasis. Specifically,

k_{14} and k_{15} characterize the calcium efflux out of the cytosol, and the parameters k_{16} and k_{17} describe calcium reuptake into the ER.

Collectively, these parameters regulate the intricate balance of calcium signaling dynamics within the cell and so ensure precise and stable control of neuronal excitability and responsiveness. Depending on the system parameters and initial conditions, these interactions can lead to either oscillatory or steady-state calcium concentration profiles.

2.3.2 Receiver Model

Intracellular calcium oscillations play a crucial role in modulating neuronal excitability and encoding information, both broadly in neuronal physiology and specifically within the context of vagal afferent neurons [93, 94]. Elevated $[Ca_c]$ significantly increases the probability of action potential generation in vagal afferent fibers, which are essential for transmitting information about gut microbial activity to the CNS. This calcium-dependent mechanism ensures subtle variations in SCFA concentrations are efficiently converted into precise electrochemical signals that propagate along the vagus nerve and ultimately influence CNS responses [13, 14].

Upon activation of the calcium signaling pathway, significant changes occur in the neuronal membrane potential that further leads to the generation of action potentials. Elevated $[Ca_c]$ enhances neuronal excitability by influencing various ion channels embedded in the neuronal membrane. The neuronal membrane potential (V_m) is governed by the balance of ionic currents flowing through different ion channels and capacitive currents. To analyze these processes, the Hodgkin-Huxley (HH) model [95] provides a comprehensive mathematical framework that describes the electrical behavior of excitable cells, such as neurons. The HH model characterizes the membrane potential V_m through differential equations. The fundamental equation governing the membrane potential is [96]:

$$C_m \frac{dV}{dt} = I_{\text{ext}} - I_{\text{Na}} - I_{\text{K}} - I_{\text{L}} - I_{\text{CaK}}, \tag{2.5}$$

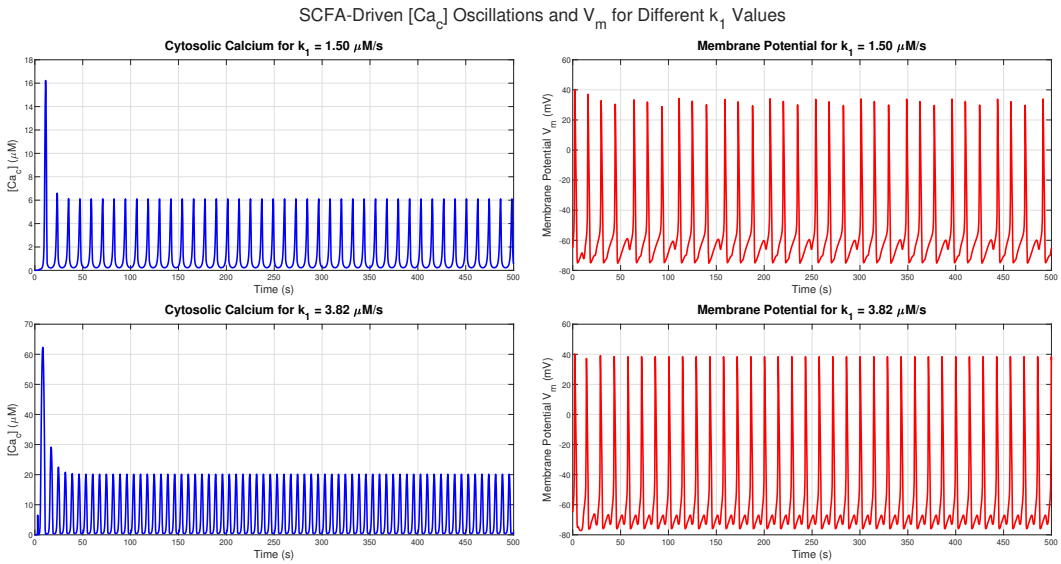

Figure 2.4: SCFA-driven cytosolic calcium oscillation and membrane potential for changing k_1 values. (a) Cytosolic calcium oscillations, and (b) Membrane potential (V_m) for $k_1 = 1.50\mu M/s$. (c) Cytosolic calcium oscillations, and (d) Membrane potential (V_m) for $k_1 = 3.82\mu M/s$,

where C_m is the membrane capacitance, I_{ext} is an externally applied current, and $I_{\text{Na}}, I_{\text{K}}, I_{\text{L}}, I_{\text{CaK}}$ represent the sodium, potassium, leak, and calcium-activated potassium currents, respectively [95, 96]. These ionic currents, which are determined by the conductances and voltages of their respective channels, control the flow of ions across the membrane and thus shape the membrane potential.

Each ionic current is defined by its conductance, gating variables, and driving force, as given below [95, 96]:

$$I_{\text{Na}} = g_{\text{Na}} m^3 h (V - E_{\text{Na}}), \tag{2.6}$$

$$I_{\text{K}} = g_{\text{K}} n^4 (V - E_{\text{K}}), \tag{2.7}$$

$$I_{\text{L}} = g_{\text{L}} (V - E_{\text{L}}), \tag{2.8}$$

$$I_{\text{CaK}} = g_{\text{CaK}} [Ca_c] (V - E_{\text{CaK}}). \tag{2.9}$$

Here, g_{Na}, g_{K}, g_{L}, and g_{CaK} are the maximum conductances for the respective ion

channels, while E_{Na}, E_{K}, E_{L}, and E_{CaK} are their corresponding reversal potentials. The gating variables m, h, and n define the probability that ion channels are open [96]:

$$\frac{dm}{dt} = \alpha_m(V)(1-m) - \beta_m(V)m, \tag{2.10}$$
$$\frac{dh}{dt} = \alpha_h(V)(1-h) - \beta_h(V)h, \tag{2.11}$$
$$\frac{dn}{dt} = \alpha_n(V)(1-n) - \beta_n(V)n. \tag{2.12}$$

The rate constants α and β for each gating variable are voltage-dependent, capturing the kinetics of channel opening and closing in response to changes in membrane potential [96]:

$$\alpha_m(V) = \begin{cases} 1.0, & V = -40 \text{ mV} \\ \frac{0.1(V+40)}{1-e^{-(V+40)/10}}, & \text{otherwise} \end{cases} \tag{2.13}$$

$$\begin{aligned} \beta_m(V) &= 4.0 \cdot e^{-(V+65)/18} \\ \alpha_h(V) &= 0.07 \cdot e^{-(V+65)/20} \\ \beta_h(V) &= \frac{1}{1+e^{-(V+35)/10}} \end{aligned} \tag{2.14}$$

$$\alpha_n(V) = \begin{cases} 0.1, & V = -55 \text{ mV} \\ \frac{0.01(V+55)}{1-e^{-(V+55)/10}}, & \text{otherwise} \end{cases} \tag{2.15}$$

$$\beta_n(V) = 0.125 \cdot e^{-(V+65)/80}$$

These voltage-dependent rate constants ensure that the gating variables accurately track changes in membrane potential, allowing ion channels to open and close at appropriate time intervals. Through this mechanism, the neuron can reliably initiate and propagate action potentials in response to voltage fluctuations [95, 97, 96].

As ionic currents and gating variables interact, they collectively shape the temporal evolution of the membrane potential. Elevated $[Ca_c]$ levels, in particular, influence the calcium-activated potassium current (I_{CaK}), enhancing the repolarization phase of the action potential. This adjustment shortens the action potential duration and reinforces the refractory period, ensuring unidirectional propagation and maintaining precise timing and firing patterns. Through these mechanisms, essential physiological information, including signals related to gut microbial activity, is encoded into coherent electrical patterns suitable for transmission.

Table 2.1 provides the Hodgkin-Huxley parameters employed in the model. The Hodgkin-Huxley framework describes the electrical characteristics of excitable cells, such as neurons, by incorporating the dynamics of voltage-gated ion channels. The parameter values are primarily adapted from established studies on neuronal excitability [95, 98], with minor adjustments (e.g., calcium-activated potassium currents) to reflect biological features relevant to vagal afferent neurons. Integrating the Hodgkin-Huxley equations with the SCFA-driven signaling ODEs enables the development of a unified framework that links molecular input signals (SCFA concentrations) to electrical outputs (action potentials) within the vagal pathway.

The parameter k_1 plays a pivotal role in the proposed model, as it directly governs

Table 2.1: Hodgkin-Huxley Model Parameters

Parameter	**Description**	**Value**
C_m	Membrane capacitance	1.0 µF/cm^2
g_{Na}	Maximum sodium conductance	120.0 mS/cm^2
g_{K}	Maximum potassium conductance	36.0 mS/cm^2
g_{L}	Leak conductance	0.3 mS/cm^2
g_{CaK}	Calcium-activated potassium conductance	0.1 mS/cm^2
E_{Na}	Sodium reversal potential	50.0 mV
E_{K}	Potassium reversal potential	−77.0 mV
E_{L}	Leak reversal potential	−54.387 mV
E_{CaK}	Calcium-activated potassium reversal potential	−80.0 mV
I_{ext}	External current	10.0 µA/cm^2

the initial production rate of activated G protein alpha subunits $[G_\alpha]$ in response to changing SCFA profile as described in Section 2.3.1. As the parameter directly associated with SCFA-GPCR binding events, k_1 establishes the responsiveness and sensitivity of the entire downstream signaling pathway. As shown in Eq. 2.1, increasing k_1 directly elevates the production of activated $[G_\alpha]$, which subsequently enhances $[PLC]$ synthesis as depicted Eq. 2.2. Higher $[PLC]$ levels then amplify calcium release from the endoplasmic reticulum, increasing cytosolic calcium oscillation frequency. This mechanism underscores why alterations in k_1 have enunciated effects on downstream intracellular processes, including cytosolic calcium dynamics and membrane potential oscillations.

As illustrated in Fig. 2.4, higher k_1 values result in more frequent cytosolic calcium oscillations, comparing Fig. 2.4(a) with Fig. 2.4(c). These enhanced oscillations elevate neuronal excitability and lead to improved, more precisely shaped action potential profiles, as illustrated in the membrane potential plots of Fig. 2.4(b)-(d). While the total number of action potentials increases with respect to higher k_1, the increment remains relatively modest, reflecting the intrinsic firing constraints of vagal afferent neurons. Overall, changes in k_1 modulate the responsiveness of the neuron and its capacity to transmit information effectively through action potentials, which further enhance the ability of the vagus nerve to convey detailed information

about the gut microbiota to the CNS.

Neurotransmitter release occurs when the membrane potential V_m reaches a threshold value of $V_{\text{th}} = 20\,\text{mV}$. This process promotes synaptic communication and ultimately allows the neuron to influence downstream targets. To capture these dynamics, the neurotransmitter concentration $[NT]$ in the synaptic cleft is modeled to incorporate both passive decay and active release triggered by neuronal firing. The neurotransmitter concentration evolves according to:

$$\frac{d[NT]}{dt} = -\frac{[NT]}{\tau_{\text{rec}}}, \tag{2.16}$$

where τ_{rec} is the neurotransmitter reuptake constant, representing the rate of neurotransmitter removal from the synaptic cleft to terminate the signal. The reuptake process ensures that the released neurotransmitter levels remain controlled, preventing continuous stimulation and helping to maintain signal fidelity. As a result, the interplay between action potential generation, neurotransmitter release, and reuptake provides a clear and physiologically relevant representation of how molecular signals, once translated into electrical impulses, drive synaptic transmission and influence neural circuits within the CNS.

Neurotransmitter release is modeled as a stochastic process that accounts the multivesicular release process [99, 100]. The number of vesicles released per action potential, k, follows a binomial distribution defined as:

$$k \sim \text{Binomial}(N, p_{\text{nt}}), \tag{2.17}$$

where N represents the total number of the vesicles within the presynaptic neuron, and p_{nt} is the probability of vesicle release per action potential. The instantaneous increase in neurotransmitter concentration resulting from the release of k vesicles is given by:

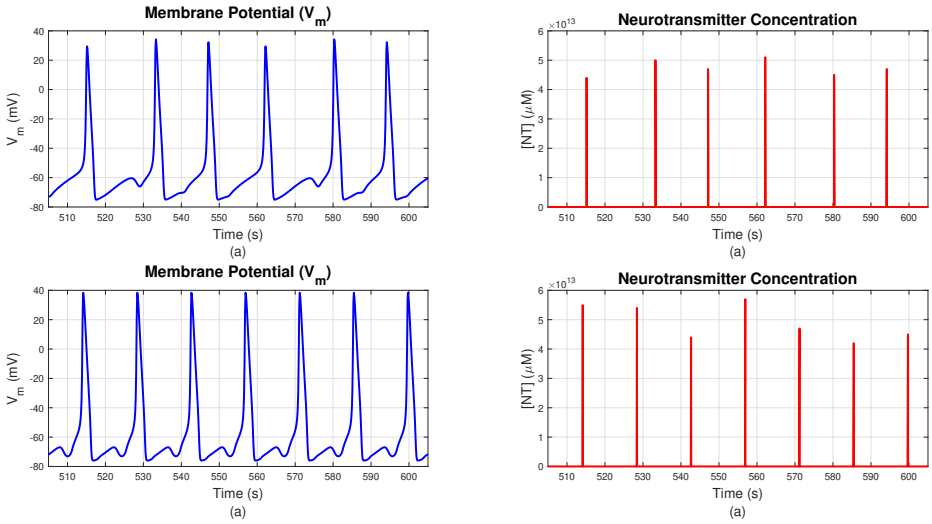

Figure 2.5: Zoomed-in view of SCFA-driven neural responses with varying GPCR activation rates. (a) Action potential generation, and (b) corresponding neurotransmitter concentration for lower activation rate ($k_1 = 1.52\,\mu$M/s); (c) Action potential generation, and (d) corresponding neurotransmitter concentration for higher activation rate ($k_1 = 3.82\,\mu$M/s).

$$\Delta[NT] = \frac{k \cdot NT_{\text{ves}}}{V_{\text{syn}}}, \tag{2.18}$$

where NT_{ves} represents the neurotransmitter amount of a vesicle and V_{syn} denotes the synaptic cleft volume. This formulation ensures that each vesicle release event delivers a definite and measured amount of neurotransmitter to the synaptic cleft, allowing precise and well-regulated synaptic signaling [99].

As illustrated in Fig. 2.5, the increase in action potential frequency with respect to higher GPCR activation leads to more frequent vesicle release events and thus elevates $[NT]$ levels in the synaptic cleft. By combining passive decay with probabilistic release, this model captures the temporal dynamics of $[NT]$ in the synaptic cleft. High neuronal activity, leading to frequent action potentials, increases vesicle release, raising $[NT]$ and thus enhancing synaptic transmission. Conversely, reuptake processes restore $[NT]$ to baseline, preventing overstimulation and ensuring

reliable communication.

Although the connection between gut-derived molecular signals and vagal neuronal activity has been previously established, this study contributes a molecular communication–based modeling framework that systematically represents key processes underlying this pathway. By incorporating SCFA-induced calcium oscillations, Hodgkin–Huxley-based action potential dynamics, and probabilistic neurotransmitter release, the proposed end-to-end model offers a structured approach to analyzing vagal signaling within the gut-brain axis. Even though the model does not aim to capture all biological complexities of the system, it highlights the key signaling mechanisms and offers a foundational framework for future investigations into gut-brain communication.

2.4 Theoretical Analysis and Simulations

In this section, the end-to-end MC model derived for SCFA-driven vagus nerve signaling in the gut-brain axis is evaluated using MATLAB-based numerical simulations. The SCFA-induced intracellular biochemical processes, including G protein activation and calcium-mediated cascades, are incorporated into the model to generate electrical action potentials and subsequent neurotransmitter release events at the synaptic terminal.

Information and communication technologies (ICT) metrics are employed to examine the overall efficacy of this communication channel. The mutual information between SCFA-induced calcium oscillations and neurotransmitter release events quantifies the information shared between these two processes, providing insight into how effectively information is transmitted through the neuronal channel [101, 102]. This metric captures the dependency between calcium signaling, which encodes information about gut microbial activity, and the resultant neurotransmitter release that propagates signals to the CNS. Concurrently, delay analysis is conducted to assess the temporal latency between calcium oscillations and neurotransmitter release, providing critical insights into the responsiveness and synchronization of the signaling pathways. By integrating these ICT metrics, we can elucidate the efficiency and

reliability of the end-to-end signaling process, highlighting potential bottlenecks and optimizing parameters for enhanced communication fidelity.

The simulations are conducted under varying G-protein activation rates (k_1) to understand better the influence of intracellular signaling parameters on the information transfer characteristics and temporal precision of the channel. Specifically, Monte Carlo simulations are conducted by sampling the SCFA-driven GPCR activation rate from independent lognormal distributions. The means of these distributions are set to a range of median values $(1.82, 2.25, 2.68, 3.10, 3.67)$, each corresponding to different types of SCFA molecules, which exhibit distinct affinities towards GPCR.

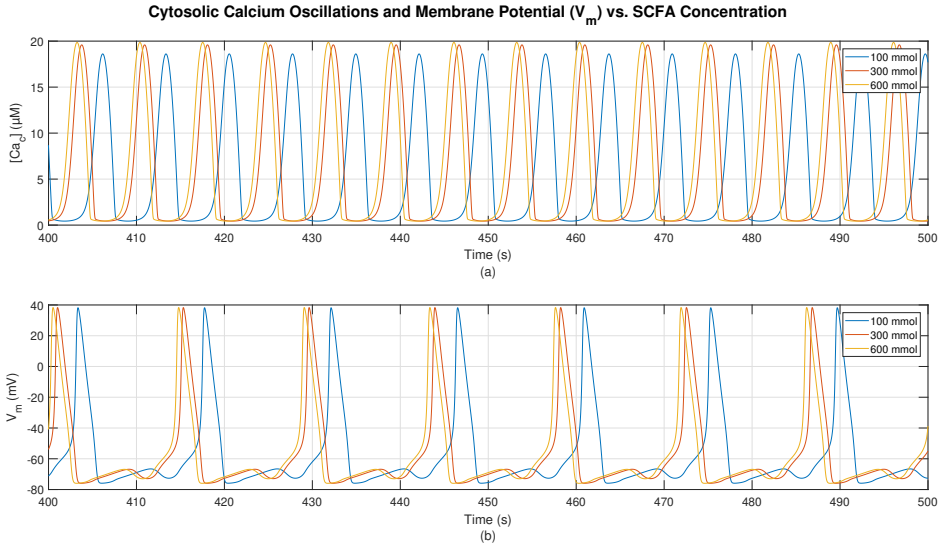

Figure 2.6: Zoomed-in view of SCFA-driven responses for varying SCFA concentrations. (a) Cytosolic calcium dynamics in response to different SCFA levels, and (b) corresponding membrane potential changes.

Higher affinity SCFAs yield increased G-protein activation rates, leading to more frequent cytosolic calcium oscillations, as demonstrated in Figure 2.4. Additionally, increasing the concentration of a specific SCFA molecule enhances receptor occupancy and consequently amplifies G-protein activation, further contributing to elevated signaling activity, as illustrated in Figure 2.6.

To provide deeper insights into SCFA-driven $[G_\alpha]$ activation dynamics, simulations are also performed across physiologically relevant SCFA concentrations (100–

600 mmol) [103]. Corresponding values of k_1 were calculated using a Michaelis-Menten relationship to represent SCFA-dependent receptor activation. Mutual information and delay metrics are computed to quantify the efficacy and responsiveness of neural communication at each concentration. Results, shown in Figure 2.7 demonstrate dose-dependent behavior, with higher SCFA concentrations yielding increased mutual information and reduced signaling delays, underscoring the importance of SCFA availability on gut-brain axis communication efficiency.

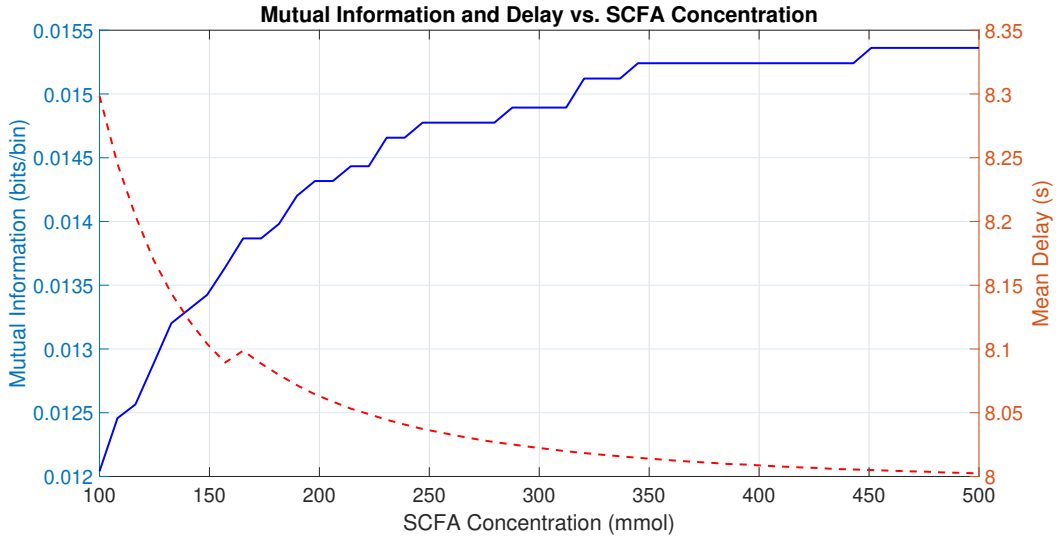

Figure 2.7: Mutual information and mean signaling delay as a function of SCFA concentration. As SCFA concentration increases, mutual information improves while signaling delay decreases, indicating enhanced communication efficiency.

The system parameters, initial conditions, and simulation details remain consistent with those outlined in the preceding sections. In addition to quantitatively exploring and characterizing the fundamental relationship between SCFAs and vagal neuronal activity, the analyses provide a rigorous framework for examining end-to-end information transfer within this complex biological signaling network. Applying information and communication technologies (ICT) to complex biological signaling pathways, such as the gut-brain axis, offers a structured and quantifiable framework to optimize communication parameters and inform the development of targeted therapeutic interventions [104]. This approach contributes to a more systematic under-

standing of the molecular and cellular communication processes underlying neurological function and behavior, and it highlights the value of information-theoretic methodologies in advancing the analysis of biological signaling systems.

2.4.1 Mutual Information

The mutual information analysis aims to quantify the statistical dependence between SCFA-induced calcium oscillations and neurotransmitter release events and serves as a fundamental metric for assessing the information transmission capacity of the neuronal communication channel. Mutual information enables the measuring of the amount of information shared between two random variables, in this case, the occurrence of calcium peaks (X) via random GPCR activation rate and the subsequent neurotransmitter release events (Y). This metric effectively measures how much knowing the state of one variable reduces the uncertainty of the other, thereby reflecting the ability of the channel to convey information.

To compute mutual information, the simulation time series is discretized into uniform time intervals with a fixed bin width (e.g., $\Delta t = 1\,\mathrm{s}$). The simulation time is set as 1000 seconds and discretized into 1-second bins, resulting in binary sequences of length 1000. We generate two binary sequences for each time bin: X for calcium events and Y for neurotransmitter release events. An element in these sequences is assigned to 1 if a corresponding event occurs within the time bin and 0 otherwise. This technique reduces complex, continuous data into discrete random variables suitable for information-theoretic computations.

After the data is discretized, the joint and marginal probabilities of the events are calculated. The joint probability $P_{XY}(x, y)$ represents the likelihood of observing a specific combination of calcium and neurotransmitter events within the same time bin. Marginal probabilities $P_X(x)$ and $P_Y(y)$ are derived by summing the joint probabilities over the possible states of the other variable. The mutual information $I(X;Y)$ is computed as:

$$I(X;Y) = \sum_{x=0}^{1} \sum_{y=0}^{1} P_{XY}(x,y) \log_2 \left(\frac{P_{XY}(x,y)}{P_X(x) P_Y(y)} \right). \tag{2.19}$$

The resulting mutual information value, measured in bits, quantifies the information transmission capacity of the neuronal channel. Higher mutual information values indicate a more efficient communication process, where intracellular calcium signaling reliably predicts following synaptic neurotransmitter release events. In the presented simulations, mutual information is computed for different values of k_1 to compare how altered G-protein activation rates affect the information-carrying capacity of the defined communication channel.

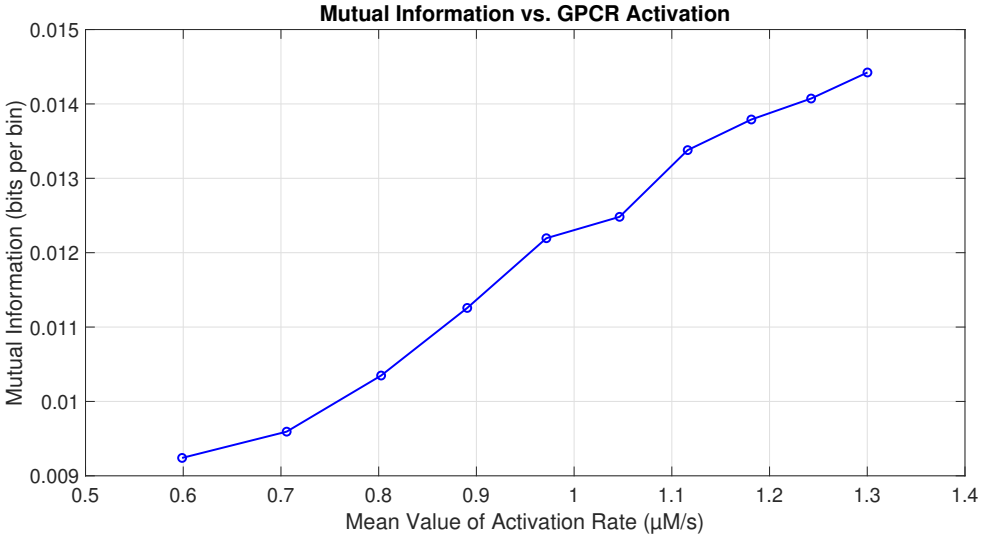

Figure 2.8: Mutual information vs GPCR activation rate.

As illustrated in Fig. 2.8, the simulation results indicate that increasing the G-protein activation rate k_1 leads to a noticeable improvement in mutual information. The activation rate k_1 depends on the type of bound SCFA and ranges between $1.52\,\mu$M/s and $3.82\,\mu$M/s [92]. This variability arises from the inherently random nature of the binding process in the gut and is effectively modeled using a lognormal distribution [105]. Specifically, for $k_1 = 1.52\,\mu$M/s, the mutual information was found to be 0.0085 bits per bin, while raising k_1 to $3.82\,\mu$M/s increased the mutual

information to 0.0110 bits per bin. Although these mutual information values are relatively modest, the enhancement observed with a higher k_1 suggests a more effective coupling between intracellular calcium signaling and synaptic neurotransmitter release.

The observed increase in mutual information aligns with the theoretical expectation that strengthening the intracellular signaling cascade leads to more reliable information encoding. As G-protein-mediated responses become more evident, the timing and occurrence of calcium oscillations gain greater predictive power regarding the subsequent release of neurotransmitters. This improved correlation implies that the channel can better convey subtle variations in SCFA-induced biochemical activity, thereby serving as a more faithful representation of underlying gut-brain communication processes.

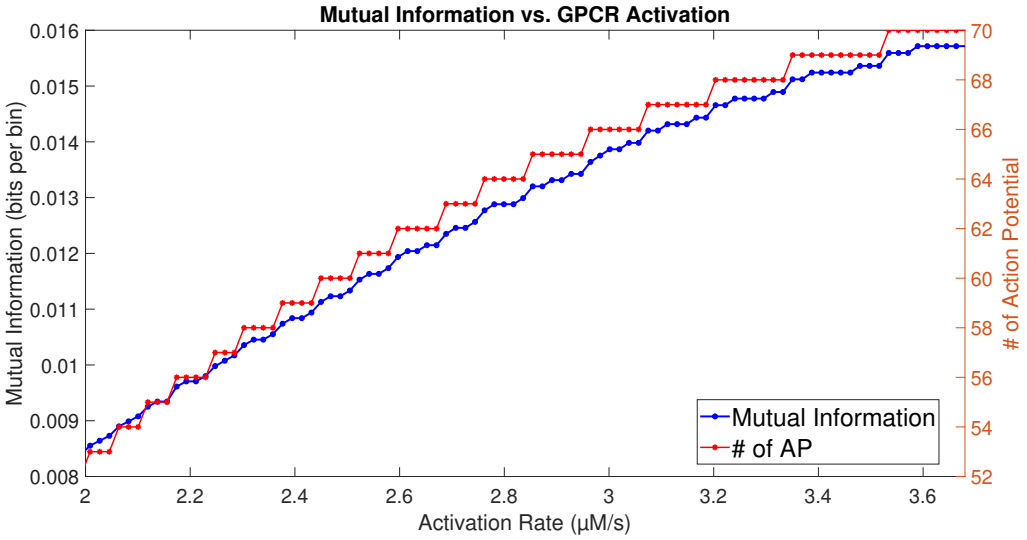

Figure 2.9: Action potential and mutual information vs GPCR activation rate.

A higher GPCR activation rate also overlaps with increased action potential frequency, driving more frequent vesicle release events. As shown in Fig. 2.9, this increased neuronal firing contributes to the rise in mutual information, as the tighter temporal alignment between calcium oscillations and action potentials augments the ability of the channel to capture subtle variations in SCFA-induced activity. Con-

sequently, strengthening the GPCR-mediated intracellular cascade not only refines the timing of neurotransmission but also increases the overall fidelity of gut-brain communication.

The obtained results align with the theoretical hypothesis that intensifying the intracellular signaling network improves information encoding. As G-protein-mediated responses become more prominent, the timing and amplitude of calcium oscillations more accurately cause neurotransmitter release, thereby expanding the capacity of the system to represent essential biochemical signals. From a broader perspective, the sensitivity of mutual information to GPCR activation rate highlights the feasibility of tuning intracellular parameters to optimize gut-brain signaling. Such insights may guide therapeutic interventions aimed at modulating GPCR activity and enhancing neural communication under pathological conditions, thus underlining the value of information-theoretic approaches in understanding complex biological networks.

2.4.2 Delay Analysis

While mutual information provides insights into the informational coupling between input and output events, delay analysis provides an important measure of the temporal dynamics inherent in the SCFA-mediated signaling pathway [1]. Specifically, it quantifies the latency between cytosolic calcium peaks and the following neurotransmitter release events. This delay designates the time required for intracellular calcium signaling to culminate in neurotransmitter release, thereby reflecting the responsiveness and synchronization of the neuronal communication channels.

The delay is computed by identifying each calcium peak within the simulation data and determining the time of the earliest neurotransmitter release event that occurs at or after that peak. The delay Δt_i for the i-th calcium peak is defined as:

$$\Delta t_i = t_{\mathrm{NT},j} - t_{\mathrm{Ca},i}, \tag{2.20}$$

where $t_{\mathrm{Ca},i}$ is the time of the i-th calcium peak, and $t_{\mathrm{NT},j}$ is the time of the earliest neurotransmitter release event observed at or following $t_{\mathrm{Ca},i}$. A distribution of delay values that characterize the temporal relationship between calcium signaling and neurotransmitter release is obtained by performing this calculation for all detected calcium peaks.

To summarize the delay characteristics, the mean, $\mu_{\Delta t}$, and the standard deviation, $\sigma_{\Delta t}$, of the signaling delay between calcium peaks and neurotransmitter release events are calculated. The metric $\mu_{\Delta t}$ represents the average latency between calcium peaks and neurotransmitter release events, while $\sigma_{\Delta t}$ quantifies the variability in these intervals. A lower mean delay indicates that information is transmitted more rapidly. Conversely, a higher standard deviation suggests more significant variability in response times, potentially affecting the reliability and synchronization of the signaling pathway.

Fig. 2.10 demonstrates that the mean and standard deviation of the delay both decrease as the GPCR activation rate, k_1, increases, reflecting more rapid and consistent signal propagation in SCFA-driven vagus nerve signaling. Since k_1 governs the SCFA-GPCR binding process and the following intracellular cascades, higher values of k_1 accelerate the calcium release and action potential generation processes. As a result, the mutual information depicted in the same figure also rises with increasing k_1, while the delay metrics drop, consistent with theoretical expectations that strengthening GPCR-mediated pathways enhances both the information transfer rate and its temporal fidelity. For example, increasing k_1 from $1.52\,\mu$M/s to $3.82\,\mu$M/s lowers the mean delay from about 9.40 s to 7.99 s and reduces the standard deviation from 4.44 s to 3.57 s. These findings demonstrate the sensitivity of the proposed communication model to an intrinsic parameter (k_1), which governs both the degree of informational coupling (via mutual information) and the timing of neural responses.

On the other hand, the obtained results confirm the expectation that SCFA-driven molecular communication along the vagus nerve is significantly slower than conventional electrical synaptic signaling. The involvement of secondary messengers,

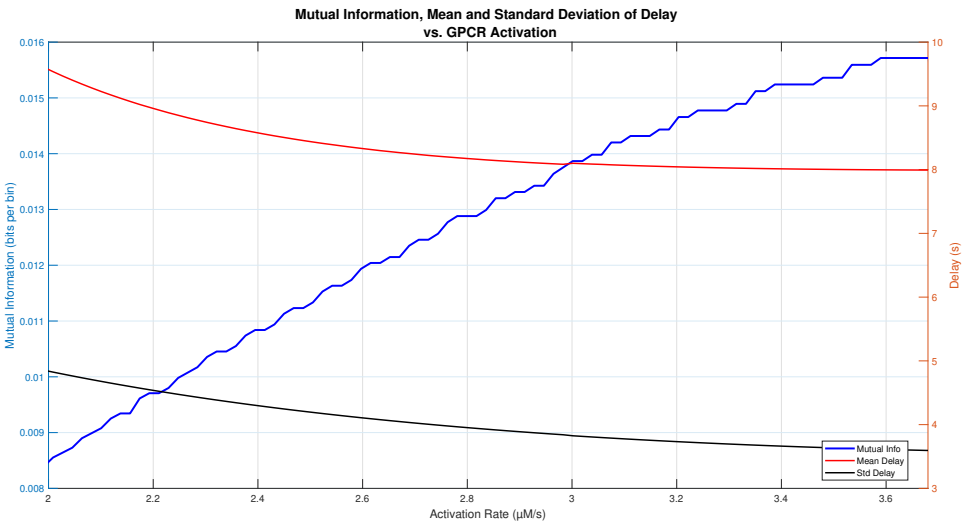

Figure 2.10: Delay vs GPCR activation rate.

receptor-ligand binding, and downstream biochemical cascades inherently introduces substantial temporal delays. Although increasing k_1 improves responsiveness, it does not fundamentally alter the time scale dominated by these biochemical processes. Consequently, the signaling pathway remains slow, consistent with the fundamental principles of molecular communication where information transmission typically involves longer time scales due to diffusion and enzymatic reaction kinetics.

Understanding the delay dynamics provides critical insights into the temporal responsiveness and synchronization of the SCFA-mediated signaling pathway, making it possible to determine how rapidly and consistently molecular events are translated into neural outputs. Characterizing the delay distribution and its sensitivity to intracellular parameters, such as k_1, highlights potential avenues for reducing latency and variability, thereby improving the speed and reliability of gut-brain communication. Beyond these temporal considerations, the complementary examination of mutual information can further elucidate the information-carrying capacity of the pathway. Integrating mutual information and delay metrics offers a comprehensive evaluation of the system's performance, illustrating how changes in intracellular kinetics influence both the fidelity and timing of information transfer. These analyses enable the identification of key factors that either enhance or impede effective

information transmission from the gut microbiota to the CNS.

Given the observed influence of k_1 on both information fidelity and signaling delay, it is important to consider how this parameter may be modulated under realistic physiological and clinical scenarios. In biological systems, k_1 is not fixed but depends on factors such as SCFA concentration, receptor density on vagal afferent neurons, and receptor-ligand binding kinetics. Changes in SCFA levels caused by diet, microbial fermentation, or host metabolism directly affect receptor activation dynamics. Pharmacological interventions or probiotics may enhance k_1 by upregulating GPCR expression or increasing receptor sensitivity, potentially improving gut-brain signaling efficiency. Conversely, pathological conditions such as dysbiosis or chronic inflammation may impair these regulatory processes, resulting in reduced k_1 and attenuated vagal signaling. Understanding the regulatory mechanisms governing k_1 may inform the development of targeted strategies to restore or strengthen vagal signaling, with implications for treating neurological and psychiatric disorders related to dysregulated gut-brain signaling.

This holistic approach deepens our understanding of molecular communication mechanisms within biological systems, identifies potential areas for optimization, and advances the investigation of the gut-brain axis. Consequently, it provides valuable insights for developing targeted therapeutic treatment techniques and enhancing overall neurological health.

2.5 Discussion

In this study, we developed a novel end-to-end MC framework to model SCFA-driven vagus nerve signaling within the GBA. The model integrates SCFA-receptor binding, intracellular calcium dynamics, Hodgkin-Huxley-based membrane potential equations, and probabilistic neurotransmitter release to capture the complete communication pathway from gut-derived SCFAs to neural activity in the brainstem.

One of the key outcomes is the role of the G-protein activation rate (k_1), which is influenced by SCFA type and concentration and varies between $1.8\,\mu$M/s and $3.7\,\mu$M/s. This rate follows a lognormal distribution, effectively modeling the in-

herent randomness of the SCFA-receptor binding process. High k_1 values enhance the sensitivity of SCFA-driven signaling and increase the fidelity of neural signal generation by promoting more frequent calcium oscillations and action potentials. However, the action potential rate remains constrained by the biophysical limits of neuronal firing, preventing disproportionate increases despite elevated GPCR activation.

The mutual information analysis reveals that higher SCFA-induced GPCR activation rates improve the information transmission capacity of the communication channel. Enhanced SCFA-mediated intracellular cascades synchronize calcium oscillations with neurotransmitter release events, thereby strengthening the correlation between SCFA concentrations and neural output. This outcome suggests that modulating intracellular signaling strength can enhance the detection and responsiveness to gut conditions, thereby increasing the robustness and precision of gut-to-CNS information flow.

Additionally, delay analysis indicates that increased activation rates reduce both the mean and variability of signaling delays. Nevertheless, SCFA-driven pathways exhibit slower communication rates than conventional electrical synapses due to the molecular nature of ligand-receptor interactions and secondary messenger dynamics. Our model proposes that adjusting enzymatic rates or receptor activation thresholds could mitigate these delays, offering potential strategies to accelerate the signaling process.

Overall, the MC-based framework demonstrates its effectiveness in explaining SCFA-driven vagus nerve signaling mechanisms and underscores the critical role of intracellular parameters in regulating the rate and reliability of gut-brain communication. This comprehensive model paves the way for exploring diverse scenarios, including different microbial compositions, pathological conditions, and pharmacological interventions, thereby guiding the development of targeted treatments to restore optimal neural communication within the GBA.

2.6 Conclusion

This chapter has presented an end-to-end molecular communication (MC) framework for short-chain fatty acid (SCFA)-driven vagus nerve signaling within the gut-brain axis (GBA). The model integrates SCFA-receptor binding kinetics, Hodgkin-Huxley-based neuron excitability, and probabilistic neurotransmitter release, providing a unified view of how gut-derived molecular signals are translated into electrical and synaptic events in the brainstem. The MC-based framework offers a robust tool for investigating how subtle variations in SCFA concentrations impact neuronal function and, eventually, influence brain activity by capturing important biochemical and electrophysiological processes.

The numerical simulations highlight that increasing the G-protein activation rate enhances both the frequency of calcium oscillations and the action potential firing rate. The resulting higher mutual information indicates a more robust link between SCFA concentration and neural output. Delay analysis further shows that increasing the activation rate reduces both the mean and standard deviation of the delay, which means the communication link is effectively sped up. Even though SCFA-driven pathways remain slower than conventional electrical synapses due to the intrinsic features of molecular communication, adjusting enzymatic rates or receptor activation thresholds can partially reduce latency, suggesting strategies to accelerate the signaling process.

From an information-theoretic perspective, the increased GPCR (G-protein coupled receptor) activation rate improves the ability of the channel to capture gut-derived signals, thereby enhancing the reliability of signal transfer to the brain. This result emphasizes the potential for developing therapeutic interventions that modify SCFA levels or receptor sensitivities to mitigate neurological and psychiatric conditions associated with gut dysbiosis or impaired gut-brain communication. By carefully analyzing how different intracellular parameters affect both the fidelity and timing of the signaling process, strategies can be developed to refine communication efficiency.

Future investigations can extend these findings by exploring different microbial compositions and disease states marked by altered gut microbiota or encompassing additional biological routes such as endocrine and immune pathways. Through this broader perspective, further progress in understanding and manipulating gut-brain communication holds promise for advancing therapeutic strategies targeting both neurological and psychiatric disorders.

While this chapter successfully characterized a complete molecular-to-neural communication link, it focused on a unidirectional pathway. However, the significant complexity of the gut-brain axis lies in its bidirectional communication nature and the crucial role of feedback in maintaining homeostasis. The insights gained from modeling this single communication pathway are therefore foundational for the next stage of this research. The subsequent chapter will build upon these principles, expanding the scope from an isolated communication channel to a system-level network by developing a closed-loop communication model.

Chapter 3

CLOSED-LOOP BIDIRECTIONAL COMMUNICATION IN THE GUT-BRAIN AXIS

3.1 Introduction

Molecular communication (MC) is a bio-inspired paradigm that utilizes molecules as information carriers, establishing a quantitative framework to analyze biological signaling networks from an information and communication theoretical perspective [1, 77]. By modeling the transmission, reception, and propagation of signaling molecules, MC provides the theoretical tools to decipher complex biological processes, contrasting with conventional electromagnetic models that cannot capture the stochastic, diffusion-based nature of these systems. The MC paradigm is foundational to the emerging concept of the Internet of Bio Nano Things (IoBNT), which envisions the integration of biological and artificial nanoscale entities into a communication network for novel applications in healthcare, diagnostics, and personalized medicine [78, 47].

The human body operates as a highly complex biological system, relying on intricate signaling networks to maintain physiological homeostasis. Understanding the communication principles that govern these networks is critical for deciphering the mechanisms underlying health and disease. MC provides the necessary analytical framework to investigate these signaling networks. A quintessential example of such a network is the gut-brain axis (GBA), which is a bidirectional communication system linking the gastrointestinal tract and the central nervous system (CNS) [17, 6]. This axis integrates the gut and its vast microbial community with the brain, forming a complex information network that influences a wide range of physiological and psychological processes [106, 32].

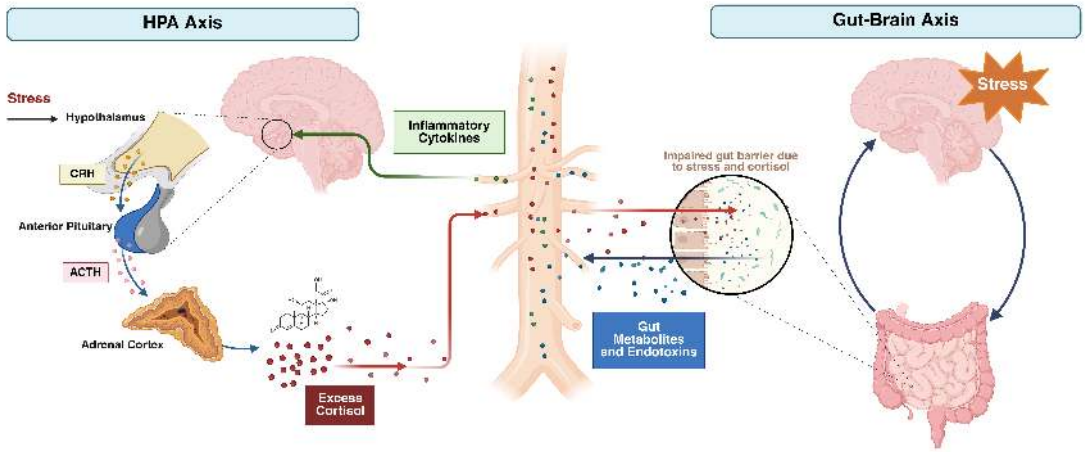

Figure 3.1: Illustration of bidirectional communication along the gut–brain axis via the HPA axis. (Created in https://BioRender.com).

The intricate communication within the GBA is facilitated by intertwined neural, immune, and endocrine channels that create a robust and dynamic network that is essential for homeostasis [107, 108]. The neural pathway provides rapid signaling through the vagus nerve and the enteric nervous system (ENS) [23, 17, 44]. The endocrine channel uses circulating neuroactive compounds often produced by the gut microbiota, while the immune channel relies on signaling molecules called cytokines to communicate with the brain [32, 109]. A principal neuroendocrine component of the GBA is the hypothalamic-pituitary-adrenal (HPA) axis, which is responsible for the core stress response system of the human body. The HPA axis operates as a closed-loop system where bottom-up signals from the gut, such as pro-inflammatory cytokines, trigger top-down neuroendocrine responses from the brain. These responses, in turn, modulate the gut environment by altering motility, secretion, and intestinal permeability, establishing a feedback cycle critical for homeostasis [110, 6]. As illustrated in Fig. 3.1, the integrity of this cycle is fundamentally dependent on the intestinal barrier, where increased permeability allows microbial-associated molecular patterns, like lipopolysaccharide (LPS), to translocate from the gut into the circulation. This translocation initiates a systemic inflammatory response that drives further bottom-up signaling through both humoral and neural

routes, perpetuating the cycle and directly impacting HPA axis regulation [17].

Dysregulation of signaling within the GBA is implicated in a broad spectrum of disorders, with strong links to stress-related physiological and psychological conditions [17, 107]. Both acute and chronic stress disrupt homeostasis by altering the composition of the gut microbiota, a state known as dysbiosis. This increases intestinal permeability, allowing pro-inflammatory molecules like LPS to translocate from the gut into the circulation, which triggers a systemic immune response [111]. This inflammatory signal activates the HPA axis, the body's primary stress response system. In a healthy individual, the HPA axis follows a cascade where corticotropin-releasing hormone (CRH) from the hypothalamus triggers the pituitary to release adrenocorticotropic hormone (ACTH), which causes the adrenal cortex to release cortisol. This cortisol then executes a negative feedback loop to restore homeostasis. However, under the persistent stimulation of chronic stress, this crucial regulatory feedback becomes impaired [110, 112, 113].

The persistent activation of the HPA axis leads to elevated levels of stress hormones like cortisol, which further weaken the gut barrier. This compromised barrier permits increased translocation of microbial components such as LPS into the bloodstream. The subsequent systemic immune response triggers the release of pro-inflammatory cytokines like interleukin 6 (IL-6) and tumor necrosis factor alpha (TNF-α), which further stimulates the HPA axis. This feedback loop sustains a state of low-grade systemic inflammation coupled with neuroendocrine dysregulation, a condition strongly implicated in the pathophysiology of mood disorders like depression and anxiety [106, 114]. The resulting state of chronic hypercortisolism impairs the HPA axis's negative feedback, leading to sustained hormone production and neurotoxic effects in brain regions critical for mood regulation, such as the hippocampus and prefrontal cortex. Evidence from both germ-free animal and clinical studies supports a causal role for the microbiota in this process, strengthening the motivation for a unified communication framework that models these microbial and host interactions [17, 6].

Given the complexity of the GBA, MC modeling is crucial for quantitatively

analyzing its signaling dynamics and uncovering the mechanisms that contribute to disease. Traditional systems-level frameworks often neglect critical features of biological signaling, such as molecular noise, spatial diffusion, and temporal delays. In contrast, MC provides a comprehensive and detailed modeling approach that intrinsically incorporates these dynamics through advection-diffusion and ligand-receptor interactions. This makes it a uniquely suitable methodology for quantitatively analyzing the intricate pathways of the GBA and deciphering how disruptions in these signaling pathways can lead to pathological states.

Existing research has established the foundation for analyzing the GBA using the MC approaches. Foundational work introduced the Microbiome-Gut-Brain Axis as a comprehensive biomolecular communication network, outlining the potential for IoBNT integration [79]. Subsequent studies have developed end-to-end MC models for specific gut-to-brain routes, including the signaling of the microbial metabolite p-cresol in the context of Autism Spectrum Disorder [43] and SCFA-driven vagus nerve signaling [44]. Concurrently, other research has explored the GBA at the synaptic scale, for instance by modeling neurotransmitter diffusion as a Molecular Quantum (MolQ) communication channel [80]. Collectively, these studies have clarified how molecular messages are produced, transported, and decoded along individual pathways and have demonstrated the value of communication-theoretic tools in this domain. However, the focus has remained mainly on unidirectional signaling or on isolated components of the axis, which limits insight into the system-level behavior that emerges when multiple channels interact within a feedback structure.

In this chapter, we address this gap by proposing a novel MC framework that models the GBA as a bidirectional, closed-loop network. While prior mathematical studies have coupled inflammatory cytokines to the HPA axis [113], a complete representation that closes the loop via the brain-to-gut pathway with its inherent time delays is still lacking. Therefore, we formulate a system of delay differential equations (DDEs) that explicitly links HPA axis activity to gut barrier integrity, thereby closing the communication loop. Utilizing the proposed model, we simulate the system's response to healthy, acute, and chronic stress profiles to characterize the transition

from homeostasis to a pathological state of hypercortisolism. Furthermore, we quantify the communication-channel performance by analyzing its stability, small-signal gain, and information-theoretic capacity, identifying key parameters that govern the system's dynamics. This approach moves beyond the analysis of individual pathways to provide a holistic, systems-level understanding of GBA dynamics in both health and disease. By conceptualizing this network as a communication channel, this chapter aims to:

- Formulate a system of delay differential equations (DDEs) to model the closed-loop dynamics between gut permeability, circulating endotoxin, pro-inflammatory cytokines (TNF-α, IL-6), and HPA axis hormones (ACTH, Cortisol).

- Simulate the response of the system to different stress profiles (healthy, acute, chronic) to characterize the transition from healthy circadian oscillations to a pathological state of hypercortisolism.

- Analyze the GBA as a communication channel by linearizing the model to derive its end-to-end transfer function.

- Quantify the channel's performance by calculating key communication metrics, including small-signal gain, bandwidth, and information-theoretic capacity, to understand how chronic stress impairs the GBA's ability to process information.

The rest of the chapter is organized as follows. Section 3.2 presents the bidirectional closed-loop molecular communication model and defines the six state variables, delay terms, and channel couplings. Section 3.3 reports the theoretical analysis and simulations, including healthy, acute, and chronic stress scenarios. It presents an analysis to identify stability thresholds and a frequency-domain analysis to quantify the channel's small-signal gain, bandwidth, and information-theoretic capacity. Section 3.4 interprets the results in the context of gut barrier control and hypothalamic-pituitary-adrenal regulation and identifies potential therapeutic targets. Section 3.5

summarizes the contributions, outlines limitations, and suggests directions for future work.

3.2 System Model

The GBA is a sophisticated, bidirectional communication network that is crucial for maintaining physiological and psychological homeostasis. The proposed framework models a vital feedback loop within this communication network, detailing the signaling mechanism between the HPA axis, immune activation, and gut barrier integrity. Under chronic stress conditions, this regulatory system transforms into a self-perpetuating process of inflammation and neuroendocrine dysregulation. The proposed model is developed to quantitatively examine these dynamics as a system of six coupled, nonlinear DDEs. The communication system is characterized by six primary signals, representing the concentrations or levels of endotoxin ($P(t)$), TNF-α ($T(t)$), IL-6 ($S(t)$), ACTH ($A(t)$), cortisol ($C(t)$), and gut permeability ($L(t)$).

3.2.1 Model Architecture and Signal Propagation

The model architecture is built upon three fundamental feedback loops that describe the communication network:

1. **The HPA Negative Feedback Loop:** Cortisol provides delayed (τ_{hpa}) negative feedback to inhibit ACTH and its own production, depicting the canonical endocrine regulatory mechanism.

2. **The Gut-to-Brain Inflammatory Pathway:** Systemic inflammation, driven by endotoxin (P) leaking from a compromised gut barrier, stimulates the HPA axis. Cytokines (T and S) promote the production of HPA hormones, i.e., ACTH and cortisol.

3. **The Brain-to-Gut Damage Pathway:** Elevated levels of cortisol increase gut permeability (L), leading to further endotoxin leakage via a delayed feedback mechanism (τ_{gut}).

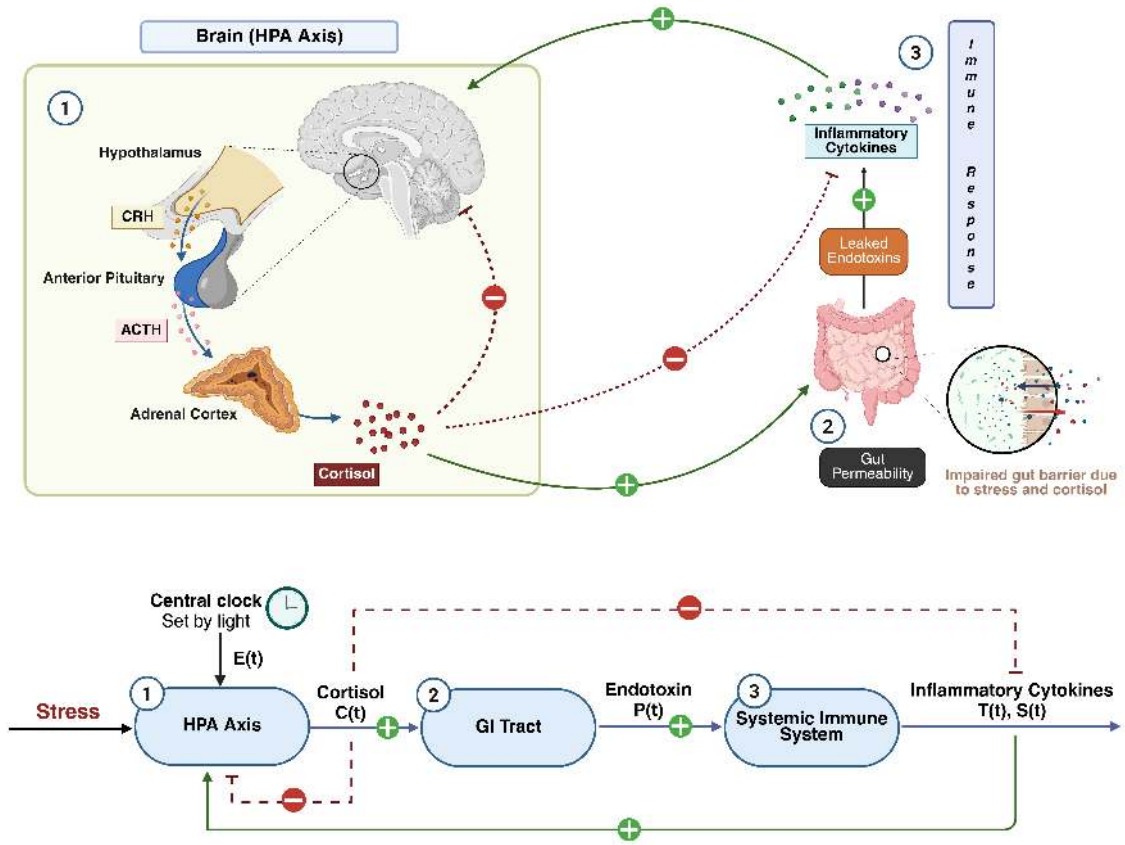

Figure 3.2: Closed-loop communication within the gut–brain axis via the HPA axis. (Created in https://BioRender.com).

These feedback loops initiate a self-perpetuating cycle under chronic stress conditions. The process begins when elevated cortisol (C) increases gut permeability (L) after a delay (τ_{gut}), allowing endotoxins (P) to enter the bloodstream. This triggers an immune response and the release of pro-inflammatory cytokines (T and S), which in turn transmit a powerful inflammatory signal back to the brain, stimulating the HPA axis to produce even more cortisol (C). This resulting surge of cortisol closes the loop by further damaging the gut barrier, thus reinforcing and sustaining the entire pathological cycle.

3.2.2 Molecular Communication Framework

Fig. 3.2 provides a schematic overview of the proposed closed-loop MC model. Within this MC framework, the system can be conceptualized as follows:

- **Input Signal**: An external stressor, which is modeled as an increase in the leakage rate of endotoxin molecules from the gut. This represents the initial trigger that perturbs the system from its healthy state.
- **Channel and Transmission Mechanism**: The entire bidirectional physiological cascade, encompassing the hormonal brain-to-gut pathway, the endotoxin-driven gut-to-immune pathway, and the cytokine-mediated immune-to-brain feedback loop.
- **Output Signal**: The plasma concentration of cortisol, $C(t)$, which reflects the system's overall response to the input stressor.

The dynamics of the proposed model are described by the rate of change for six key state variables ($L(t)$, $P(t)$, $T(t)$, $S(t)$, $A(t)$, $C(t)$). The following equations form a coupled system in which the output of one physiological process serves as the input to another. This interconnected structure mathematically defines the vital feedback loops that govern GBA regulation. The communication process is initiated by the **Brain → Gut** pathway, where the final output of the HPA axis, cortisol, modulates the integrity of the intestinal barrier. The state of gut permeability, $L(t)$, is modeled as a dynamic balance between cortisol-induced damage and the gut's natural repair mechanisms:

$$\frac{dL(t)}{dt} = \underbrace{k_{\text{damage}} \left(\frac{C(t-\tau_{\text{gut}})^{n_{\text{gut}}}}{C_{\text{half}}^{n_{\text{gut}}} + C(t-\tau_{\text{gut}})^{n_{\text{gut}}}} \right)}_{\text{Damage from Cortisol}} - \underbrace{k_{\text{repair}}(L(t) - L_{\text{base}})}_{\text{Natural Repair}}, \tag{3.1}$$

where the first term models the damage inflicted by past cortisol levels, $C(t-\tau_{\text{gut}})$, using a Hill function. This captures a nonlinear saturating effect where the damage rate increases with cortisol concentration but eventually plateaus. The time delay τ_{gut} accounts for hormonal circulation and cellular response time. The second term represents the gut's intrinsic capacity for self-repair, modeled as a linear process that drives the permeability level $L(t)$ back toward its healthy baseline L_{base}.

A compromised gut barrier allows endotoxin molecules to pass from the intestinal lumen into the bloodstream, initiating the **Gut** $\rightarrow$ **Immune** signaling pathway. The dynamics of the resulting plasma endotoxin concentration, $P(t)$, which serves as the input signal for the inflammation process, are described by:

$$\begin{aligned}\frac{dP(t)}{dt} = &\underbrace{k_{\text{leak}}L(t)}_{\text{Leakage from Gut}} - \underbrace{e_P P(t)}_{\text{Natural Clearance}} \\ &\underbrace{- d_1 \left(\frac{T(t)}{x_1 + T(t)}\right)\left(\frac{S(t)}{x_2 + S(t)}\right) P(t)}_{\text{Immune-Mediated Clearance}}.\end{aligned} \tag{3.2}$$

The production of endotoxin is proportional to the gut permeability (L) and modulated by the leakage rate k_{leak}, which is a result of the stress input. Endotoxin is subsequently cleared from circulation via a natural, first-order elimination process at a rate e_P, and also through a more potent clearance by the immune system, which is dependent on the pro-inflammatory cytokines TNF-α (T) and IL-6 (S).

The presence of endotoxin in the bloodstream triggers a pro-inflammatory cytokine cascade, starting with the production of TNF-α, whose dynamics are modeled as:

$$\frac{dT(t)}{dt} = -e_T T(t) + \underbrace{k\frac{P(t)}{x_3 + P(t)}}_{\text{Stimulation by LPS}} + \underbrace{\left(\frac{d_2}{x_4 + C(t)} + \frac{d_3}{x_5 + S(t)}\right)\left(\frac{T(t)}{x_6 + T(t)}\right)}_{\text{Self-Stimulation (Inhibited by Cortisol \& IL-6)}}. \tag{3.3}$$

The production of TNF-α is driven by endotoxin (P), a process modeled with Michaelis-Menten kinetics to capture saturation effects. The equation also incorporates a positive feedback term where TNF-α stimulates its production to amplify the immune signal rapidly. This self-amplification is tightly regulated, suppressed by the anti-inflammatory effects of both cortisol (C) and the secondary cytokine IL-6 (S), providing a crucial control mechanism.

TNF-α then stimulates the production of IL-6, a secondary cytokine with both pro- and anti-inflammatory roles. The dynamics of $S(t)$ are given by:

$$\frac{dS(t)}{dt} = -e_S S(t) + \underbrace{d_4\left(\frac{1}{x_7 + C(t)}\right)\left(\frac{T(t)}{x_8 + T(t)}\right)}_{\text{Stimulation by TNF-}\alpha\text{ (inhibited by cortisol)}}. \tag{3.4}$$

This equation shows that IL-6 is produced in response to TNF-α levels. The synthesis of IL-6 is strongly inhibited by cortisol, highlighting cortisol's systemic role in modulating and ultimately suppressing the inflammatory cascade.

The circulating cytokines transmit an inflammatory signal to the brain, representing the **Gut** $\rightarrow$ **Brain** pathway, which directly influences the HPA axis. The dynamics of the ACTH (A) model the pituitary's response, which is driven by the body's internal clock and feedback from both cortisol and the immune system:

$$\frac{dA(t)}{dt} = -e_A A(t) + \underbrace{(hE(t))\frac{c^{m_1}}{c^{m_1} + C(t-\tau_{\text{hpa}})^{m_1}}}_{\text{Circadian Drive and Cortisol Inhibition}} + \underbrace{d_5 \left(\frac{S(t)}{x_9 + S(t)}\right)\left(\frac{T(t)}{x_{10} + T(t)}\right)}_{\text{Stimulation by Cytokines}}. \tag{3.5}$$

ACTH (A) production is driven by a baseline stimulus h and modulated by a 24-hour circadian rhythm $E(t)$. This production is inhibited by delayed negative feedback from cortisol, $C(t-\tau_{\text{hpa}})$, and is stimulated by the inflammatory cytokines S and T, which convey the molecular alarm signals from the periphery to CNS.

Finally, cortisol (C) is the terminal output of the HPA axis, and its production completes the multiple feedback loops within the communication system. The cortisol dynamics are described by:

$$\frac{dC(t)}{dt} = -e_C C(t) + \underbrace{\alpha \frac{A(t-\tau_{\text{hpa}})^{m_2}}{a^{m_2} + A(t-\tau_{\text{hpa}})^{m_2}}}_{\text{Stimulation by ACTH}} + \underbrace{d_6 \left(\frac{S(t)}{x_{11} + S(t)}\right)\left(\frac{T(t)}{x_{12} + T(t)}\right)}_{\text{Stimulation by Cytokines}}. \tag{3.6}$$

Cortisol (C) is produced in response to past levels of ACTH ($A(t-\tau_{\text{hpa}})$). The inflammatory cytokines (S and T) also directly stimulate the cortisol production, providing a parallel pathway for the immune system to amplify the stress response. The produced cortisol then acts back on the gut and the immune cells, closing the overall gut-brain communication loop.

The system of coupled DDEs, with parameters specified in Table 3.1, forms the mathematical basis of our molecular communication framework for the closed-

Table 3.1: Model Parameters

Parameter	Description	Value
HPA Axis		
h	Baseline for ACTH production	7.66 (pg/mL)/min [113]
c	Half-saturation for cortisol inhibition	6.11 μg/dL [113]
m_1	Hill coefficient for cortisol inhibition	4 (dimensionless) [113]
α	Max production rate of cortisol	0.28 (μg/dL)/min [113]
a	Half-saturation for ACTH stimulation	21 pg/mL [113]
m_2	Hill coefficient for ACTH stimulation	4 (dimensionless) [113]
e_A	Elimination rate of ACTH	0.04 min^{-1} [113]
e_C	Elimination rate of Cortisol	0.01 min^{-1} [113]
τ_{hpa}	Time delay for HPA axis	10 min [113]
Immune System		
k	Production rate of TNF-α from LPS	0.0504 (ng/cL)/min [113]
e_P	Elimination rate of LPS	0.05 min^{-1} [113]
e_T	Elimination rate of TNF-α	0.038 min^{-1} [113]
e_S	Elimination rate of IL-6	0.02 min^{-1} [113]
Gut Permeability		
k_{damage}	Rate of cortisol-induced gut damage	0.002 min^{-1}
k_{repair}	Natural gut repair rate	0.05 min^{-1}
k_{leak}	Time-varying LPS leakage rate	scenario-specific (min^{-1})
L_{base}	Baseline healthy gut permeability	0.1 (dimensionless)
C_{half}	Cortisol half-saturation	15 μg/dL
n_{gut}	Hill coefficient	2 (dimensionless)
τ_{gut}	Time delay for cortisol	120 min

loop GBA. The parameter values for the HPA axis and immune components are adopted from the validated model by Malek et al. [113], ensuring a physiologically grounded core. The novel gut permeability parameters were estimated to align with established physiological behavior. This MC-based model systematically represents the key processes underlying the stress-induced pathological cycle by integrating the HPA axis, peripheral immune signaling, and gut barrier dynamics. Although this framework does not aim to capture all the biological complexities of the GBA, it highlights the critical signaling mechanisms and feedback loops that govern system stability. Therefore, the proposed end-to-end model offers a structured approach to

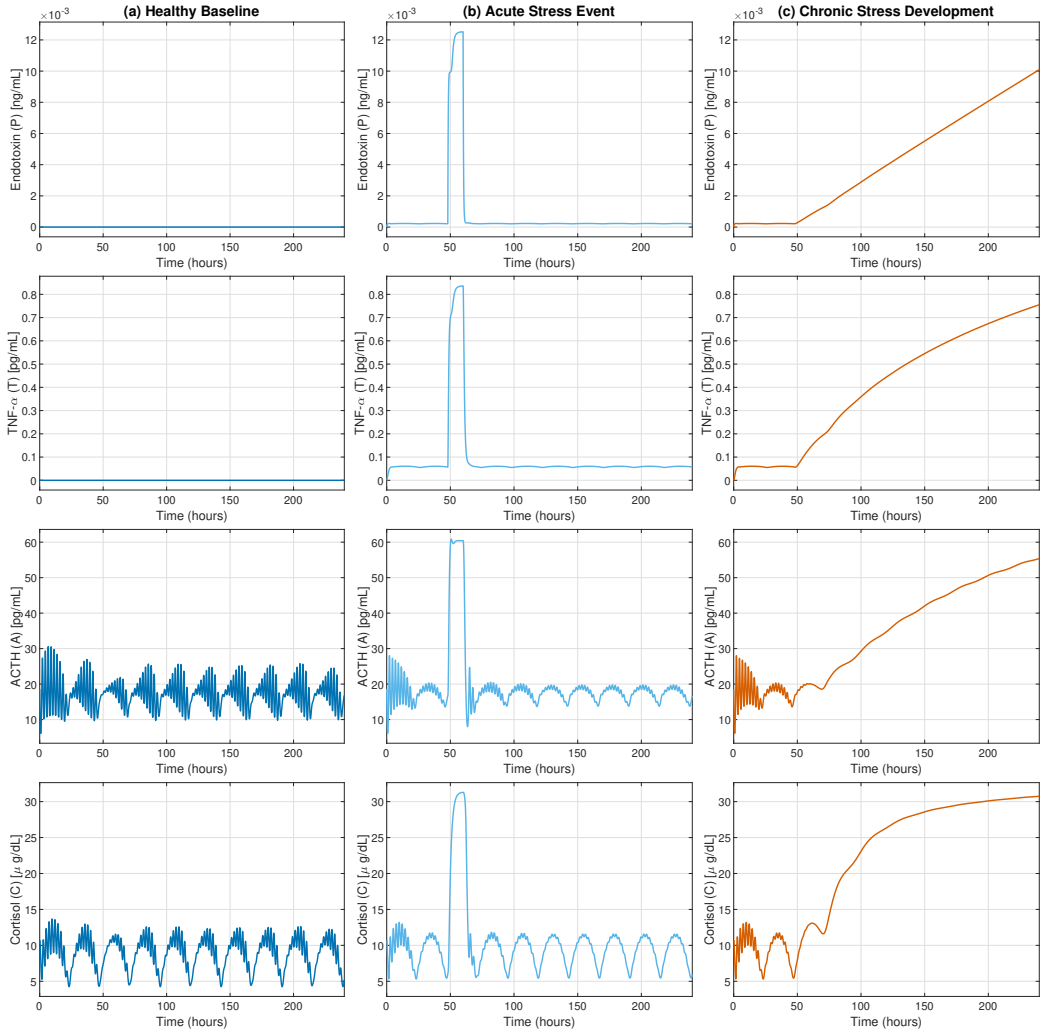

Figure 3.3: Comparative dynamics of the GBA network under three simulated stress scenarios. The columns depict the system's response to (a) a Healthy Baseline, (b) an Acute Stress event (a 12-hour pulse starting at hour 48), and (c) a Chronic Stress profile (initiated at hour 48). The rows display the time-course for the key signaling molecules: Endotoxin, TNF-α, ACTH, and Cortisol.

quantitatively analyze how the GBA responds to stress, providing a foundational basis for the theoretical analysis and the following numerical simulations.

3.3 Theoretical Analysis and Simulations

To investigate the dynamics of the proposed closed-loop GBA network, numerical simulations of the system of DDEs defined in Section 3.2 are conducted. The primary

objective of this analysis is to characterize the system's transition from a healthy, homeostatic state to a pathological, dysregulated state under different stress conditions. The DDE system was solved numerically in MATLAB using the `dde23` solver. The end-to-end system model is simulated under three distinct scenarios, each initiated by a different external stress input profile. The results, shown in Fig. 3.3, display the system's temporal response over a 10-day period.

3.3.1 Time-Domain Response to Stress Scenarios

Healthy Baseline In the healthy baseline scenario, the system represents a non-stressed state governed by its internal regulatory signaling mechanisms. As depicted in Fig. 3.3(a), the HPA axis operates under its canonical negative feedback, where cortisol production maintains stable circadian oscillations. Consequently, the effect of cortisol on the intestinal barrier is negligible, and gut permeability (L) is kept at a low baseline by natural repair processes. This ensures that the gut-to-brain inflammatory pathway, depicted in Fig. 3.2, remains quiescent. Circulating levels of endotoxin molecules and the pro-inflammatory cytokine TNF-α are therefore kept at basal concentrations, reflecting an intact gut barrier and an inactive immune state. This scenario demonstrates that in the absence of significant stressors, the GBA network successfully maintains homeostasis.

Acute Stress An acute stress event is modeled as a transient, 12-hour increase in the gut leakage rate k_{leak} starting at hour 48. This perturbation raises circulating endotoxin, which triggers a rapid cytokine response and, in turn, stimulates the HPA axis. The HPA axis activation causes a surge in ACTH and cortisol that overrides the normal circadian rhythm, as seen in Fig. 3.3(b). After the τ_{gut} delay, this elevated cortisol increases gut permeability, leading to a temporary dysfunction of the gut barrier.

The resulting temporary gut barrier dysfunction allows a further influx of endotoxin into systemic circulation, which activates the gut-to-brain inflammatory communication channel. This acts as a potent molecular signal, initiating a tran-

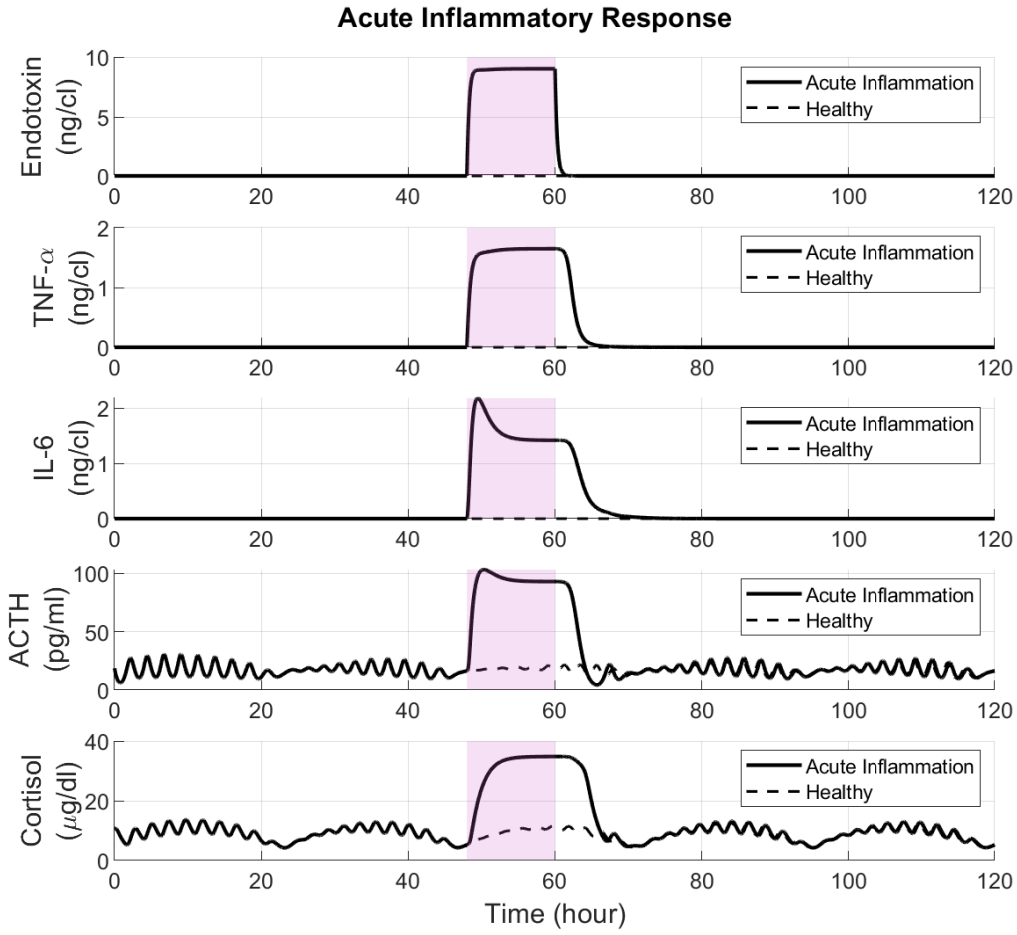

Figure 3.4: Dynamics of the acute inflammatory cascade following a transient endotoxin leakage.

sient but robust inflammatory cascade characterized by a sharp rise in TNF-α and subsequently IL-6 as illustrated in Fig. 3.4. These circulating cytokine molecules constitute a secondary, delayed stimulatory signal that propagates back to the HPA axis, amplifying the initial cortisol peak and closing the bidirectional communication loop depicted in Fig. 3.2. Once the external stressor is removed, the hyperactivation of the HPA axis ceases, resulting in a fall in cortisol levels. This facilitates the repair of the gut barrier, which terminates the endotoxin leakage and the subsequent inflammatory feedback signal. Within approximately 48 hours (Fig. 3.4), the system returns to its homeostatic circadian rhythm, underlining its capacity to manage and

recover from acute physiological challenges effectively.

Chronic Stress Scenario Chronic stress is modeled as a sustained elevation of k_{leak}, which causes persistent activation of the HPA axis. This continuous primary input leads to chronically elevated cortisol levels, representing a dysregulated neuroendocrine output. This signal propagates down the brain-to-gut pathway, where the sustained high cortisol inflicts continuous damage on the intestinal barrier, leading to a progressive and lasting increase in gut permeability. As shown in Fig. 3.3(c), this sustained permeability results in chronic endotoxin leakage, establishing a state of persistent, low-grade systemic inflammation due to elevated endotoxin and TNF-α.

This inflammatory signal that feeds back to the brain via the gut-to-brain pathway. This feedback route, as conceptualized in Fig. 3.2, becomes the dominant driver of HPA axis activity, overriding the canonical negative feedback mechanism. Unlike in the acute scenario, the system fails to recover and instead enters the pathological state. It becomes trapped in a self-reinforcing loop where elevated cortisol damages the gut barrier and leads to more inflammation that drives cortisol even higher. This demonstrates how a chronic stressor can push the GBA network past a tipping point, locking it into a diseased state characterized by a complete loss of circadian rhythm and a flat profile of hypercortisolism.

3.3.2 Bifurcation Analysis and Tipping Points

To investigate the system's resilience to stress, a one-parameter bifurcation analysis was performed to identify the critical thresholds at which the GBA network transitions from healthy to pathological state. The analysis involved systematically sweeping the constant external stress input, represented by the k_{leak}, across a range of values. For each stress level, the stability of the resulting cortisol oscillation was quantified to map the response of the end-to-end communication system.

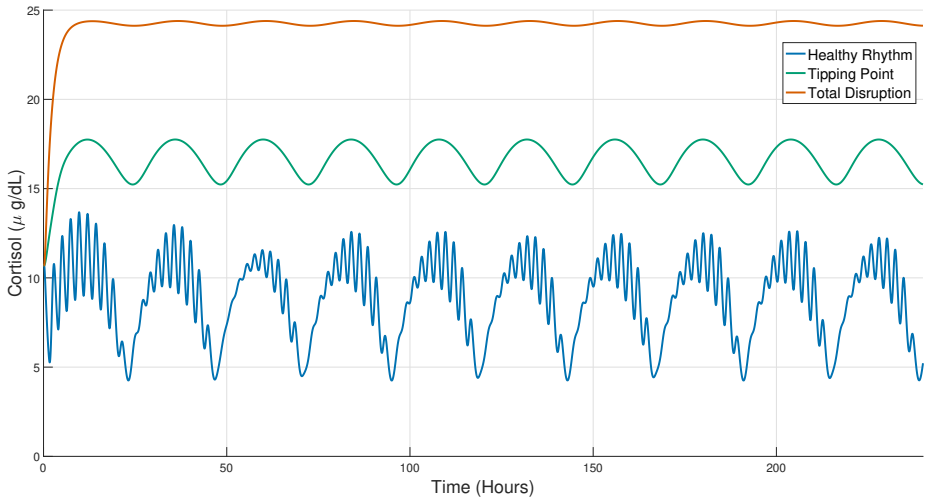

Figure 3.5: Results of the numerical bifurcation sweep identifying critical thresholds for system stability.

The results of this analysis are summarized in Fig. 3.5, which compares the system's steady-state cortisol dynamics at three key identified points.

1. *Healthy Rhythm:* In the absence of external stress, the system exhibits robust, stable circadian oscillations. This represents a healthy, homeostatic state where the HPA axis's natural negative feedback loop is dominant. This state corresponds to a resilient channel capable of efficiently processing signals.

2. *The Tipping Point:* As the stress level increases, the system reaches its first critical threshold at a stress input leading $k_{\text{leak}} \approx 1.52$ min^{-1}. At this tipping point, the pathological positive feedback from the gut-to-brain inflammatory pathway becomes strong enough to compete with the HPA axis's regulatory negative feedback, significantly dampening the cortisol rhythm and marking the onset of a dysregulated state.

3. *Total Disruption:* A further increase in stress pushes the system past a second threshold that represents $k_{\text{leak}} \approx 2.04$ min^{-1}. After this point, the self-perpetuating inflammatory feedback loop completely overpowers the system's

natural regulation, and the circadian oscillation ceases entirely. The system becomes locked in a stable pathological state of hypercortisolism, which corresponds to a state of communication failure with a severely compromised ability to process information.

This bifurcation analysis, therefore, reveals that the shift from health state to pathology is not gradual but occurs at distinct tipping points. This denotes a fundamental change in the system's dynamics. The following section provides a detailed frequency-domain analysis to deepen the understanding of the changes in the channel properties that drive this resilience loss.

3.3.3 Frequency Domain Analysis

To further characterize the GBA as a communication channel, the time-domain simulations are complemented by a frequency-domain analysis. Since the system model described in Sec. 3.2 is nonlinear and includes explicit delays, a small-signal analysis is performed. In this method, the system is linearized about a stable operating point, from which a transfer function characterizing the response to small perturbations is derived. For this analysis, the six-state DDE system is defined in the following compact state-space form:

$$\begin{aligned} \dot{x}(t) &= f\big(x(t),\, x(t-\tau_{\mathrm{hpa}}),\, x(t-\tau_{\mathrm{gut}}),\, u(t)\big) \\ y(t) &= C(t), \end{aligned} \tag{3.7}$$

where the state vector $x(t)$ and its time derivative $\dot{x}(t)$ are column vectors defined as:

$$x(t) = \begin{bmatrix} P(t) \\ T(t) \\ S(t) \\ A(t) \\ C(t) \\ L(t) \end{bmatrix}, \qquad \dot{x}(t) = \begin{bmatrix} dP(t)/dt \\ dT(t)/dt \\ dS(t)/dt \\ dA(t)/dt \\ dC(t)/dt \\ dL(t)/dt \end{bmatrix}. \tag{3.8}$$

Within this state-space framework, the input is defined as $u(t) \triangleq k_{\text{leak}}(t)$, and the output $y(t)$ is the cortisol concentration, selected via the vector $\mathbf{C}_{\text{out}} = [0, 0, 0, 0, 1, 0]$. The function f represents the complete set of six coupled differential equations from Section 3.2. To linearize the system, a stationary operating point, $x^\star$, must first be found. This equilibrium state is determined by fixing the time-varying circadian drive at its mean, $E(t) \equiv \bar{E}$, setting the input to a constant baseline value, $u^\star$, and numerically solving the algebraic system $f(x^\star, x^\star, x^\star, u^\star) = 0$.

The nonlinear system is then approximated by a linear model that is valid for small perturbations, $\delta x(t) = x(t) - x^\star$, around this equilibrium. A first-order Taylor expansion yields the linear model:

$$\begin{aligned} \delta\dot{x}(t) = \mathbf{J}_0\, \delta x(t) + \mathbf{J}_{\text{hpa}}\, \delta x(t - \tau_{\text{hpa}}) \\ + \mathbf{J}_{\text{gut}}\, \delta x(t - \tau_{\text{gut}}) + \mathbf{B}\, \delta u(t), \end{aligned} \tag{3.9}$$

The system matrices are the Jacobians, which are composed of the partial derivatives of the system function f evaluated at the equilibrium point ($|_\star$). The instantaneous Jacobian, $\mathbf{J}_0$, is a 6x6 matrix describing the immediate influence of each state variable on every other:

$$\mathbf{J}_0 = \left.\frac{\partial f}{\partial x}\right|_\star = \begin{bmatrix} \frac{\partial(dP/dt)}{\partial P} & \cdots & \frac{\partial(dP/dt)}{\partial L} \\ \vdots & \ddots & \vdots \\ \frac{\partial(dL/dt)}{\partial P} & \cdots & \frac{\partial(dL/dt)}{\partial L} \end{bmatrix}_\star . \tag{3.10}$$

The matrices representing the delayed feedback effects are sparse, as they isolate only the specific delayed interactions. The matrix $\mathbf{J}_{\text{hpa}}$ captures the delayed HPA axis feedback. Since only the equations for dA/dt and dC/dt depend on delayed cortisol and ACTH respectively, its form is:

$$\mathbf{J}_{\text{hpa}} = \left.\frac{\partial f}{\partial x_{\text{hpa}}}\right|_\star = \begin{bmatrix} 0 & 0 & 0 & 0 & 0 & 0 \\ 0 & 0 & 0 & 0 & 0 & 0 \\ 0 & 0 & 0 & 0 & 0 & 0 \\ 0 & 0 & 0 & 0 & \frac{\partial(dA/dt)}{\partial C(t-\tau_{\text{hpa}})} & 0 \\ 0 & 0 & 0 & \frac{\partial(dC/dt)}{\partial A(t-\tau_{\text{hpa}})} & 0 & 0 \\ 0 & 0 & 0 & 0 & 0 & 0 \end{bmatrix}_\star . \tag{3.11}$$

Similarly, $\mathbf{J}_{\text{gut}}$ captures only the delayed effect of cortisol on gut permeability:

$$\mathbf{J}_{\text{gut}} = \left.\frac{\partial f}{\partial x_{\text{gut}}}\right|_\star = \begin{bmatrix} 0 & 0 & 0 & 0 & 0 & 0 \\ 0 & 0 & 0 & 0 & 0 & 0 \\ 0 & 0 & 0 & 0 & 0 & 0 \\ 0 & 0 & 0 & 0 & 0 & 0 \\ 0 & 0 & 0 & 0 & 0 & 0 \\ 0 & 0 & 0 & 0 & \frac{\partial(dL/dt)}{\partial C(t-\tau_{\text{gut}})} & 0 \end{bmatrix}_\star . \tag{3.12}$$

The input matrix $\mathbf{B}$ represents how the input perturbation $u(t)$ affects the system's states Since $u(t)$ only appears in the equation for dP/dt, the $\mathbf{B}$ is obtained as:

$$\mathbf{B} = \left.\frac{\partial f}{\partial u}\right|_{\star} = \begin{bmatrix} \partial(dP/dt)/\partial u \\ 0 \\ 0 \\ 0 \\ 0 \\ 0 \end{bmatrix}_{\star} = \begin{bmatrix} L^{\star} \\ 0 \\ 0 \\ 0 \\ 0 \\ 0 \end{bmatrix}. \tag{3.13}$$

Note that the linearization of the product term $k_{\text{leak}}L(t)$ from the endotoxin equation yields two distinct components. The first, which enters the input matrix $\mathbf{B}$, shows that the input's effect is scaled by the baseline permeability $L^{\star}$. The second, which is added to the instantaneous Jacobian matrix $\mathbf{J}_0$, reflects that the baseline leakage rate $u^{\star}$ modulates the coupling between permeability and endotoxin.

Applying the Laplace Transform to the linearized model (3.9) converts the system into the following algebraic equation in the frequency domain ($s = j\omega$):

$$sX(s) = \left(\mathbf{J}_0 + \mathbf{J}_{\text{hpa}}e^{-s\tau_{\text{hpa}}} + \mathbf{J}_{\text{gut}}e^{-s\tau_{\text{gut}}}\right)X(s) + \mathbf{B}\,U(s). \tag{3.14}$$

The output of the end-to-end communication channel is the cortisol concentration, $Y(s)$, which is selected from the state vector using the vector $\mathbf{C}_{\text{out}} = [0, 0, 0, 0, 1, 0]$. The end-to-end transfer function, $H(s)$, is obtained by taking the ratio of this specific output to the input, $H(s) = Y(s)/U(s)$:

$$H(s) = \mathbf{C}_{\text{out}}\left(s\mathbf{I} - \mathbf{J}_0 - \mathbf{J}_{\text{hpa}}e^{-s\tau_{\text{hpa}}} - \mathbf{J}_{\text{gut}}e^{-s\tau_{\text{gut}}}\right)^{-1}\mathbf{B}. \tag{3.15}$$

The transfer function in (3.15) provides a complete input-to-output description of the linearized system. In this expression, the vector $\mathbf{C}_{\text{out}}$ selects cortisol as the output, and $\mathbf{B}$ maps the input signal to its initial state. The matrix $\mathbf{J}_0$ captures the

instantaneous system dynamics, while the exponential terms containing $\mathbf{J}_{\text{hpa}}$ and $\mathbf{J}_{\text{gut}}$ incorporate the crucial feedback delays.

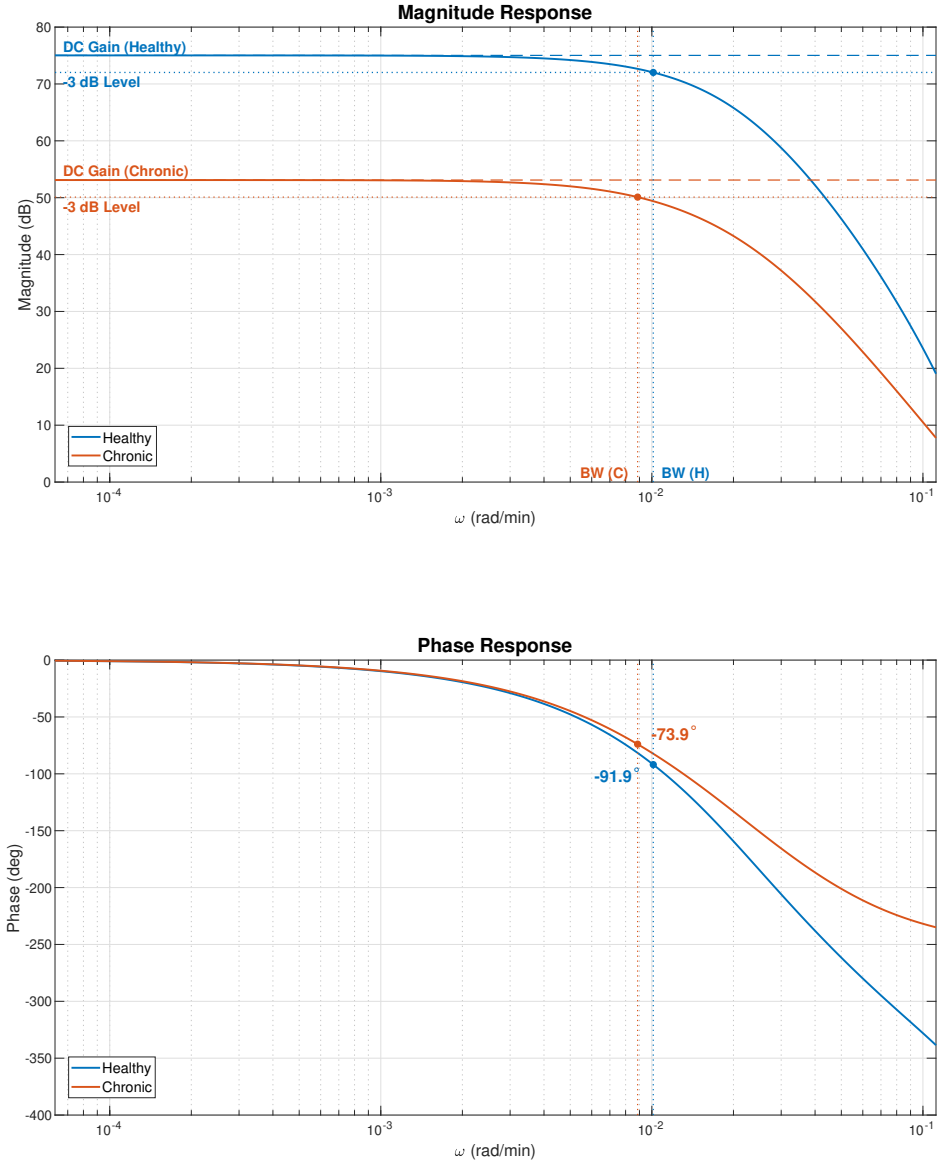

Figure 3.6: Magnitude and phase response of the linearized GBA channel.

The frequency response of the GBA channel, obtained by evaluating the transfer function at $s = j\omega$, reveals its core signal-processing characteristics. As illustrated

in Fig. 3.6, the channel behaves as a high-order low-pass filter. This behavior is governed by the slow biochemical elimination and repair kinetics, which enable the system to naturally attenuate rapid, high-frequency fluctuations. The explicit time delays in the model introduce a substantial, frequency-dependent phase lag, a critical factor that governs the system's closed-loop stability. Since the model is linearized around a fixed point by freezing the circadian input $E(t)$ at its mean, it does not capture the dominant 24-hour resonance of the full nonlinear system. A more rigorous treatment would require periodic (Floquet) linearization. It is important to note that this linearization operation is valid only in the vicinity of a locally asymptotically stable equilibrium point, $x^\star$. Outside this stable regime, the frequency response is not predictive.

3.3.4 Quantitative Performance Metrics: DC Gain and Bandwidth

The transfer function, (3.15), provides a basis for quantifying the channel's performance using standard metrics. Two key metrics, the static (DC) gain and the bandwidth, are used to summarize the end-to-end behavior of the linearized GBA channel.

The DC gain is found by evaluating the transfer function at zero frequency:

$$H(0) \;=\; -\,\mathbf{C}_{\text{out}}\big(\mathbf{J}_0 + \mathbf{J}_{\text{hpa}} + \mathbf{J}_{\text{gut}}\big)^{-1}\mathbf{B}. \tag{3.16}$$

A large magnitude of $|H(0)|$ indicates strong amplification of a persistent change in gut leakage into a steady offset in cortisol. As the system's operating point approaches a bifurcation threshold (a tipping point), the total system matrix, $\mathbf{J}_\Sigma \triangleq \mathbf{J}_0 + \mathbf{J}_{\text{hpa}} + \mathbf{J}_{\text{gut}}$, becomes ill-conditioned, causing $|H(0)|$ to grow significantly. The DC gain therefore serves as an indicator for the system's proximity to a loss of stability.

The responsiveness of the channel is characterized by its bandwidth. The half-power bandwidth, $\omega_{3\text{dB}}$, is a standard metric defined as the frequency at which the

channel's gain drops to $1/\sqrt{2}$ (or -3 dB) of its DC value:

$$|H(j\omega_{3\mathrm{dB}})| = \frac{|H(0)|}{\sqrt{2}}. \tag{3.17}$$

The DC gain $|H(0)|$ quantifies the steady-state sensitivity to persistent changes in k_{leak}, whereas the half-power bandwidth $\omega_{3\mathrm{dB}}$ summarizes the channel's responsiveness to changing inputs. As illustrated in Fig. 3.6, the healthy operating point exhibits a broader effective passband than the chronic state, consistent with the bandwidth narrowing expected near a loss of resilience. These two metrics provide the basis for interpreting the information-theoretic results that follow.

3.3.5 Information-Theoretic Channel Capacity

The transfer function provides a basis for calculating the channel's information-theoretic capacity, which defines the maximum rate of reliable information transmission for small perturbations. To perform this calculation, the linearized GBA channel is modeled as a continuous-time, single-input single-output (SISO) system with additive noise:

$$y(t) = \big(h * u\big)(t) + n(t), \tag{3.18}$$

where $h(t)$ is the impulse response corresponding to the transfer function $H(s)$, $u(t)$ is the input perturbation to k_{leak}, and $n(t)$ is a zero-mean, stationary Gaussian noise process with power spectral density (PSD) $S_n(\omega)$. The input signal is constrained by an average power budget, P_{av}:

$$\frac{1}{2\pi}\int_{-\infty}^{\infty} S_u(\omega)\, d\omega \le P_{av}, \tag{3.19}$$

For a stable LTI channel with wide-sense stationary Gaussian noise, a power-

constrained Gaussian input achieves the Shannon capacity, which is defined as [115]:

$$C = \frac{1}{2\pi} \int_{-\infty}^{\infty} \log_2 \left(1 + \frac{|H(j\omega)|^2 \, S_u^\star(\omega)}{S_n(\omega)} \right) d\omega, \tag{3.20}$$

where $S_u^\star(\omega)$ is the optimal input power spectrum that maximizes the capacity. This optimal spectrum is found using the "water-filling" algorithm, which strategically allocates more power to frequencies where the channel gain is high and the noise is low:

$$S_u^\star(\omega) \;=\; \max \left\{ 0,\; \mu - \frac{S_n(\omega)}{|H(j\omega)|^2} \right\}, \tag{3.21}$$

where the constant μ (the "water level") is chosen to satisfy the total power constraint, $\dfrac{1}{2\pi} \displaystyle\int_{-\infty}^{\infty} S_u^\star(\omega) \, d\omega = P_{\text{av}}$.

The water-filling algorithm allocates input power strategically to maximize information flow. It assigns more power to frequencies with a higher signal-to-noise ratio (SNR) density, given by the term $|H(j\omega)|^2/S_n(\omega)$. For a low-pass channel such as the GBA, this generally concentrates power within the effective passband. However, the allocation is not a hard cutoff at a specific frequency but smoothly follows the entire SNR profile. A crucial property of this formula is that capacity depends on the channel's magnitude response, $|H(j\omega)|$, and the noise PSD. The channel's phase response does not affect the total capacity. In our model, the physiological time delays ($\tau_{\text{hpa}}, \tau_{\text{gut}}$) are critical because they indirectly alter the capacity by reshaping the magnitude response, as captured in the transfer function (3.15).

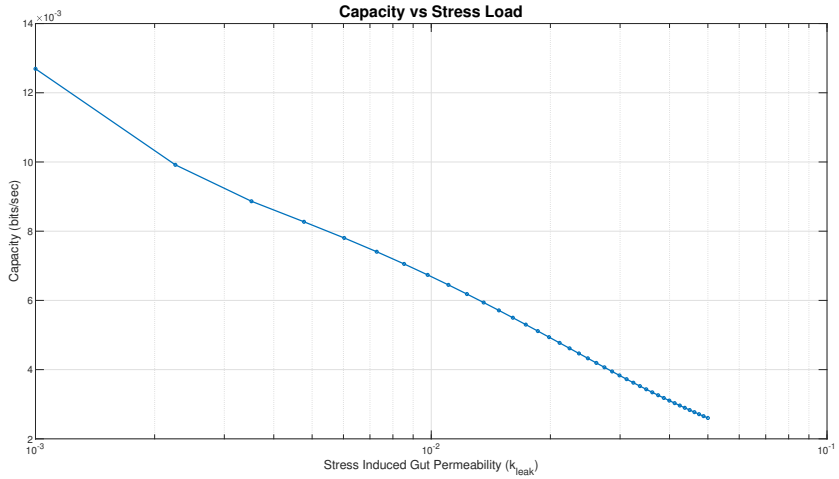

Figure 3.7: Information-theoretic channel capacity as a function of stress-induced leakage rate (k_{leak}).

The capacity in (3.20) is a small-signal upper bound for the linearized, stable operating point with Gaussian noise and an average-power constraint. The achievable rate in a real biological context would be lower due to factors such as non-Gaussian disturbances and physiological amplitude constraints on the signaling molecules. As the transfer function $H(s)$ depends on the equilibrium, the capacity is also operating-point dependent. As shown in Fig. 3.7, this capacity varies as the system transitions from healthy to stressed states, revealing that increasing chronic stress levels progressively degrade the channel's ability to transmit information reliably.

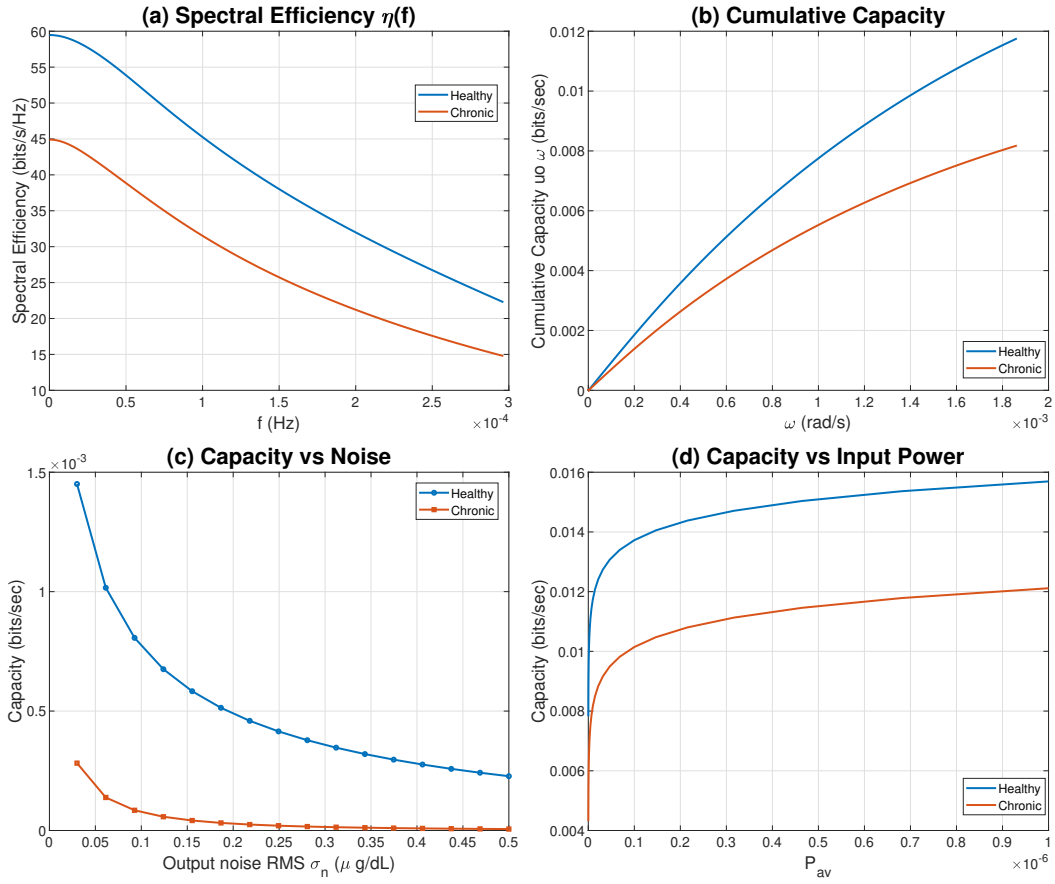

Figure 3.8: Detailed analysis of channel capacity for healthy and chronic stress states.

To further examine the communication impairment, Fig. 3.8 provides a detailed comparison between the healthy and chronic stress operating points. In Fig. 3.8 (a), the spectral efficiency $\eta(f)$ (bits/s/Hz) is concentrated at low frequencies f, and the healthy state exhibits a higher peak and a broader effective passband, consistent with a wider usable bandwidth. In Fig. 3.8(b), the cumulative capacity $C(\omega) = \int_0^{\omega} \eta\big(\omega'/(2\pi)\big)\, \frac{d\omega'}{2\pi}$ (with ω in rad/s) rises more rapidly and reaches a larger value in the healthy state, confirming greater total information throughput. In Fig. 3.8 (c), capacity decreases monotonically as the output noise level increases, while the healthy state preserves a consistent advantage that indicates superior robustness. In Fig. 3.8 (d), capacity increases concavely with the input power budget and shows diminishing returns at high power. The healthy state achieves higher

rates for any fixed power, demonstrating better power efficiency. Collectively, the results quantify the communication performance deficit under chronic stress since chronic stress squeezes the usable spectrum, reduces passband gain, and limits the information processing capability of the GBA channel. The outcomes demonstrate that the pathological state is characterized not only by hormonal dysregulation but also by a fundamental impairment in the ability to process and transmit information reliably and efficiently.

3.4 Discussion

This work introduces a novel molecular communication framework that models the gut-brain axis (GBA) as a closed-loop system governed by delayed feedback mechanisms. The proposed model, which integrates gut barrier dynamics with the canonical HPA axis and peripheral immune signaling, enables a quantitative analysis of how bidirectional communication governs the body's response to stress for changing conditions. The time-domain simulations reveal the GBA's two distinct operational regimes. In the healthy state, HPA axis-driven negative feedback dominates, enabling the stable circadian cortisol rhythms observed in Fig. 3.3(a). The system demonstrates rapid recovery from acute stressors (Fig. 3.3(b) and Fig. 3.4) since the end-to-end channel behaves as a high-order low-pass filter around its homeostatic operating point. This low-pass characteristic, which arises from the slow biochemical kinetics and explicit time delays, allows the system to attenuate transient, high-frequency perturbations effectively. However, a sustained stress input ignites a pathological positive feedback loop where cortisol-induced gut damage drives inflammation, which in turn stimulates more cortisol release. This self-reinforcing cycle leads to the collapse of circadian oscillations shown in Fig. 3.3(c). Although the delay-induced phase is negligible at very low frequencies, it accumulates with frequency and progressively erodes the effectiveness of negative feedback. This explains why short, high-frequency perturbations are attenuated while prolonged inputs can shift the operating point and unlock the self-reinforcing loop.

The transition from a healthy to a pathological state is not gradual but occurs at

critical thresholds identified as tipping points in the bifurcation analysis of Fig. 3.5. As the system approaches these thresholds, it exhibits a clear signature of critical slowing down, resulting in a significant narrowing of its communication bandwidth (Fig. 3.6). This narrowing mathematically corresponds to the dominant eigenvalues of the system's Jacobian matrix approaching the imaginary axis, indicating longer recovery times. While the approach to a bifurcation is typically marked by increasing static gain, comparison of the final stable equilibria reveals that the DC gain is substantially lower in the chronic state than in the healthy one. This occurs because the chronic high-cortisol equilibrium drives the system into a saturated regime. At this high operating point, the nonlinear Hill functions in the model desensitize the feedback loops, reducing the system's local linear sensitivity to small perturbations. Therefore, the pathological state is characterized by a communication channel that is both less responsive, as shown by the narrower bandwidth, and less sensitive to persistent inputs, as reflected by the reduced DC gain.

An information-theoretic analysis translates these dynamic changes into quantitative performance metrics. The chronic stress state is characterized by a compressed usable spectrum, reduced total throughput, and lower resilience to noise, as detailed in Fig. 3.7 and Fig. 3.8. This degradation in communication performance directly results from the altered channel transfer function, $H(s)$, in the chronic state. Channel capacity is fundamentally determined by integrating the spectral efficiency, which is a function of the signal-to-noise ratio (SNR), across the usable frequency spectrum. As shown in Fig. 3.6, the chronic equilibrium results in a channel with a lower passband gain ($|H|$) and a narrower bandwidth. These changes directly reduce the SNR over the frequencies, which lowers the spectral efficiency. When integrated, this diminished spectral efficiency results in a lower total channel capacity, as confirmed by the water-filling evaluation. This analysis demonstrates that the pathology involves not just hormonal dysregulation but a fundamental degradation of the GBA's ability to transmit information reliably. This suggests that communication metrics such as channel capacity could serve as holistic biomarkers of GBA health.

The simulation outcomes validate the proposed end-to-end closed-loop commu-

nication model. The stable circadian rhythms in the healthy baseline confirm the proper implementation of the HPA axis's dominant negative feedback loop. The system's ability to recover from acute stress validates the low-pass filter characteristic created by the model's slow biochemical kinetics, which correctly attenuates transient perturbations. Finally, the simulated collapse into a chronic state of hypercortisolism confirms that the model accurately captures the pathological positive feedback loop that emerges when sustained stress engages the system's nonlinearities and time delays. These observations show that the proposed framework successfully maps core physiological mechanisms to their expected dynamic behaviors.

The proposed framework also illustrates potential therapeutic targets for restoring healthy communication. The results suggest that interventions aimed at strengthening gut barrier integrity, enhancing the clearance of inflammatory molecules, or weakening the stimulatory coupling between cytokines and the HPA axis are all expected to increase system resilience. This modeling approach thus enables the in-silico exploration of treatments designed to shift the system's operating point away from the pathological region and restore robust information flow within the GBA.

3.5 Conclusion

This chapter introduces a novel, end-to-end molecular communication framework which models the gut-brain axis as a fully integrated, closed-loop system. The model is formulated as a system of six coupled delay differential equations that explicitly unites three critical physiological subsystems, namely the integrity of the gut barrier, the dynamics of pro-inflammatory cytokines, and the neuroendocrine signaling of the HPA axis. This unified structure provides a powerful tool for investigating how bidirectional communication between the gut and brain governs the body's response to stress.

The developed communication framework uncovers the fundamental mechanism of stress-induced pathology. Quantitative analysis demonstrates that prolonged stress drives the GBA past a tipping point, shifting its dynamics from a stable state of negative feedback to a pathological one dominated by a self-perpetuating

positive feedback loop. This study quantifies this state transition using communication theory, establishing a direct link between the loss of physiological stability and a severe degradation in channel performance. The pathological state is characterized by a reduced bandwidth, lower information capacity, and decreased robustness to molecular noise. This framework provides a novel understanding that GBA dysregulation is a fundamental impairment of the body's information processing, rather than just a hormonal imbalance.

This comprehensive model enables the uncovering of communication mechanisms within the GBA, paving the way for unprecedented applications to explore diverse scenarios and communication pathways. By systematically linking physiological conditions to information processing metrics such as passband gain, effective bandwidth, noise resilience, and channel capacity, this framework enables the in-silico screening of therapeutic interventions. This communication-centric approach promises to re-establish reliable information flow, offering new possibilities for treating stress-related disorders. As the culminating work of this thesis, these results complete the progression from unidirectional (Chapters 1–2) to closed-loop modeling of the GBA, establishing a quantitative basis for IoBNT-guided diagnostic and therapeutic strategies. Future work will focus on validating these predictions with clinical data and extending the model to include other key signaling pathways for patient-specific personalization.

Chapter 4

CONCLUSION

This thesis has established a novel and rigorous foundation for understanding and quantitatively analyzing the gut-brain axis by conceptualizing it as a complex, multi-scale communication network. This work is founded on the principle that the intricate signaling connecting the gut, microbiome, and the nervous system can be deciphered as a sophisticated information processing system. To achieve this, we employed the principles of Molecular Communication (MC) to translate biological signaling mechanisms into a structured engineering framework by mapping the physiological components to quantifiable communication counterparts i.e., transmitters, propagation channels, and receivers. MC approaches address the inherent challenges of the GBA signaling, including its stochasticity, nonlinearity, and multi-modal signaling pathways. The developed MC-based framework allows for the quantitative assessment of the system performance using metrics such as impulse response, mutual information, signaling delay, and channel capacity.

Building on this foundation, the thesis provides a deepened understanding of the gut-brain axis in a deliberate, step-by-step manner. The investigation begins with the fundamental process of molecular transport, modeling the propagation of a single microbial metabolite. Then, it advances to analyze the complete molecular-to-neural transduction process, from receptor binding event to action potential generation and neurotransmitter release. The research culminates in a system-level analysis of a bidirectional, closed-loop network, creating a coherent framework that connects microscopic biochemical signaling events to macroscopic health and disease condition.

The detailed conclusions reached in the chapters are given below.

In the Chapter 1, we introduced a foundational MC-based channel model for p-

cresol signaling in autism spectrum disorder (ASD), establishing the first communication-theoretic analysis of this specific gut-brain pathway. The model characterized the flow-dominant propagation of p-cresol molecules from the gut environment through the bloodstream to the brain, accounting for advection-diffusion dynamics in cylindrical blood vessels. We derived the impulse response of this biological channel and analyzed how key physiological parameters, including blood vessel diameter, transmitter-receiver distance, and receiver dimensions, affect signal propagation characteristics. Numerical simulations validated our theoretical derivations and demonstrated that elevated p-cresol concentrations resulting from gut dysbiosis lead to enhanced system response and rapid inhibition of dopamine β-hydroxylase enzymes in the brain. This work established the fundamental MC framework for analyzing microbial metabolite signaling through GBA. It provided crucial insights into how altered gut microbiota composition can directly affect brain chemistry through well-defined communication channels. The results showed that increasing the transmitter-receiver distance could prolong the system's response time, while increasing blood vessel diameter decreased the observation probability of signaling molecules. This work successfully applied communication engineering principles to provide a baseline for understanding the physical layer of gut-brain axis communication. The resulting quantitative framework directly links gut dysbiosis to a specific neurological outcome, affirming the power of this approach for analyzing biological pathways [43].

Chapter 2 presented a comprehensive end-to-end model for short-chain fatty acid (SCFA)-driven vagus nerve signaling within the GBA. We developed an integrated framework that captures the entire communication channel from molecular binding events to neural information transmission, including SCFA-receptor binding kinetics, intracellular G-protein and calcium signaling dynamics, Hodgkin-Huxley-based action potential generation, and probabilistic neurotransmitter release mechanisms. Through extensive numerical simulations and information-theoretic analysis, we quantified the performance of this hybrid molecular-neural channel using mutual information and delay metrics. The outcomes demonstrated that the G-protein

activation rate, governed by SCFA type and concentration, acts as a critical parameter determining channel efficiency. Higher activation rates yielded increased mutual information and reduced signaling delays, indicating more reliable and faster information transfer. The analysis revealed that, within physiological ranges, higher SCFA concentrations increased mutual information and reduced transmission delays, establishing a quantitative link between microbial metabolite levels and neural communication efficiency. This work provided the first quantitative analysis of how gut-derived molecular signals are transduced into neural information, revealing the inherent trade-offs between signaling fidelity and speed and establishing a crucial link between microbial metabolism and neural communication [44].

In Chapter 3, the research culminated in a novel, system-level model that captures the essential bidirectional and feedback-driven nature of the GBA. This chapter introduced a closed-loop network model integrating the hypothalamic-pituitary-adrenal (HPA) axis, immune signaling, and gut barrier integrity, formulated as a system of nonlinear delay differential equations. Simulations of healthy, acute, and chronic stress scenarios demonstrated the system's transition from stable circadian oscillations to a pathological state of sustained hypercortisolism. The bifurcation analysis identified the critical tipping points where the system loses resilience. Furthermore, frequency-domain analysis of the linearized channel quantified the system's information-theoretic capacity. It demonstrated that chronic stress markedly impaired communication performance that was characterized by reduced bandwidth, decreased channel capacity, and diminished noise resilience compared to the healthy state. This model demonstrates that gut-brain axis pathology is not just a biochemical imbalance, but rather a fundamental information processing failure, marked by the breakdown of feedback control and a collapse of the network's communication capacity [45].

Collectively, these contributions establish a powerful new framework for studying the GBA. This thesis has demonstrated that molecular communication theory provides an exceptionally robust framework for describing intra-body networks by translating complex biological mechanisms into explicit channel models with quan-

tifiable metrics. The most significant insight from this work is that GBA-related disorders can be fundamentally comprehended as communication system failures rather than only biochemical imbalances. For instance, the collapse into pathological states represents a fatal impairment of the body's information processing capabilities, characterized by damaged feedback loops, increased noise, and ultimately a complete loss of channel capacity.

The MC perspective has profound implications for both research and clinical applications. It provides a principled methodology for identifying therapeutic targets to restore healthy information flow through strategies such as improving channel reliability, reducing systemic noise, or retuning feedback control mechanisms. Furthermore, the models developed in this thesis lay the essential theoretical groundwork for future Internet of Bio-Nano Things (IoBNT) applications, providing the necessary channel knowledge to design smart devices that can effectively sense, diagnose, and modulate biological signaling pathways in a safe and targeted manner.

Limitations and Future Work

Although the models presented in this thesis are based on established physiology, they are also necessarily abstractions of an immense biological complexity. Acknowledging this limitation highlights clear avenues for future research. For instance, future research could expand the pathway models to include a broader range of signaling molecules and their competitive interactions (cross-talk). Similarly, the system-level model from Chapter 3, while capturing a critical feedback loop, could be extended to incorporate other parallel pathways, such as direct vagal immune signaling, to create an even more holistic representation.

The several exciting research avenues emerge from this thesis are:

- **Model Validation and Personalization:** The next critical next step is to validate the model predictions against experimental and clinical data. This would involve using time-series data of hormone levels, cytokine concentrations, and gut permeability markers from animal models or human subjects

to rigorously test and refine the models. Furthermore, by integrating multi-omics data (e.g., metagenomics, metabolomics) from groups of patients, these frameworks could be parameterized for specific individuals, paving the way for personalized medicine and patient-specific predictions of disease progression or treatment response.

- **Exploring Other Pathologies:** The analytical framework developed in this thesis is highly adaptable. Future work can extend this approach to investigate the communication failures implicated in other GBA-related disorders. For instance, the models could be modified to explore altered serotonergic signaling in depression, the role of alpha-synuclein propagation in Parkinson's disease, or the specific patterns of visceral hypersensitivity that characterize irritable bowel syndrome (IBS).

- **Designing IoBNT Interventions:** The models developed in this thesis serve as a powerful in silico testbed for designing and optimizing novel therapeutic strategies based on IoBNT principles. For instance, the framework could be used to simulate a synthetic probiotic that operates in a closed-loop, sensing inflammatory markers in the gut and releasing a therapeutic molecule in response. The proper channel models would be crucial for this design process, as they allow for the prediction of the dose-response dynamics and timing required to restore homeostasis, which in turn could significantly accelerate the development of these advanced technologies.

- **Network-Level Analysis:** This thesis has primarily focused on characterizing individual communication links and specific feedback loops. However, the GBA operates as a network with multiple parallel neural, endocrine, and immune pathways that constantly interact. A significant avenue for future research is to apply the principles of network information theory to analyze this system as a whole. Such an approach could investigate fundamental questions, including how information is routed and prioritized across different channels,

how the system manages interference between competing signals, and how it allocates resources to achieve robust, adaptive communication and maintain system-level homeostasis.

In conclusion, this thesis has demonstrated the remarkable capacity of applying information and communication theory to one of the most complex signaling systems in the human body. By establishing a rigorous, quantitative foundation for the GBA, this work not only advances our fundamental understanding of intra-body communication but also paves the way for a new generation of diagnostic and therapeutic strategies designed to restore and maintain the body's vital communication pathways.

BIBLIOGRAPHY

[1] O. B. Akan, H. Ramezani, T. Khan, N. A. Abbasi, and M. Kuscu, "Fundamentals of molecular information and communication science," *Proceedings of the IEEE*, vol. 105, no. 2, pp. 306–318, 2016.

[2] M. Seyedi, B. Kibret, D. T. Lai, and M. Faulkner, "A survey on intrabody communications for body area network applications," *IEEE Transactions on Biomedical Engineering*, vol. 60, no. 8, pp. 2067–2079, 2013.

[3] T. Nakano, *Molecular communication*. Cambridge University Press, 2013.

[4] D. Malak and O. B. Akan, "Molecular communication nanonetworks inside human body," *Nano Communication Networks*, vol. 3, no. 1, pp. 19–35, 2012.

[5] B. Atakan, O. B. Akan, and S. Balasubramaniam, "Body area nanonetworks with molecular communications in nanomedicine," *IEEE Communications Magazine*, vol. 50, no. 1, pp. 28–34, 2012.

[6] E. A. Mayer, "Gut feelings: the emerging biology of gut–brain communication," *Nature Reviews Neuroscience*, vol. 12, no. 8, pp. 453–466, 2011.

[7] L. R. Johnson, *Physiology of the gastrointestinal tract*. Elsevier, 2006.

[8] H. M. Said, *Physiology of the gastrointestinal tract*. Academic Press, 2018.

[9] Y. Kim and T. A. Pritts, "The gastrointestinal tract," in *Geriatric trauma and critical care*. Springer, 2017, pp. 35–43.

[10] A. R. Gunawardene, B. M. Corfe, and C. A. Staton, "Classification and functions of enteroendocrine cells of the lower gastrointestinal tract," *International journal of experimental pathology*, vol. 92, no. 4, pp. 219–231, 2011.

[11] R. Pabst, "The anatomical basis for the immune function of the gut," *Anatomy and embryology*, vol. 176, no. 2, pp. 135–144, 1987.

[12] A. Heintz-Buschart and P. Wilmes, "Human gut microbiome: function matters," *Trends in microbiology*, vol. 26, no. 7, pp. 563–574, 2018.

[13] B. Dalile, L. Van Oudenhove, B. Vervliet, and K. Verbeke, "The role of short-chain fatty acids in microbiota–gut–brain communication," *Nature reviews Gastroenterology & hepatology*, vol. 16, no. 8, pp. 461–478, 2019.

[14] Y. P. Silva, A. Bernardi, and R. L. Frozza, "The role of short-chain fatty acids from gut microbiota in gut-brain communication," *Frontiers in endocrinology*, vol. 11, p. 508738, 2020.

[15] C. R. Martin, V. Osadchiy, A. Kalani, and E. A. Mayer, "The brain-gut-microbiome axis," *Cellular and molecular gastroenterology and hepatology*, vol. 6, no. 2, pp. 133–148, 2018.

[16] T. G. Dinan and J. F. Cryan, "The microbiome-gut-brain axis in health and disease," *Gastroenterology Clinics*, vol. 46, no. 1, pp. 77–89, 2017.

[17] J. F. Cryan *et al.*, "The microbiota-gut-brain axis," *Physiological reviews*, 2019.

[18] P. J. Kennedy, J. F. Cryan, T. G. Dinan, and G. Clarke, "Kynurenine pathway metabolism and the microbiota-gut-brain axis," *Neuropharmacology*, vol. 112, pp. 399–412, 2017.

[19] V. F. Monteiro-Cardoso, M. Corlianò, and R. R. Singaraja, "Bile acids: a communication channel in the gut-brain axis," *NeuroMolecular Medicine*, vol. 23, no. 1, pp. 99–117, 2021.

[20] J. B. Furness, "The enteric nervous system and neurogastroenterology," *Nature reviews Gastroenterology & hepatology*, vol. 9, no. 5, pp. 286–294, 2012.

[21] E. A. Mayer, K. Nance, and S. Chen, "The gut–brain axis," *Annual review of medicine*, vol. 73, no. 1, pp. 439–453, 2022.

[22] T. G. Dinan and J. F. Cryan, "Brain-gut-microbiota axis and mental health," *Biopsychosocial Science and Medicine*, vol. 79, no. 8, pp. 920–926, 2017.

[23] B. Bonaz, T. Bazin, and S. Pellissier, "The vagus nerve at the interface of the microbiota-gut-brain axis," *Frontiers in neuroscience*, vol. 12, p. 49, 2018.

[24] H.-R. Berthoud and W. L. Neuhuber, "Functional and chemical anatomy of the afferent vagal system," *Autonomic Neuroscience*, vol. 85, no. 1-3, pp. 1–17, 2000.

[25] R. A. Travagli and L. Anselmi, "Vagal neurocircuitry and its influence on gastric motility," *Nature Reviews Gastroenterology & Hepatology*, vol. 13, no. 7, pp. 389–401, 2016.

[26] S. M. Brierley, T. J. Hibberd, and N. J. Spencer, "Spinal afferent innervation of the colon and rectum," *Frontiers in cellular neuroscience*, vol. 12, p. 467, 2018.

[27] E. Agostoni, J. Chinnock, M. D. B. Daly, and J. Murray, "Functional and histological studies of the vagus nerve and its branches to the heart, lungs and abdominal viscera in the cat," *The Journal of physiology*, vol. 135, no. 1, pp. 182–205, 1957.

[28] D. V. Bohórquez, R. A. Shahid, A. Erdmann, A. M. Kreger, Y. Wang, N. Calakos, F. Wang, R. A. Liddle *et al.*, "Neuroepithelial circuit formed by innervation of sensory enteroendocrine cells," *The Journal of clinical investigation*, vol. 125, no. 2, pp. 782–786, 2015.

[29] P. D. Cani and C. Knauf, "How gut microbes talk to organs: the role of endocrine and nervous routes," *Molecular metabolism*, vol. 5, no. 9, pp. 743–752, 2016.

[30] R. E. Steinert, C. Feinle-Bisset, L. Asarian, M. Horowitz, C. Beglinger, and N. Geary, "Ghrelin, cck, glp-1, and pyy (3–36): secretory controls and physiological roles in eating and glycemia in health, obesity, and after rygb," *Physiological reviews*, vol. 97, no. 1, pp. 411–463, 2017.

[31] A. Farzi, E. E. Fröhlich, and P. Holzer, "Gut microbiota and the neuroendocrine system," *Neurotherapeutics*, vol. 15, no. 1, pp. 5–22, 2018.

[32] G. Clarke, R. M. Stilling, P. J. Kennedy, C. Stanton, J. F. Cryan, and T. G. Dinan, "Minireview: gut microbiota: the neglected endocrine organ," *Molecular endocrinology*, vol. 28, no. 8, pp. 1221–1238, 2014.

[33] S. Negi, D. K. Das, S. Pahari, S. Nadeem, and J. N. Agrewala, "Potential role of gut microbiota in induction and regulation of innate immune memory," *Frontiers in immunology*, vol. 10, p. 2441, 2019.

[34] B. Ruder, R. Atreya, and C. Becker, "Tumour necrosis factor alpha in intestinal homeostasis and gut related diseases," *International journal of molecular sciences*, vol. 20, no. 8, p. 1887, 2019.

[35] R. Dantzer, J. C. O'connor, G. G. Freund, R. W. Johnson, and K. W. Kelley, "From inflammation to sickness and depression: when the immune system subjugates the brain," *Nature reviews neuroscience*, vol. 9, no. 1, pp. 46–56, 2008.

[36] A. Rutsch, J. Kantsjö, and F. Ronchi, "The gut-brain axis: how microbiota and host inflammasome influence brain physiology and pathology. front immunol 11: 604179," 2020.

[37] A. H. Miller, V. Maletic, and C. L. Raison, "Inflammation and its discontents: the role of cytokines in the pathophysiology of major depression," *Biological psychiatry*, vol. 65, no. 9, pp. 732–741, 2009.

[38] J. F. Cryan and S. O'mahony, "The microbiome-gut-brain axis: from bowel to behavior," *Neurogastroenterology & Motility*, vol. 23, no. 3, pp. 187–192, 2011.

[39] Y. Ringel, "The gut microbiome in irritable bowel syndrome and other functional bowel disorders," *Gastroenterology Clinics*, vol. 46, no. 1, pp. 91–101, 2017.

[40] C. Benakis, C. Martin-Gallausiaux, J.-P. Trezzi, P. Melton, A. Liesz, and P. Wilmes, "The microbiome-gut-brain axis in acute and chronic brain diseases," *Current opinion in neurobiology*, vol. 61, pp. 1–9, 2020.

[41] E. A. Mayer, R. Knight, S. K. Mazmanian, J. F. Cryan, and K. Tillisch, "Gut microbes and the brain: paradigm shift in neuroscience," *Journal of Neuroscience*, vol. 34, no. 46, pp. 15 490–15 496, 2014.

[42] G. Sharon, T. R. Sampson, D. H. Geschwind, and S. K. Mazmanian, "The central nervous system and the gut microbiome," *Cell*, vol. 167, no. 4, pp. 915–932, 2016.

[43] B. E. Ortlek and O. B. Akan, "Communication theoretical analysis of p-cresol signaling in gut-brain axis with autism spectrum disorder," in *ICC 2023-IEEE International Conference on Communications*. IEEE, 2023, pp. 4482–4487.

[44] B. E. Ortlek and O. B. Akan, "Modeling and analysis of scfa-driven vagus nerve signaling in the gut-brain axis via molecular communication," *IEEE Transactions on Molecular, Biological, and Multi-Scale Communications*, 2025.

[45] B. E. Ortlek and O. B. Akan, "Gut-brain axis as a closed-loop molecular communication network," *arXiv preprint arXiv:2509.07911*, 2025.

[46] I. F. Akyildiz and J. M. Jornet, "The internet of nano-things," *IEEE Wireless Communications*, vol. 17, no. 6, pp. 58–63, 2010.

[47] I. F. Akyildiz, M. Pierobon, S. Balasubramaniam, and Y. Koucheryavy, "The internet of bio-nano things," *IEEE Communications Magazine*, vol. 53, no. 3, pp. 32–40, 2015.

[48] E. A. Mayer, K. Tillisch, A. Gupta *et al.*, "Gut/brain axis and the microbiota," *The Journal of clinical investigation*, vol. 125, no. 3, pp. 926–938, 2015.

[49] L. H. Morais, H. L. Schreiber IV, and S. K. Mazmanian, "The gut microbiota–brain axis in behaviour and brain disorders," *Nature Reviews Microbiology*, vol. 19, no. 4, pp. 241–255, 2021.

[50] Q. Li, Y. Han, A. B. C. Dy, and R. J. Hagerman, "The gut microbiota and autism spectrum disorders," *Frontiers in cellular neuroscience*, vol. 11, p. 244313, 2017.

[51] C. Lord *et al.*, "Autism spectrum disorder," *Nature reviews Disease primers*, vol. 6, no. 1, p. 5, 2020.

[52] C. Lord, M. Elsabbagh, G. Baird, and J. Veenstra-Vanderweele, "Autism spectrum disorder," *The Lancet*, vol. 392, no. 10146, pp. 508–520, 2018.

[53] E. Y. Hsiao, "Gastrointestinal issues in autism spectrum disorder," *Harvard review of psychiatry*, vol. 22, no. 2, pp. 104–111, 2014.

[54] C. A. Erickson, K. A. Stigler, M. R. Corkins, D. J. Posey, J. F. Fitzgerald, and C. J. McDougle, "Gastrointestinal factors in autistic disorder: a critical review," *Journal of autism and developmental disorders*, vol. 35, no. 6, p. 713, 2005.

[55] D. L. Coury, P. Ashwood, A. Fasano, G. Fuchs, M. Geraghty, A. Kaul, G. Mawe, P. Patterson, and N. E. Jones, "Gastrointestinal conditions in children with autism spectrum disorder: developing a research agenda," *Pediatrics*, vol. 130, no. Supplement_2, pp. S160–S168, 2012.

[56] B. Sankowski, K. Księżarczyk, E. Raćkowska, S. Szlufik, D. Koziorowski, and J. Giebułtowicz, "Higher cerebrospinal fluid to plasma ratio of p-cresol sulfate and indoxyl sulfate in patients with parkinson's disease," *Clinica Chimica Acta*, vol. 501, pp. 165–173, 2020.

[57] J. F. White, "Intestinal pathophysiology in autism," *Experimental Biology and Medicine*, vol. 228, no. 6, pp. 639–649, 2003.

[58] V. Saurman, K. G. Margolis, and R. A. Luna, "Autism spectrum disorder as a brain-gut-microbiome axis disorder," *Digestive diseases and sciences*, vol. 65, no. 3, pp. 818–828, 2020.

[59] A. Fattorusso, L. Di Genova, G. B. Dell'Isola, E. Mencaroni, and S. Esposito, "Autism spectrum disorders and the gut microbiota," *Nutrients*, vol. 11, no. 3, p. 521, 2019.

[60] E. Y. Hsiao *et al.*, "The microbiota modulates gut physiology and behavioral abnormalities associated with autism," *Cell*, vol. 155, no. 7, p. 1451, 2013.

[61] S. M. Finegold *et al.*, "Pyrosequencing study of fecal microflora of autistic and control children," *Anaerobe*, vol. 16, no. 4, pp. 444–453, 2010.

[62] S. R. Elsden, M. G. Hilton, and J. M. Waller, "The end products of the metabolism of aromatic amino acids by clostridia," *Archives of microbiology*, vol. 107, no. 3, pp. 283–288, 1976.

[63] G. M. Whited and D. T. Gibson, "Toluene-4-monooxygenase, a three-component enzyme system that catalyzes the oxidation of toluene to p-cresol in pseudomonas mendocina kr1." *Journal of bacteriology*, vol. 173, no. 9, pp. 3010–3016, 1991.

[64] V. Cafaro, E. Notomista, P. Capasso, and A. Di Donato, "Mutation of glutamic acid 103 of toluene o-xylene monooxygenase as a means to control the

catabolic efficiency of a recombinant upper pathway for degradation of methylated aromatic compounds," *Applied and environmental microbiology*, vol. 71, no. 8, pp. 4744–4750, 2005.

[65] S. Liabeuf, T. B. Drüeke, and Z. A. Massy, "Protein-bound uremic toxins: new insight from clinical studies," *Toxins*, vol. 3, no. 7, pp. 911–919, 2011.

[66] R. De Smet, J. Van Kaer, B. Van Vlem, A. De Cubber, P. Brunet, N. Lameire, and R. Vanholder, "Toxicity of free p-cresol: a prospective and cross-sectional analysis," *Clinical Chemistry*, vol. 49, no. 3, pp. 470–478, 2003.

[67] P. J. Goodhart, W. E. DeWolf Jr, and L. I. Kruse, "Mechanism-based inactivation of dopamine. beta.-hydroxylase by p-cresol and related alkylphenols," *Biochemistry*, vol. 26, no. 9, pp. 2576–2583, 1987.

[68] W. Shaw, "Dopamine excess and/or norepinephrine and epinephrine deficiency in autistic patients due to prenatal and/or postnatal deficiency of dopamine beta-hydroxylase," *J Orthomol Med*, vol. 36, no. 1, 2020.

[69] D. Pavăl, "A dopamine hypothesis of autism spectrum disorder," *Developmental neuroscience*, vol. 39, no. 5, pp. 355–360, 2017.

[70] P. Bermudez-Martin *et al.*, "The microbial metabolite p-cresol induces autistic-like behaviors in mice by remodeling the gut microbiota," *BioRxiv*, 2020.

[71] V. Jamali, A. Ahmadzadeh, W. Wicke, A. Noel, and R. Schober, "Channel modeling for diffusive molecular communication—a tutorial review," *Proceedings of the IEEE*, vol. 107, no. 7, pp. 1256–1301, 2019.

[72] R. Daneman and A. Prat, "The blood–brain barrier," *Cold Spring Harbor perspectives in biology*, vol. 7, no. 1, p. a020412, 2015.

[73] W. Wicke, T. Schwering, A. Ahmadzadeh, V. Jamali, A. Noel, and R. Schober, "Modeling duct flow for molecular communication," in *2018 IEEE Global Communications Conference (GLOBECOM)*. IEEE, 2018, pp. 206–212.

[74] B. Zlokovic, "Blood–brain barrier and neurovascular mechanisms of neurodegeneration and injury," 2009.

[75] J. C. Fiala and K. M. Harris, "Dendrite structure," *Dendrites*, vol. 2, pp. 1–11, 1999.

[76] R. Ågren, T. M. Stepniewski, H. Zeberg, J. Selent, and K. Sahlholm, "Dopamine d2 receptor agonist binding kinetics—role of a conserved serine residue," *International journal of molecular sciences*, vol. 22, no. 8, p. 4078, 2021.

[77] N. Farsad, H. B. Yilmaz, A. Eckford, C.-B. Chae, and W. Guo, "A comprehensive survey of recent advancements in molecular communication," *IEEE Communications Surveys & Tutorials*, vol. 18, no. 3, pp. 1887–1919, 2016.

[78] M. Kuscu and B. D. Unluturk, "Internet of bio-nano things: A review of applications, enabling technologies and key challenges," *arXiv preprint arXiv:2112.09249*, 2021.

[79] I. F. Akyildiz, J. Chen, M. Ghovanloo, U. Guler, T. Ozkaya-Ahmadov, M. Pierobon, A. F. Sarioglu, and B. D. Unluturk, "Microbiome-gut-brain axis as a biomolecular communication network for the internet of bio-nanothings," *IEEE access*, vol. 7, pp. 136 161–136 175, 2019.

[80] B. Maitra and O. B. Akan, "Molecular quantum (molq) communication channel in the gut-brain axis synapse," *IEEE Transactions on Molecular, Biological, and Multi-Scale Communications*, 2024.

[81] S. Breit, A. Kupferberg, G. Rogler, and G. Hasler, "Vagus nerve as modulator of the brain–gut axis in psychiatric and inflammatory disorders," *Frontiers in psychiatry*, vol. 9, p. 44, 2018.

[82] M. Rosas-Ballina *et al.*, "Acetylcholine-synthesizing t cells relay neural signals in a vagus nerve circuit," *Science*, vol. 334, no. 6052, pp. 98–101, 2011.

[83] Y. B. Wang, G. De Lartigue, and A. J. Page, "Dissecting the role of subtypes of gastrointestinal vagal afferents," *Frontiers in Physiology*, vol. 11, p. 643, 2020.

[84] C. Goswami, Y. Iwasaki, and T. Yada, "Short-chain fatty acids suppress food intake by activating vagal afferent neurons," *The Journal of nutritional biochemistry*, vol. 57, pp. 130–135, 2018.

[85] M. Carabotti, A. Scirocco, M. A. Maselli, and C. Severi, "The gut-brain axis: interactions between enteric microbiota, central and enteric nervous systems," *Annals of gastroenterology: quarterly publication of the Hellenic Society of Gastroenterology*, vol. 28, no. 2, p. 203, 2015.

[86] K. J. O'Riordan, M. K. Collins, G. M. Moloney, E. G. Knox, M. R. Aburto, C. Fülling, S. J. Morley, G. Clarke, H. Schellekens, and J. F. Cryan, "Short chain fatty acids: microbial metabolites for gut-brain axis signalling," *Molecular and Cellular Endocrinology*, vol. 546, p. 111572, 2022.

[87] C. Guo, Y.-J. Huo, Y. Li, Y. Han, and D. Zhou, "Gut-brain axis: Focus on gut metabolites short-chain fatty acids," *World journal of clinical cases*, vol. 10, no. 6, p. 1754, 2022.

[88] S. Longo, S. Rizza, and M. Federici, "Microbiota-gut-brain axis: Relationships among the vagus nerve, gut microbiota, obesity, and diabetes," *Acta diabetologica*, vol. 60, no. 8, pp. 1007–1017, 2023.

[89] A. Majumdar, I. P. Siva Venkatesh, and A. Basu, "Short-chain fatty acids in the microbiota–gut–brain axis: role in neurodegenerative disorders and viral infections," *ACS Chemical Neuroscience*, vol. 14, no. 6, pp. 1045–1062, 2023.

[90] W. Xiao, J. Su, X. Gao, H. Yang, R. Weng, W. Ni, and Y. Gu, "The microbiota-gut-brain axis participates in chronic cerebral hypoperfusion by disrupting the metabolism of short-chain fatty acids," *Microbiome*, vol. 10, no. 1, p. 62, 2022.

[91] B. Bonaz, V. Sinniger, and S. Pellissier, "The vagus nerve in the neuro-immune axis: implications in the pathology of the gastrointestinal tract," *Frontiers in immunology*, vol. 8, p. 1452, 2017.

[92] U. Kummer, L. F. Olsen, C. J. Dixon, A. K. Green, E. Bornberg-Bauer, and G. Baier, "Switching from simple to complex oscillations in calcium signaling," *Biophysical journal*, vol. 79, no. 3, pp. 1188–1195, 2000.

[93] M. J. Berridge, "Neuronal calcium signaling," *Neuron*, vol. 21, no. 1, pp. 13–26, 1998.

[94] A. McQuate, E. Latorre-Esteves, and A. Barria, "A wnt/calcium signaling cascade regulates neuronal excitability and trafficking of nmdars," *Cell reports*, vol. 21, no. 1, pp. 60–69, 2017.

[95] M. Häusser, "The hodgkin-huxley theory of the action potential," *Nature neuroscience*, vol. 3, no. 11, pp. 1165–1165, 2000.

[96] A. L. Hodgkin and A. F. Huxley, "A quantitative description of membrane current and its application to conduction and excitation in nerve," *The Journal of physiology*, vol. 117, no. 4, p. 500, 1952.

[97] A. L. Hodgkin and A. F. Huxley, "Action potentials recorded from inside a nerve fibre," *Nature*, vol. 144, no. 3651, pp. 710–711, 1939.

[98] B. P. Bean, "The action potential in mammalian central neurons," *Nature Reviews Neuroscience*, vol. 8, no. 6, pp. 451–465, 2007.

[99] W. Yu and L. Lin, "Modeling and evaluation of vesicle release mechanisms in neuro-spike communication," *IEEE Transactions on NanoBioscience*, vol. 21, no. 3, pp. 416–424, 2022.

[100] H. Ramezani and O. B. Akan, "Information capacity of vesicle release in neuro-spike communication," *IEEE Communications Letters*, vol. 22, no. 1, pp. 41–44, 2017.

[101] M. Civas and O. B. Akan, "Rate of information flow across layered neuro-spike network in the spinal cord," *IEEE transactions on nanobioscience*, vol. 19, no. 3, pp. 368–377, 2020.

[102] H. Ramezani, T. Khan, and O. B. Akan, "Information theoretical analysis of synaptic communication for nanonetworks," in *IEEE INFOCOM 2018-IEEE Conference on Computer Communications*. IEEE, 2018, pp. 2330–2338.

[103] T. Ikeda, A. Nishida, M. Yamano, and I. Kimura, "Short-chain fatty acid receptors and gut microbiota as therapeutic targets in metabolic, immune, and neurological diseases," *Pharmacology & therapeutics*, vol. 239, p. 108273, 2022.

[104] G. Aceto, V. Persico, and A. Pescapé, "The role of information and communication technologies in healthcare: taxonomies, perspectives, and challenges," *Journal of Network and Computer Applications*, vol. 107, pp. 125–154, 2018.

[105] C. Furusawa, T. Suzuki, A. Kashiwagi, T. Yomo, and K. Kaneko, "Ubiquity of log-normal distributions in intra-cellular reaction dynamics," *Biophysics*, vol. 1, pp. 25–31, 2005.

[106] J. F. Cryan and T. G. Dinan, "Mind-altering microorganisms: the impact of the gut microbiota on brain and behaviour," *Nature reviews neuroscience*, vol. 13, no. 10, pp. 701–712, 2012.

[107] S. Grenham, G. Clarke, J. F. Cryan, and T. G. Dinan, "Brain–gut–microbe communication in health and disease," *Frontiers in physiology*, vol. 2, p. 94, 2011.

[108] H. T. Ding, Y. Taur, and J. T. Walkup, "Gut microbiota and autism: key concepts and findings," *Journal of autism and developmental disorders*, vol. 47, no. 2, pp. 480–489, 2017.

[109] S. El Aidy, T. G. Dinan, and J. F. Cryan, "Immune modulation of the brain-gut-microbe axis," p. 146, 2014.

[110] A. G. Bertollo, C. F. Santos, M. D. Bagatini, and Z. M. Ignácio, "Hypothalamus-pituitary-adrenal and gut-brain axes in biological interaction pathway of the depression," *Frontiers in Neuroscience*, vol. 19, p. 1541075, 2025.

[111] K. Kasarello, A. Cudnoch-Jedrzejewska, and K. Czarzasta, "Communication of gut microbiota and brain via immune and neuroendocrine signaling," *Frontiers in microbiology*, vol. 14, p. 1118529, 2023.

[112] T. G. Dinan, E. M. Quigley, S. M. Ahmed, P. Scully, S. O'Brien, L. O'Mahony, S. O'Mahony, F. Shanahan, and P. N. Keeling, "Hypothalamic-pituitary-gut axis dysregulation in irritable bowel syndrome: plasma cytokines as a potential biomarker?" *Gastroenterology*, vol. 130, no. 2, pp. 304–311, 2006.

[113] H. Malek, M. M. Ebadzadeh, R. Safabakhsh, A. Razavi, and J. Zaringhalam, "Dynamics of the hpa axis and inflammatory cytokines: insights from mathematical modeling," *Computers in Biology and Medicine*, vol. 67, pp. 1–12, 2015.

[114] G. S. Tofani, S.-J. Leigh, C. E. Gheorghe, T. F. Bastiaanssen, L. Wilmes, P. Sen, G. Clarke, and J. F. Cryan, "Gut microbiota regulates stress responsivity via the circadian system," *Cell metabolism*, vol. 37, no. 1, pp. 138–153, 2025.

[115] T. M. Cover, *Elements of information theory*. John Wiley & Sons, 1999.